REPORT NO.
UCB/EERC-78/07
APRIL 1978

EARTHQUAKE ENGINEERING RESEARCH CENTER

STUDIES OF STRUCTURAL RESPONSE TO EARTHQUAKE GROUND MOTION

by

OSCAR A. LOPEZ
ANIL K. CHOPRA

A report on research conducted under Grant ENV76-04264
from the National Science Foundation.

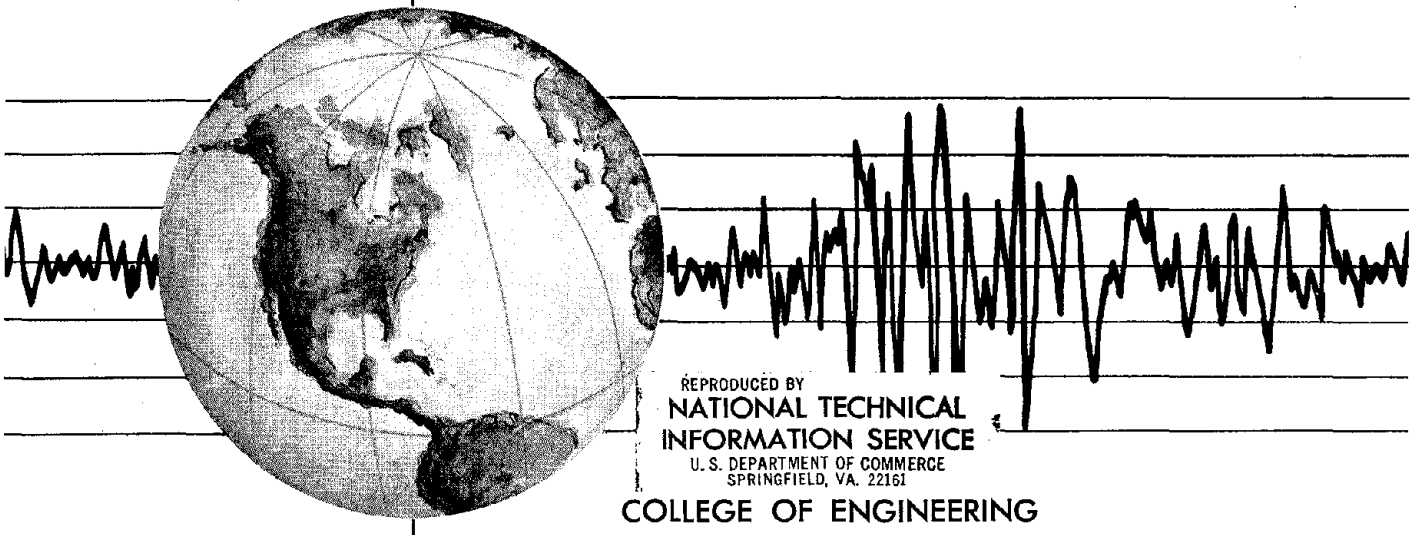

COLLEGE OF ENGINEERING

UNIVERSITY OF CALIFORNIA · Berkeley, California

BIBLIOGRAPHIC DATA SHEET	1. Report No. NSF/RA- 780117	2.	3. Recipient's Accession No. PB282790
4. Title and Subtitle Studies of Structural Response to Earthquake Ground Motion			5. Report Date April 1978 6.
7. Author(s) Oscar A. Lopez and Anil K. Chopra			8. Performing Organization Rept. No. 78/07
9. Performing Organization Name and Address Earthquake Engineering Research Center University of California, Richmond Field Station 47th Street and Hoffman Blvd. Richmond, California 94804			10. Project/Task/Work Unit No. 11. Contract/Grant No. ENV 76-04264
12. Sponsoring Organization Name and Address National Science Foundation 1800 G Street, N.W. Washington, D.C. 20550			13. Type of Report & Period Covered 14.
15. Supplementary Notes			

16. Abstracts

The response of linear elastic and nonlinear hysteretic systems having a single degree of freedom to recorded and simulated ground motions is studied. The objective is to evaluate whether the commonly used simulated motions are appropriate for predicting inelastic response of structures and elastic response of long period structures.

Eight simulated motions were generated to model properties of horizontal ground motions recorded during four earthquakes. The simulated motions are sample functions of a white noise process passed through a SDOF filter and multiplied by a temporal intensity functions. Two versions, corresponding to parabolic and 'standard' base line corrections (BLC), of each of the simulated and recorded accelerograms were considered.

The following general conclusions are deduced. Simulated ground motions should be subjected to the standard BLC, because it results in more reliable ground velocities and displacements, which in turn would lead to more reliable predictions of response of long period structures. Furthermore, the spectral density of the underlying random process, from which the simulated motions are obtained, should be modified to be more representative of the frequency content of recorded motions, especially in the low frequency range. Such an improved model can be expected to lead to better agreement, over a broad range of periods, in the average response spectra of simulated and recorded motions, for elastic as well as inelastic systems.

The response of idealized one-story structural systems to earthquake ground motion is computed with the objective of evaluating the effects of gravity loads and vertical ground motions. It is shown that the coupling between lateral and vertical deformations created by yielding in the system must be considered in order to predict the plastic part of vertical deformations due to horizontal ground motion. However, simpler analysis without such deformation coupling, but with reduction of lateral yield strength due to gravity load, would generally by satisfactory for predicting the lateral response of the system.

It is shown that the principal effect of the vertical component of ground motion is to superpose elastic vertical oscillations about the gradually growing vertical deformation that resulted from yielding due to horizontal ground motion alone. Lateral deformations are not influenced significantly by vertical ground motion; hence they may be determined from analysis of response to horizontal ground motion only.

18. Availability Statement Release Unlimited	19. Security Class (This Report) UNCLASSIFIED	
	20. Security Class (This Page) UNCLASSIFIED	22. Price A05 / MF A01

STUDIES OF STRUCTURAL RESPONSE TO EARTHQUAKE GROUND MOTION

by

Oscar A. Lopez

Anil K. Chopra

A Report on Research Conducted under

Grant ENV76-04264 from the National Science Foundation

Report No. UCB/EERC-78-07
Earthquake Engineering Research Center
University of California
Berkeley, California

April, 1978

ABSTRACT

This study of response of simple structural systems to earthquake ground motion is presented in two parts:

Part One

The response of linear elastic and nonlinear hysteretic systems having a single degree of freedom to recorded and simulated ground motions is studied. The objective is to evaluate whether the commonly used simulated motions are appropriate for predicting inelastic response of structures and elastic response of long period structures.

Eight simulated motions were generated to model properties of horizontal ground motions recorded during four earthquakes. The simulated motions are sample functions of a white noise process passed through a SDOF filter and multiplied by a temporal intensity functions. Two versions, corresponding to parabolic and 'standard' base line corrections (BLC), of each of the simulated and recorded accelerograms were considered.

The following general conclusions are deduced. Simulated ground motions should be subjected to the standard BLC, because it results in more reliable ground velocities and displacements, which in turn would lead to more reliable predictions of response of long period structures. Furthermore, the spectral density of the underlying random process, from which the simulated motions are obtained, should be modified to be more representative of the frequency content of recorded motions, especially in the low frequency range. Such an improved model can be expected to lead to better agreement, over a broad range of periods, in the average response spectra of simulated and recorded motions, for elastic as well as inelastic systems.

Part Two

The response of idealized one-story structural systems to earthquake ground motion is computed with the objective of evaluating the effects of gravity loads and vertical ground motions. It is shown that the coupling between lateral and vertical deformations created by yielding in the system must be considered in order to predict the plastic part of vertical deformations due to horizontal ground motion. However, simpler analysis without such deformation coupling, but with reduction of lateral yield strength due to gravity load, would generally by satisfactory for predicting the lateral response of the system.

It is shown that the principal effect of the vertical component of ground motion is to superpose elastic vertical oscillations about the gradually growing vertical deformation that resulted from yielding due to horizontal ground motion alone. Lateral deformations are not influenced significantly by vertical ground motion; hence they may be determined from analysis of response to horizontal ground motion only.

ACKNOWLEDGEMENTS

This research investigation was supported in part by Grant No. ENV76-04264 from the National Science Foundation. Additional support was provided by the fellowship Mr. Oscar A. Lopez received from Consejo Nacional de Investigaciones Cientificas y Tecnologicas, Venezuela during his graduate study.

This report also constitutes Mr. Lopez's doctoral dissertation which has been submitted to the University of California, Berkeley. The dissertation committee consisted of Professors A.K. Chopra (Chairman), J. Penzien and B.A. Bolt.

The writers are grateful to Professor Penzien for his advice during the course of this research and to Professor Bolt for reviewing the manuscript.

TABLE OF CONTENTS

Page

PREFACE

This study of response of simple structural systems to earthquake ground motion is organized in two parts:

Part One - Structural Response to Simulated Earthquake Motions, and

Part Two - Effects of Gravity Loads and Vertical Ground Motion on Earthquake Response of Buildings.

PART ONE

Structural Response to Simulated Earthquake Motions

INTRODUCTION

Study of probabilistic aspects of earthquake response of structures requires at least several ground motions recorded under a similar set of conditions: Magnitude of the earthquake, source mechanism, distance to the causative fault, geology between the fault and the recording station, local soil conditions, etc. From this point of view, the present collection of strong-motion accelerograms is far from adequate. Procedures for simulation of earthquake motions have therefore been developed for probabilistic studies of earthquake response. The motions are simulated as member functions of a random process model appropriate for recorded motions under a particular set of conditions.

Earthquake accelerograms have been modeled by random processes of varying complexity including stationary white noise (1), stationary Gaussian process with spectral density derived from average undamped velocity spectra of recorded accelerograms (2), a nonstationary process which consists of a stationary process multiplied by an envelope function which describes the temporal variation of the intensity of the process (3,4,5,6), and a nonstationary process with frequency content varying with time (7). Another approach to simulation of ground motions is to idealize the generation of an earthquake as a series of closely spaced focii along the rupturing fault (8). Successively, each focus or small rupture is assumed to radiate seismic waves with appropriate characteristics. Superposition of the waves from all the focii results in the complete simulated ground motion. Comparison of elastic response spectra for recorded and simulated motions have usually been the basis for evaluating the quality of the simulation

model. In a recent study, however, parameters for the nonstationary model mentioned above were determined specifically for inelastic response studies (9). The durations of the three phases--quadratic build up, constant value and exponential decay--of the envelope function for intensity were determined to minimize the mean simulation error in deformation spectra and dissipated hysteretic energy for elastic-perfectly-plastic systems.

Ground motions simulated as sample functions of a nonstationary random process, consisting of a stationary Gaussian process multiplied by a time dependent intensity function, possess many of the important properties of recorded earthquake accelerograms. In particular, simulated and recorded accelerograms have been shown to result in similar average response spectra for linearly elastic systems with vibration periods less than 3 secs (5). However, these or similar simulated motions have also been employed in probabilistic studies of inelastic response of systems (5,6) and as design earthquakes for structures with long natural periods of vibration, such as very tall buildings, offshore oil-drilling platforms and long span bridges. The objective of this study is to evaluate whether these widely used simulated motions are indeed appropriate for predicting inelastic response of structures and elastic response of long period structures.

IDEALIZED SYSTEMS

A one-story building is idealized as a shear type structure with total mass concentrated at the top deck, which is assumed to be rigid and the deflection is due only to lateral deformation in the columns, resulting in a system with one degree of freedom. In addition to a

linearly elastic case, two bilinear hysteretic force-deformation relations are considered: Elastic-perfectly-plastic and bilinear strain hardening with post-yield stiffness equal to one-tenth of the initial elastic stiffness.

The elastic stiffness $k_e = \frac{4\pi^2}{T^2} \frac{W}{g}$ where W = total weight of the structure, T = natural period of linear vibration, and g = acceleration of gravity. The yield strength $F_y = 2KCW$ where K = a numerical coefficient in the Uniform Building Code (UBC) depending on the structural system, selected herein as 0.67, the value recommended for ductile moment resisting frames; $C = 0.05/T^{1/3}$ is the base shear coefficient in an earlier edition of the UBC (10). The yield strength for the system has been taken as twice the UBC design values, to account for the difference between yield and design stresses as well as for the strengthening influence of non-structural components. Energy dissipation in the structure due to effects other than yielding is represented by viscous damping with the damping ratio ξ selected as 0.05.

RECORDED AND SIMULATED MOTIONS

The ground motion records listed in Table 1 are representative of ground motions on firm ground in the region of strong shaking during earthquakes of magnitude 6.5 to 7.5. The maximum values of acceleration, integrated velocity and displacement, and spectrum intensity for 5 per cent damping ratio ($SI_{0.05}$) are listed in Table 1 for two versions of each of the eight accelerograms: The original digitization with parabolic base line correction (11) and the more recent digitization with "standard" base line correction (12). The latter version, now considered as the "standard" data for recorded accelerograms, is presented in Fig. 1.

Eight simulated motions were generated to model the properties of the above mentioned recorded motions. The random process model including its parameter values and the simulation procedure adopted herein is essentially indentical to earlier studies (4-6). The simulation procedure consisted of generating samples of stationary Gaussian white noise; multiplying the white noise by an intensity function of time (Fig. 2) to represent a segment of strong shaking at constant intensity preceded by a quadratic build-up of intensity and followed by an exponential decay in intensity; passing the resulting function through a second order linear filter with frequency = 2.5 cps (5π rads/sec) and damping ratio = 60% to impart the desired frequency content, as indicated by the spectral density (Fig. 2), and finally performing a baseline correction on the filtered function. The eight simulated motions were all scaled by the same factor such that the average spectrum intensity $SI_{0.05}$ for the ensemble would be 1.36m, the $SI_{0.05}$ value for the S00E component of the El Centro 1940 motion.

The maximum values of acceleration, integrated velocity and displacement and spectrum intensity for 5% damping of two versions of the resulting motions are listed in Table 2; the two versions correspond to the two types of base line corrections mentioned above. The simulated accelerograms with standard base line correction are presented in Fig. 3.

Each recorded accelerogram was normalized so that its spectrum intensity $SI_{0.05}$ = 1.36 m, the $SI_{0.05}$ value of the S00E component of the El Centro 1940 motion. The average values of the ground motion parameters--maximum acceleration, integrated velocity and displacement, and spectrum intensity--for the resulting ensemble of normalized

recorded motions are presented in Table 3, along with the corresponding values for the ensemble of simulated motions.

The type of base line correction affects recorded and simulated motions similarly, with little influence on accelerations, some what more change in velocities, and large influence on displacements (Tables 1, 2 and 3). With standard base line correction, the average values of maximum displacements are only one-third of the values with parabolic base line correction (Table 3); also see Ref. (13).

Because of the scaling criteria adopted, the average spectrum intensity is the same for the two ensembles. However, the average value of maximum acceleration for simulated motions is significantly smaller than for recorded motions, maximum velocity is significantly larger, and maximum displacement is approximately twice as large (Table 3).

Each of the recorded and simulated accelerograms has a large number of zero crossings. An acceleration pulse is defined as the portion of an accelerogram between any neighbor pair of zero crossings. The area of the acceleration pulse controls the response of structures with fundamental period much longer than the duration of the pulse. For this reason it was of interest to examine the statistics of pulse areas in recorded and simulated motions. Two histograms for areas of acceleration pulses are presented in Fig. 4. One is the average across the ensemble of recorded motions and the other across the ensemble of simulated motions, both with standard base line correction. Simulated accelerograms contain a larger number of small pulses (area < 5 in/sec) and a smaller number of large pulses (area > 5 in/sec), relative to recorded accelerograms.

ELASTIC RESPONSE SPECTRA

Previous studies (5) have shown that elastic response spectra for simulated and recorded ground motions, both with parabolic base line correction, are similar for vibration periods up to 3 sec. In light of the observed differences in the properties of simulated and recorded ground motions, especially as influenced by the base line correction (BLC), it is of interest to re-examine their elastic response spectra, especially in the range of longer vibration periods.

The pseudo velocity response spectrum for 5% damping ratio was computed, using a standard computer program (14), for each member of four ensembles of ground motions: Normalized recorded motions with parabolic BLC, simulated motions with parabolic BLC, normalized recorded motions with standard BLC and simulated motions with standard BLC. The resulting spectra were averaged separately over each ensemble of ground motions. The average response spectra were plotted on longarithmic scales with the ordinate representing the pseudo-velocity, PS_v, and the abcissa the natural period of vibration of the system, T (Figs. 5-8). The values of pseudo-acceleration, PS_a, and displacement, S_d, can be determined directly from the diagonal scales. Also shown in Figs. 5-8 are the values of maximum ground acceleration, velocity and displacement averaged separately over each ensemble (Table 3).

When presented in this form, the response spectrum approaches the maximum ground acceleration at the left end for very short vibration periods and the maximum ground displacement at the right end for very long vibration periods. The response spectrum is most influenced by ground accelerations in the short period region, by ground displacements in the long period region, and by ground velocities in the intermediate

period region where the pseudo velocity is essentially independent of vibration period (15).

Previous comparisons of average response spectra for recorded and simulated ground motions have usually been for motions with parabolic BLC and in the vibration period range less than 3 sec. A similar comparison but for a longer range of vibration periods is presented in Fig. 5. Consistent with average values of maximum ground acceleration, velocity and displacement for the two ensembles, the response spectrum for simulated motions is smaller in the short period region but larger in the intermediate and long period regions, relative to the spectrum for recorded motions. In the long period region, discrepancy between the two spectra tends to increase with vibration period, and for very long periods would reach a factor of approximately 2, consistent with the ratio of average values of maximum ground displacement for the two ensembles. However, the discrepancy at 15 sec period is not much larger than it is at some shorter periods, for example 0.6 sec.

When the average response spectrum for simulated motions with parabolic BLC is compared with the corresponding spectrum for what are now considered as standard data for recorded accelerograms, a large discrepancy is apparent in the long period range, whereas the comparison has not changed much in the short and intermediate periods (Fig. 6). For longer periods, the two spectra diverge so greatly, because maximum displacements from simulated accelerograms are approximately six times the value from recorded accelerograms.

The important effect of the base line correction on the response spectrum in the long period range is seen in Fig. 7. The average

response spectrum for the ensemble of recorded motions is essentially the same for vibration periods up to 2 sec., independent of the type--parabolic or standard -- of BLC. However, the response spectrum is increasingly sensitive to the base line correction as vibration periods increase beyond 2 sec. The standard BLC reduces the ground displacement to approximately one-third the value associated with parabolic BLC (Fig. 7, Table 3), leading to similar reduction in the response spectrum at very long periods.

Simulated motions with parabolic BLC are unsatisfactory in the sense that, in the long period region, their response spectrum is unacceptably large compared to the response spectrum based on standard data set for the recorded motions (Fig. 6). Because response spectrum in the long period range is strongly dependent on the base line correction employed (Fig. 7), it seemed that the first step in improving simulated motions would be to subject them to the standard BLC. Comparison of the average response spectrum for the resulting ensemble of simulated motions (Tables 2 and 3) with the corresponding spectrum for recorded motions indicates that discrepancy in the long period range has decreased (Fig. 8). Over the entire period range, discrepancy between the two response spectra is now similar to what was observed in Fig. 5. This is consistent with the data presented in Table 3, indicating that the ratio between ensemble averages for simulated and recorded motions of the ground acceleration, velocity and displacement are essentially independent of the type of base line correction.

Discrepancy between average response spectra for recorded and simulated ground motions depends, in part, on how the motions are normalized. When the two ensembles were normalized to have the same

average spectrum intensity for 5% damping, the discrepancy is indicated in Fig. 8: The average response spectrum for simulated motions, as compared to the spectrum for recorded motions is smaller for vibration periods less than 1 sec, but larger for longer periods; the area under the two spectra in the period range 0.1 to 2.5 sec is, of course, the same because of the normalization criterion. If the two ensembles had been normalized to have the same average value of maximum ground acceleration, their response spectra would have been in very good agreement in the short period region, where they are most influenced by ground accelerations. However, this would be at the expense of increased discrepancy between the two spectra in the intermediate and long period regions. At intermediate periods, response spectra are most influenced by ground velocities and better agreement between the two spectra can obviously be achieved by normalizing the two ensembles to have the same average value of maximum ground velocity. However, in comparison with Fig. 8, this would worsen agreement between the two spectra in the short period region. In the long period region, where response spectra are most influenced by ground displacements, it would be necessary to match average values of maximum displacement of the two ground motion ensembles to achieve good agreement between the two response spectra. However, in comparison to Fig. 8, this would considerably worsen agreement between the two spectra in the short and intermediate period regions. Considering the two spectra over a limited range of vibration periods, normalization based on maximum acceleration, velocity or displacement--whichever is appropriate for the particular range--would provide a better agreement than normalization based on spectrum intensity.

However, when a broad period range is considered, response spectra for simulated and recorded motions are significantly different in shape, indicating that their frequency content, on the average, is not the same. In order to achieve better agreement between the two response spectra, the spectral density of the random process employed as a model for earthquake accelerograms (Fig. 2) should be modified to be more representative of the frequency content of recorded motions over a broad range of frequencies.

CHARACTERISTICS OF ELASTIC AND INELASTIC RESPONSES

The computed response of linearly elastic and elastic-perfectly-plastic hysteretic systems, both with small amplitude elastic vibration period 0.4 sec, to three simulated motions is presented in Fig. 9. The deformation response of both systems has been normalized by the yield displacement of the hysteretic system. (Note that the yield strength of this hysteretic system = 0.24 W, not the same as indicated in the section on "idealized systems".) A visual comparison of the time variation of deformation for the two systems indicates significant difference in their behavior: Responses of the elastic system are oscillatory about the initial equilibrium position, and have the appearance of a sinusoid of frequency equal to the natural frequency of the system f = 2.5 cps, but with slowly varying random amplitude and phase. On the other hand, responses of the elastic-perfectly-plastic hysteretic system are characterized by a few large increments in the plastic part of the deformation, each causing a shift in the equilibrium position about which the structure subsequently oscillates until the next large increment in plastic part of the deformation occurs. Thus,

there are several equilibrium positions about which the structure oscillates during the earthquake motion.

In order to identify the factors that influence structural response, simulated accelerogram no. 5 (Fig. 3) and the responses of the elastic system and of the elastic-perfectly-plastic hysteretic system to this simulated motion are all presented in Fig. 10 to the same time scale. Also included is the time variation of the rate of the energy input to the system by the ground motion, normalized with respect to the elastic strain energy at yield point (Appendix A). The three acceleration pulses immediately preceding the three largest increments in the plastic part of the drift, as well as the energy input ΔE to the system by these pulses, are identified. Pulses b and c having similar areas produce significantly different incremental plastic deformation Δv^P (defined in Fig. 11), whereas pulses a and c having dissimilar areas produced similar incremental plastic deformation.

This lack of correlation between pulse area and incremental plastic deformation is further indicated in Fig. 11 where areas of pulses and associated incremental plastic deformations are plotted. Although deformation has a tendency to increase with pulse area, the relationship between the two is neither simple nor direct. Acceleration pulses a and c input similar amounts of energy to the inelastic system, while pulse b inputs less energy (Fig. 10), thus indicating that pulses with larger areas do not necessarily input greater energy to the system. However, it is apparent (Fig. 10) that the larger incremental plastic deformations are roughly proportional to the energy input to the system by acceleration pulses that immediately preceded the deformations.

The other simulated motion shown (Fig. 10) has been obtained from simulated motion no. 5 by deleting the shaded pulse a' immediately preceding pulse a; in all other respects the two motions are identical. This slight modification in the ground motion altered the state--displacement, velocity and acceleration--of the system preceding acceleration pulse a, resulting in significant change in the incremental plastic deformation and the energy input to the system by this pulse, and the maximum response during the earthquake. However, the energy input and incremental plastic deformations due to pulses b and c as well as the oscillatory, elastic portion of the response remained virtually unchanged. In contrast, the response of the elastic system was virtually unaffected by modification of the ground motion (Fig. 10). It is therefore concluded that effects of smaller pulses or maximum response of elastic systems are negligible but they may be significant in the case of inelastic systems.

INELASTIC RESPONSE SPECTRA

It was seen in the preceding section that earthquake response of inelastic systems is quite sensitive to details of the ground motion, in particular to acceleration pulses with small area, whereas response of elastic systems is relatively insensitive. It has also been noted that simulated motions considered herein contain many more smaller acceleration pulses than recorded motions (Fig. 4). It is therefore of interest to see whether the simulated motions are as suitable to determine the response of inelastic systems as they are in determining the response of elastic systems.

Responses of the idealized system described earlier, with several values of low amplitude vibration period T, varying between 0.2

and 7 sec., to the ensembles of recorded and simulated ground motions, both with the standard base line correction, were computed. For each period value, response was analyzed for two bilinear hysteretic systems: Elastic-perfectly-plastic and bilinear strain hardening; the response of corresponding linearly elastic systems had already been computed to obtain the elastic response spectra presented in a preceding section.

Results are summarized in the form of average response spectra which were obtained as follows: Maximum displacements for the three types of systems--elastic, elastic-perfectly-plastic and bilinear strain hardining--having the same low amplitude vibration period were normalized by yield displacement of bilinear systems. These normalized maximum displacements were averaged separately over the two ensembles of ground motions, and plotted against vibration period in the form of average response spectra for the three types of systems and two ensembles of ground motions (Fig. 12). For each type of system, the ratio of the ordinates of the average response spectra for simulated and recorded ground motions is presented in Fig. 13 as a function of vibration period. This figure may also be interpreted as a plot of error in the average response spectrum for simulated motions, relative to the corresponding spectrum for recorded motions, expressed as a percentage of the ordinates of the latter.

For all three types of structural systems, the average response spectrum for simulated motions is smaller than the spectrum for recorded motions at shorter vibration periods, but larger for the longer vibration periods (Fig. 12), with the ratio of maximum displacements due to simulated and recorded motions growing with increase in vibration period. Errors are largest for elastic-perfectly-plastic

systems over much of the period range, and roughly the same for linearly elastic and strain hardening hysteretic systems. Most structures exhibit strain hardening in plastic deformation, and Fig. 13 therefore indicates that in the average sense, simulated motions used herein are appropriate for determining the maximum response of such structures in their inelastic range of behavior, to the same degree as they are suitable for predicting elastic response.

CONCLUSIONS

The type of base line correction (BLC), whether parabolic or 'standard', affects recorded and simulated ground motions similarly, with little influence on accelerations, somewhat more change in velocities, and large influence on displacements. Simulated ground motions to be used for response analysis of structures with long natural periods of vibration should be subjected to the standard BLC, because it is known to result in more reliable ground velocities and displacements, which in turn would lead to more reliable predictions of response of such structures.

However, even with the standard BLC, simulated ground motions--which are sample functions of a white noise process passed through a SDOF filter and multiplied by a temporal intensity function--have significantly different properties compared to recorded motions. On the average, maximum ground displacements for simulated motions are about twice of those for recorded motions, and the shape of the two average response spectra are significantly dissimilar. In order to achieve better agreement between the two response spectra over a broad range of periods, the spectral density of the underlying random

process, from which the simulated motions are obtained, should be modified to be more representative of the frequency content of recorded motions.

An improved random process model which leads to better agreement between elastic response spectra for simulated and recorded motions over a broad range of periods ($0.2 < T < 7$ sec.) can be expected to lead to similarly improved agreement in response spectra for inelastic systems.

REFERENCES

1. Bycroft, G. N., "White Noise Representation of Earthquakes," Journal of the Engineering Mechanics Division, ASCE, Vol. 86, No. EM2, April 1960, pp. 1-6.

2. Housner, G. W. and Jennings, P. C., "Generation of Artificial Earthquakes," Journal of the Engineering Mechanics Division, ASCE, Vol. 90, No. EM1, February 1964, pp. 114-150.

3. Amin, M., H. S. Ts'ao, and A. H.-S. Ang, "Significance of Non-stationarity of Earthquake Motions," Proceedings, Fourth World Conference on Earthquake Engineering, Santiago, Chile, 1969, A-1, pp. 97-114.

4. Jennings, P. C., Housner, G. W. and Tsai, N. C., "Simulated Earthquake Motions," Report No. EERL 68-10, Earthquake Engineering Research Laboratory, California Institute of Technology, Pasadena, California, April 1968.

5. Ruiz, Patricio and Penzien, Joseph, "Probabilistic Study of the Behavior of Structures During Earthquakes," EERC No. 69-3, Earthquake Engineering Research Center, University of California, Berkeley, California, March 1969.

6. Murakami, M. and Penzien, J., "Nonlinear Response Spectra for Probabilistic Seismic Design and Damage Assessment of Reinforced Concrete Structures," Report No. EERC 75-38, Earthquake Engineering Research Center, University of California, Berkeley, California, November 1975.

7. Kubo, T. and Penzien, J., "Time and Frequency Domain Analysis of Three Dimensional Ground Motions, San Fernando Earthquake," Report No. EERC 76-6, Earthquake Engineering Research Center, University of California, Berkeley, California, March 1976.

8. Rascon, O. A. and C. A. Cornell, "A Physically Based Model to Simulate Strong Earthquake Record on Firm Ground," Proceedings, Fourth World Conference on Earthquake Engineering, Santiago, Chile, 1969, A-1, pp. 84-96.

9. Kameda, H. and Ang, A. H.-S., "Simulation of Strong Earthquake Motions for Inelastic Structural Response," Proceedings, Sixth World Conference on Earthquake Engineering, Vol. 2, New Delhi, 1977, pp. 149-154.

10. "Uniform Building Code," International Conference of Buildings Officials, 1970.

11. Berg, G. V. and Housner, G. W., "Integrated Velocity and Displacement of Strong Earthquake Ground Motion," Bulletin of the Seismological Society of America, Vol. 51, No. 2, April 1961, pp. 175-189.

12. Hudson, D. E. and Brady, A. G., "Strong Motion Earthquake Accelerograms," EERL No. 71-50, Earthquake Engineering Research Laboratory, California Institute of Technology, Pasadena, California, September 1971.

13. Trifunac, M. D., "Low Frequency Digitization Errors and a New Method for Zero Base Line Correction of Strong-Motion Accelerograms," Report No. EERL 70-07, Earthquake Engineering Research Laboratory, California Institute of Technology, Pasadena, California, September 1970.

14. Nigam, N. C. and Jennings, P. C., "Digital Calculation of Response Spectra from Strong-Motion Earthquake Records," Earthquake Engineering Research Laboratory, California Institute of Technology, Pasadena, California, June 1968.

15. Veletsos, A. S., Newmark, N. M. and Chelapati, C. V., "Deformation Spectra for Elastic and Elastoplastic Systems Subjected to Ground Shock and Earthquake Motions," Proceedings, Third World Conference on Earthquake Engineering, Vol. 2, New Zealand, 1965, pp. 663-680.

TABLE 1: PROPERTIES OF RECORDED GROUND MOTIONS

EARTHQUAKE: LOCATION & DATE		ACCELEROGRAPH SITE	PARABOLIC BASE LINE CORRECTION					STANDARD BASE LINE CORRECTION				
			COMPONENT	GROUND MOTION MAXIMA Accel.	Vel. (cm/sec)	Displ. (cm)	SPECTRUM INTENSITY SI (m) 0.05	COMPONENT	GROUND MOTION MAXIMA Accel.	Vel. (cm/sec)	Displ. (cm)	SPECTRUM INTENSITY SI (m) 0.05
Imperial Valley	May 18, 1940	El Centro, Imperial Valley Irrigation District	S00E	0.32 g	38.59	28.70	1.39	S00E	0.35 g	33.46	12.46 (10.9)*	1.36
			S90W	0.23 g	36.19	50.70	1.02	S90W	0.21 g	36.93	20.06 (19.8)	1.14
Lower California	Dec. 30, 1934	El Centro, Imperial Valley	N90E	0.18 g	19.20	19.18	0.53	N90E	0.18 g	11.57	6.19 (3.7)	0.47
			N00E	0.26 g	31.29	29.23	0.79	N00E	0.16 g	20.84	5.47 (4.2)	0.55
Western Washington	Apr. 13, 1949	Olympia, Washington, Highway Test Lab	S10E	0.19 g	18.97	18.21	0.75	S04E	0.16 g	21.42	10.31 (8.5)	0.75
			S80W	0.32 g	22.47	40.00	0.89	S86W	0.28 g	17.10	9.32 (10.4)	0.80
Kern County	July 21, 1952	Taft, Lincoln School Tunnel	N21E	0.18 g	13.66	22.02	0.60	N21E	0.16 g	15.71	6.97 (5.5)	0.58
			S69E	0.16 g	19.64	24.43	0.66	S69E	0.18 g	17.71	6.58 (6.0)	0.65

*Periods > 15 sec. filtered out from the displacements; see Ref. (11)

TABLE 2: PROPERTIES OF SIMULATED GROUND MOTIONS

SIMULATION NO.	PARABOLIC BASE LINE CORRECTION				STANDARD BASE LINE CORRECTION			
	GROUND MOTION MAXIMA			SPECTRUM	GROUND MOTION MAXIMA			SPECTRUM
	ACCELERATION	VELOCITY (cm/sec)	DISPLACEMENT (cm)	INTENSITY SI (m) 0.05	ACCELERATION	VELOCITY (cm/sec)	DISPLACEMENT (cm)	INTENSITY SI (m) 0.05
1	0.28 g	56.13	62.86	1.40	0.28 g	52.26	22.54 (23.29)*	1.41
2	0.23 g	55.56	82.19	1.07	0.21 g	54.69	51.97 (46.61)	1.07
3	0.27 g	46.41	93.32	1.41	0.25 g	46.26	26.73 (29.34)	1.42
4	0.34 g	43.12	52.45	1.32	0.31 g	36.86	37.97 (31.83)	1.32
5	0.27 g	58.94	129.42	1.36	0.25 g	39.48	27.89 (28.59)	1.35
6	0.31 g	33.20	79.45	1.39	0.27 g	31.25	19.80 (17.01)	1.39
7	0.31 g	70.19	192.85	1.60	0.28 g	49.56	49.40 (50.38)	1.60
8	0.31 g	53.54	91.08	1.31	0.29 g	50.07	29.91 (31.50)	1.30
AVERAGE VALUES:	0.29 g	52.14	97.95	1.36	0.27 g	45.05	33.28 (32.32)	1.36

*Periods > 15 sec. filtered out from the displacements; see Ref. (11)

TABLE 3: PROPERTIES OF GROUND MOTIONS

ENSEMBLE AVERAGES				
ENSEMBLE AND TYPE OF BLC	GROUND MOTION MAXIMA			SPECTRUM INTENSITY $SI_{0.05}$ (m)
	ACCELERATION	VELOCITY (cm/sec)	DISPLACEMENT (cm)	
RECORDED MOTIONS				
•Parabolic BLC	0.39 g	41.1	48.5	1.36
•Standard BLC	0.38 g	37.8	16.5	1.36
SIMULATED MOTIONS				
•Parabolic BLC	0.29 g	52.1	98.0	1.36
•Standard BLC	0.27 g	45.1	33.3	1.36
RATIO OF ENSEMBLE AVERAGES FOR SIMULATED AND RECORDED MOTIONS				
•Parabolic BLC	0.74	1.27	2.02	1.00
•Standard BLC	0.71	1.19	2.02	1.00

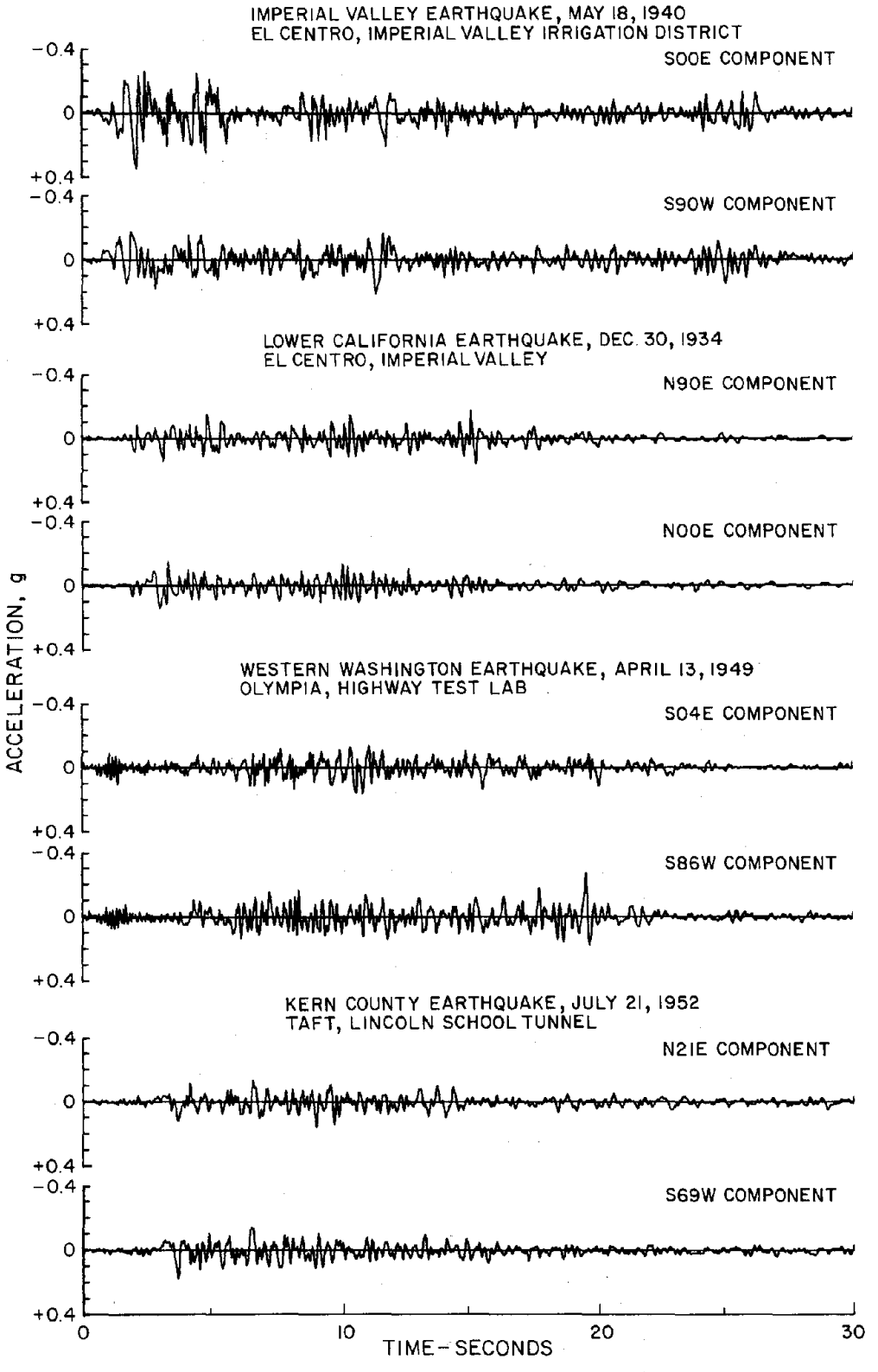

FIG. 1 RECORDED ACCELEROGRAMS WITH STANDARD BASE LINE CORRECTION.

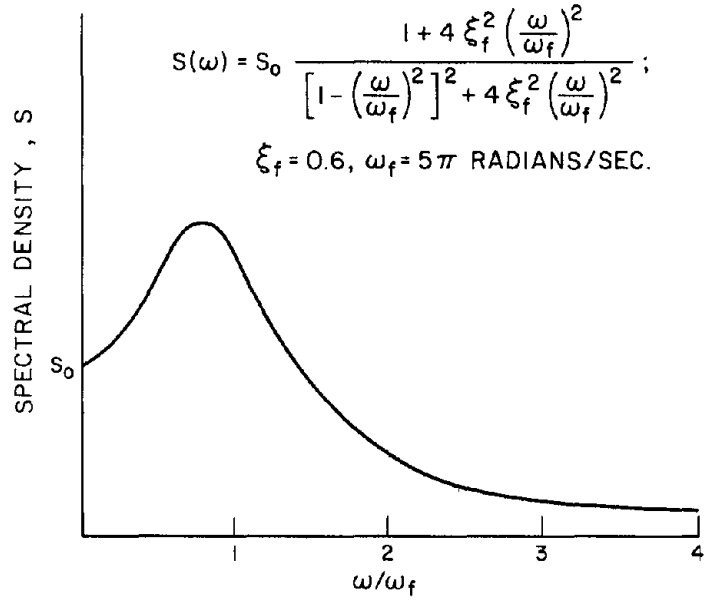

(a) SPECTRAL DENSITY OF FILTERED WHITE NOISE ACCELERATION

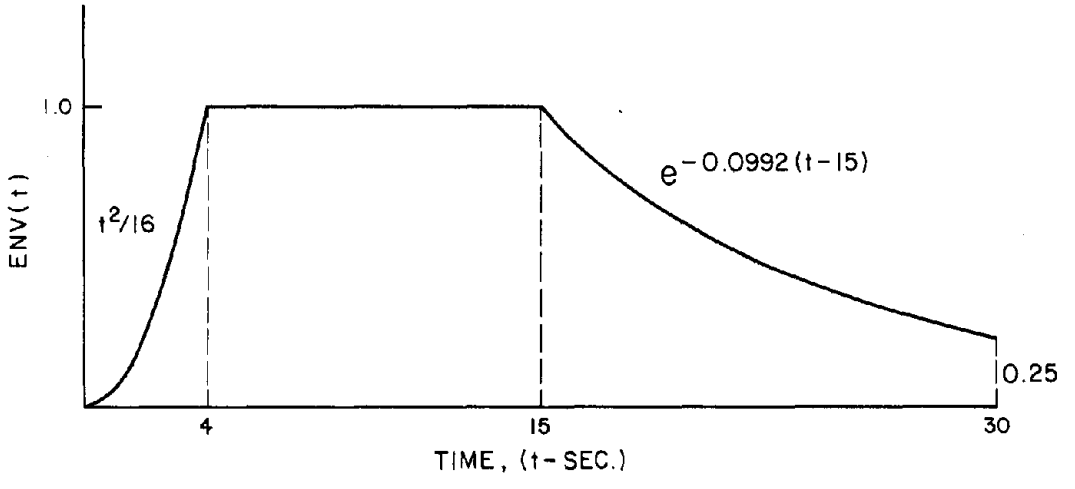

(b) INTENSITY - TIME FUNCTION

FIG. 2 SIMULATED GROUND MOTION: SPECTRAL DENSITY AND INTENSITY TIME-FUNCTION (4-6).

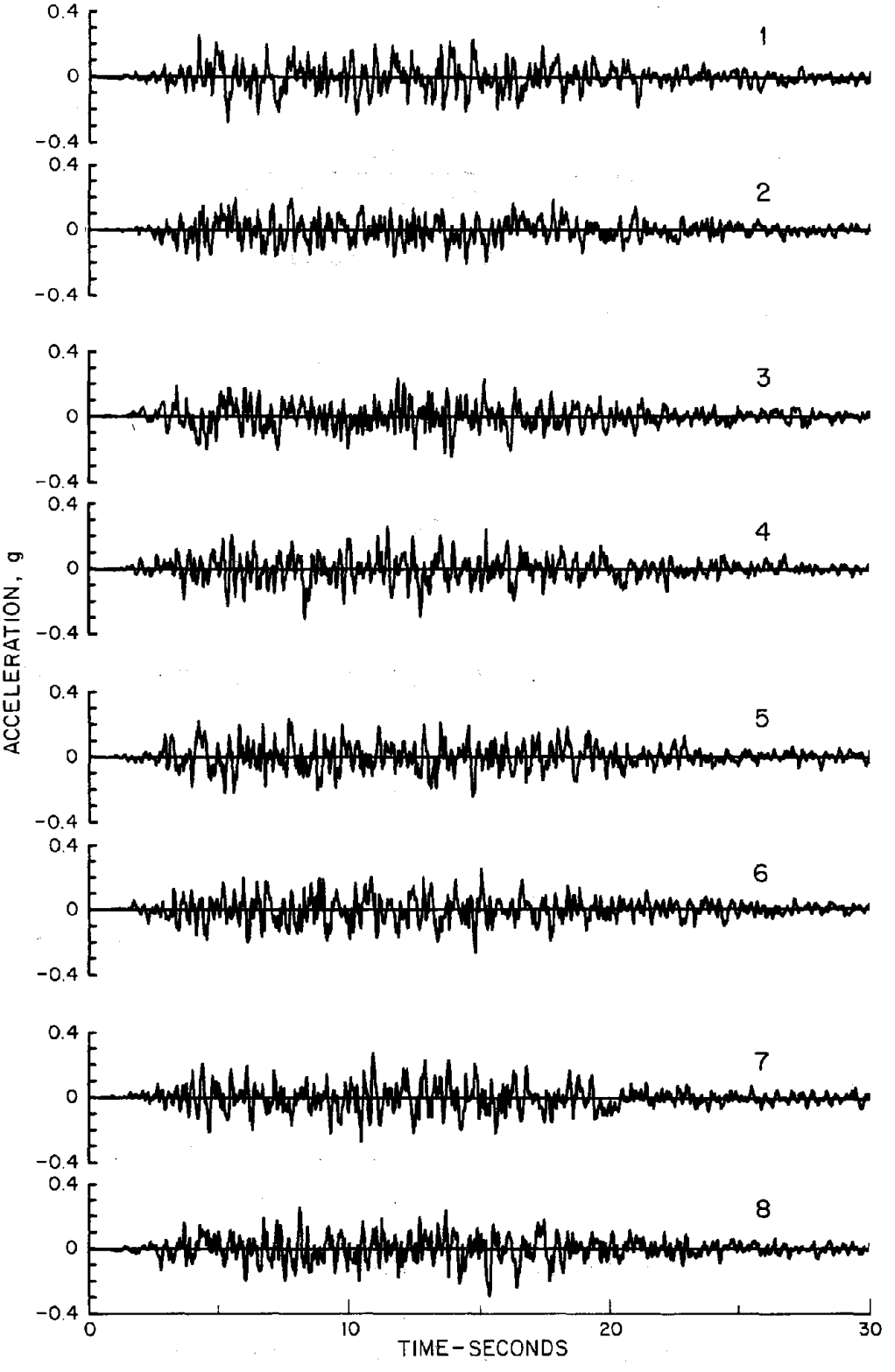

FIG. 3 SIMULATED ACCELEROGRAMS.

AVERAGE NUMBER OF PULSES PER ACCELEROGRAM

PULSE AREA, A (IN./SEC.)	RECORDED MOTIONS*	SIMULATED MOTIONS*
A > 10	11	8
5 ≤ A ≤ 10	29	27
A < 5	189	228

*STANDARD BASE LINE CORRECTION

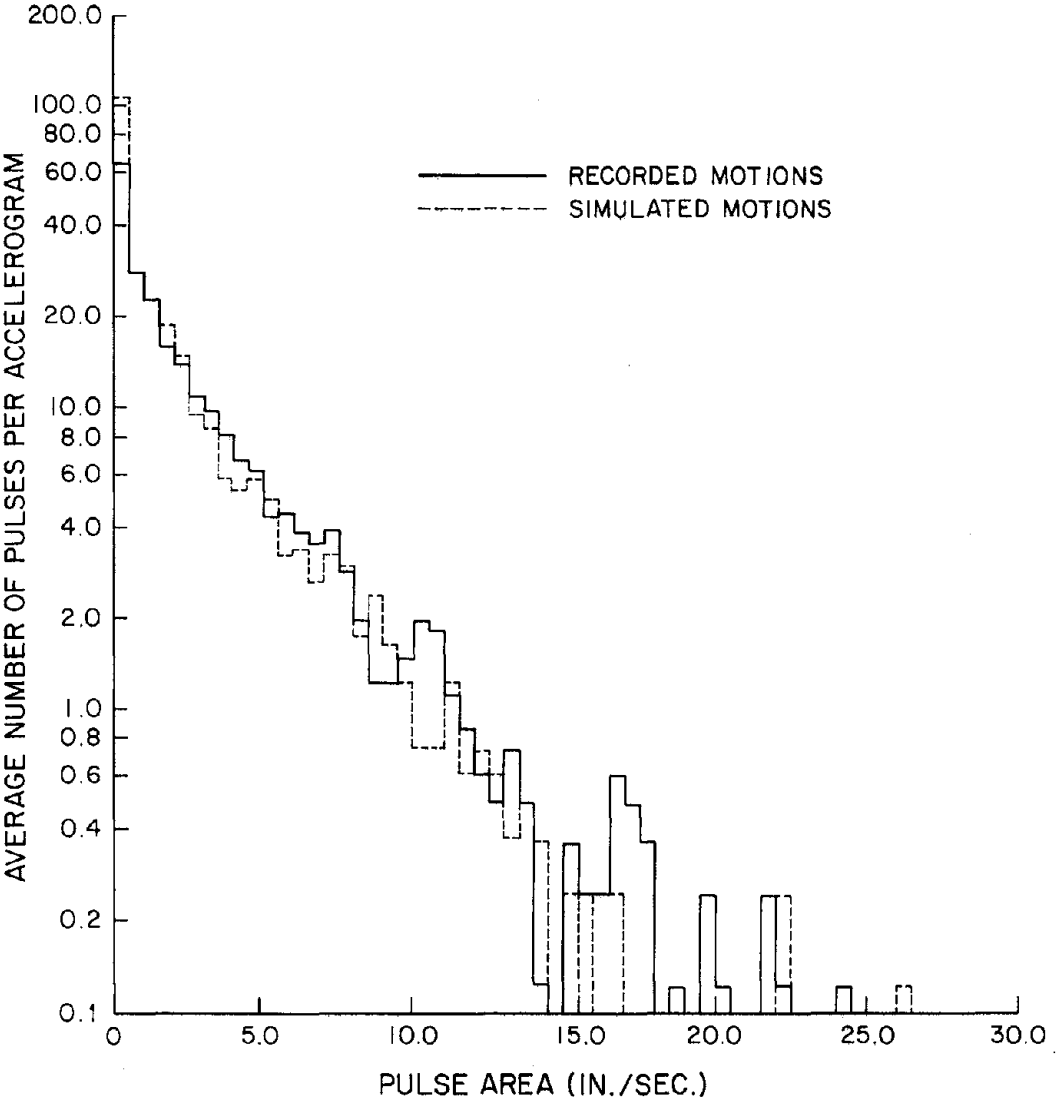

FIG. 4 HISTOGRAMS FOR AREAS OF ACCELERATION PULSES.

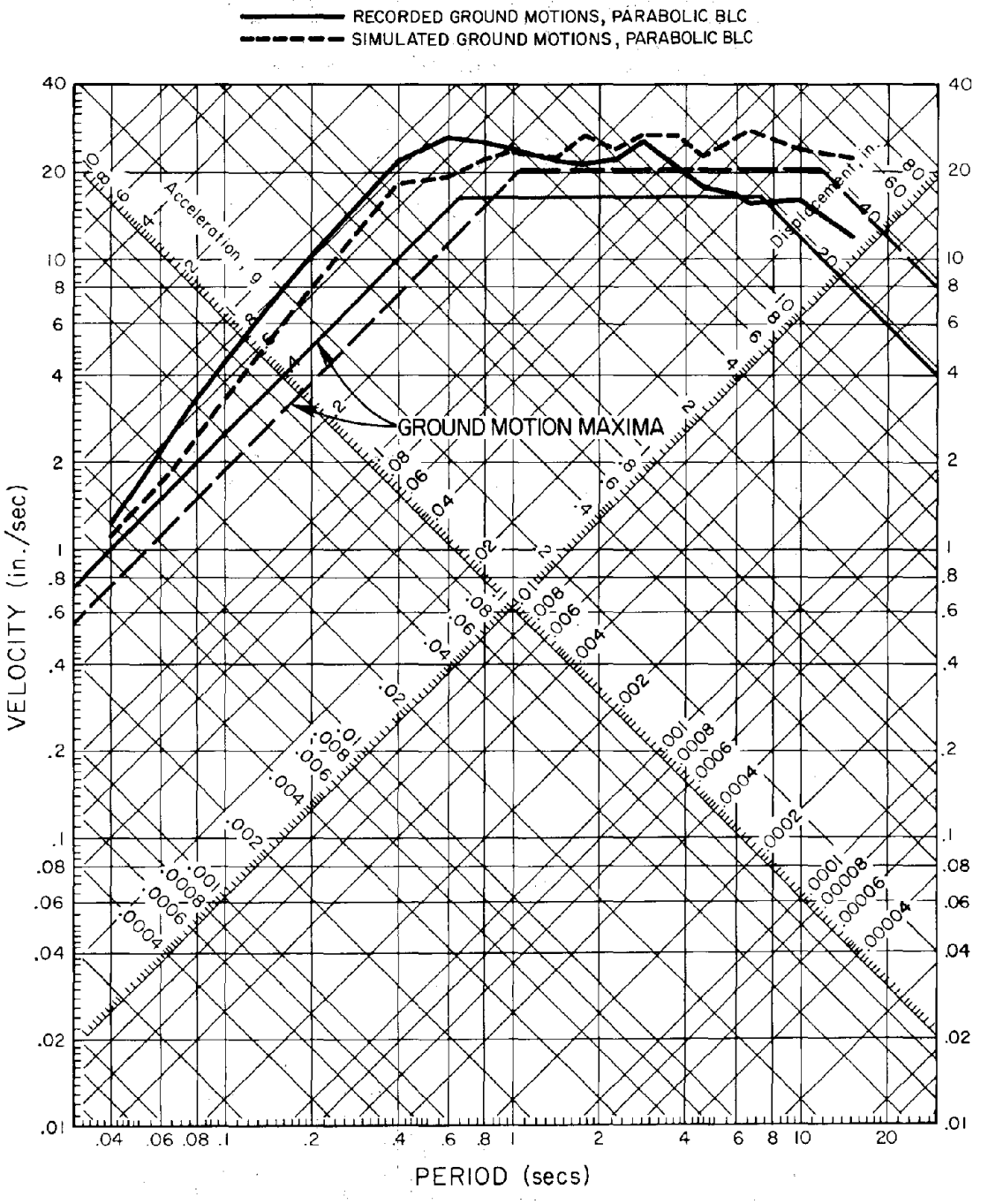

FIG. 5 AVERAGE RESPONSE SPECTRA FOR 5% DAMPING.

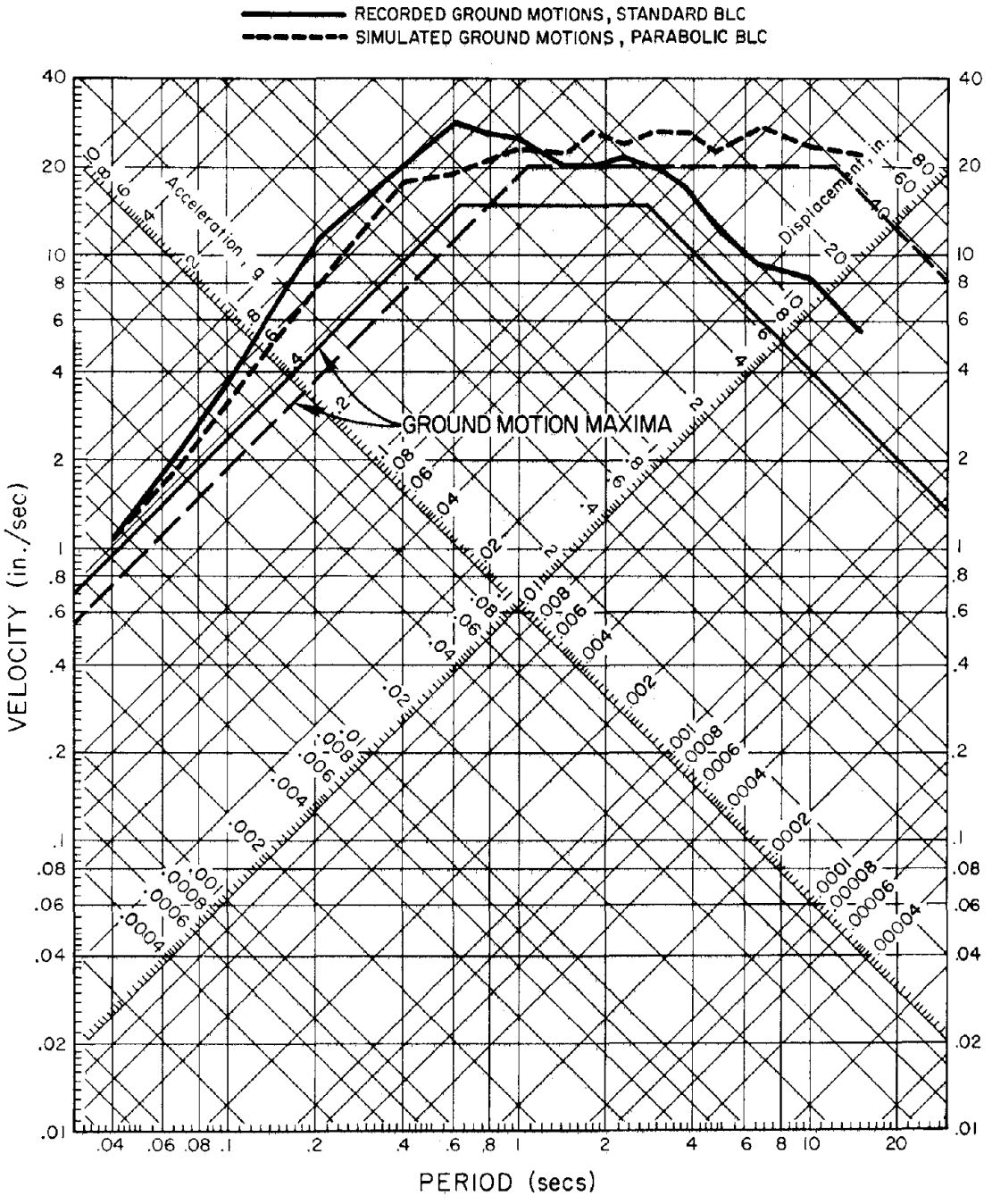

FIG. 6 AVERAGE RESPONSE SPECTRA FOR 5% DAMPING.

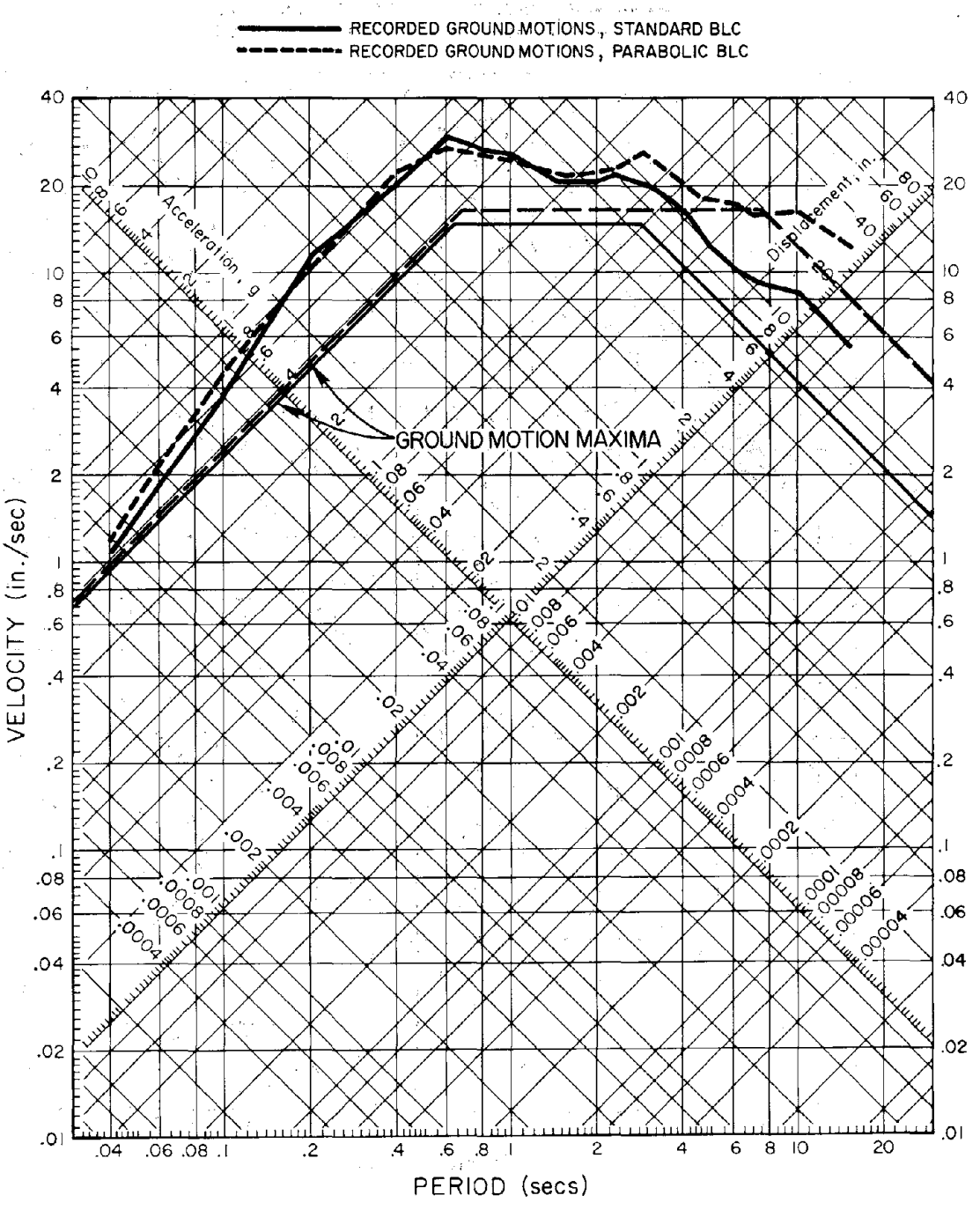

FIG. 7 AVERAGE RESPONSE SPECTRA FOR 5% DAMPING.

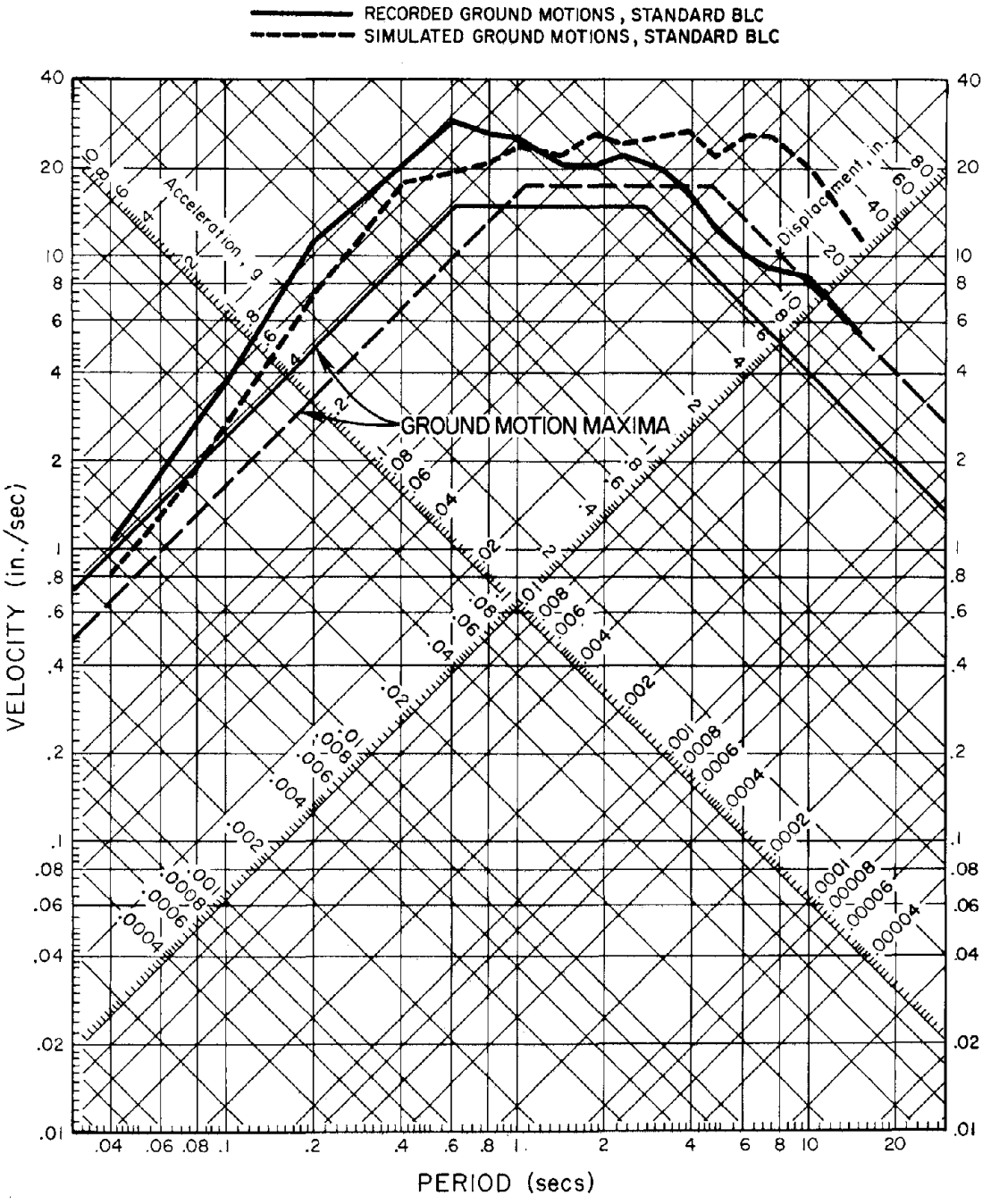

FIG. 8 AVERAGE RESPONSE SPECTRA FOR 5% DAMPING.

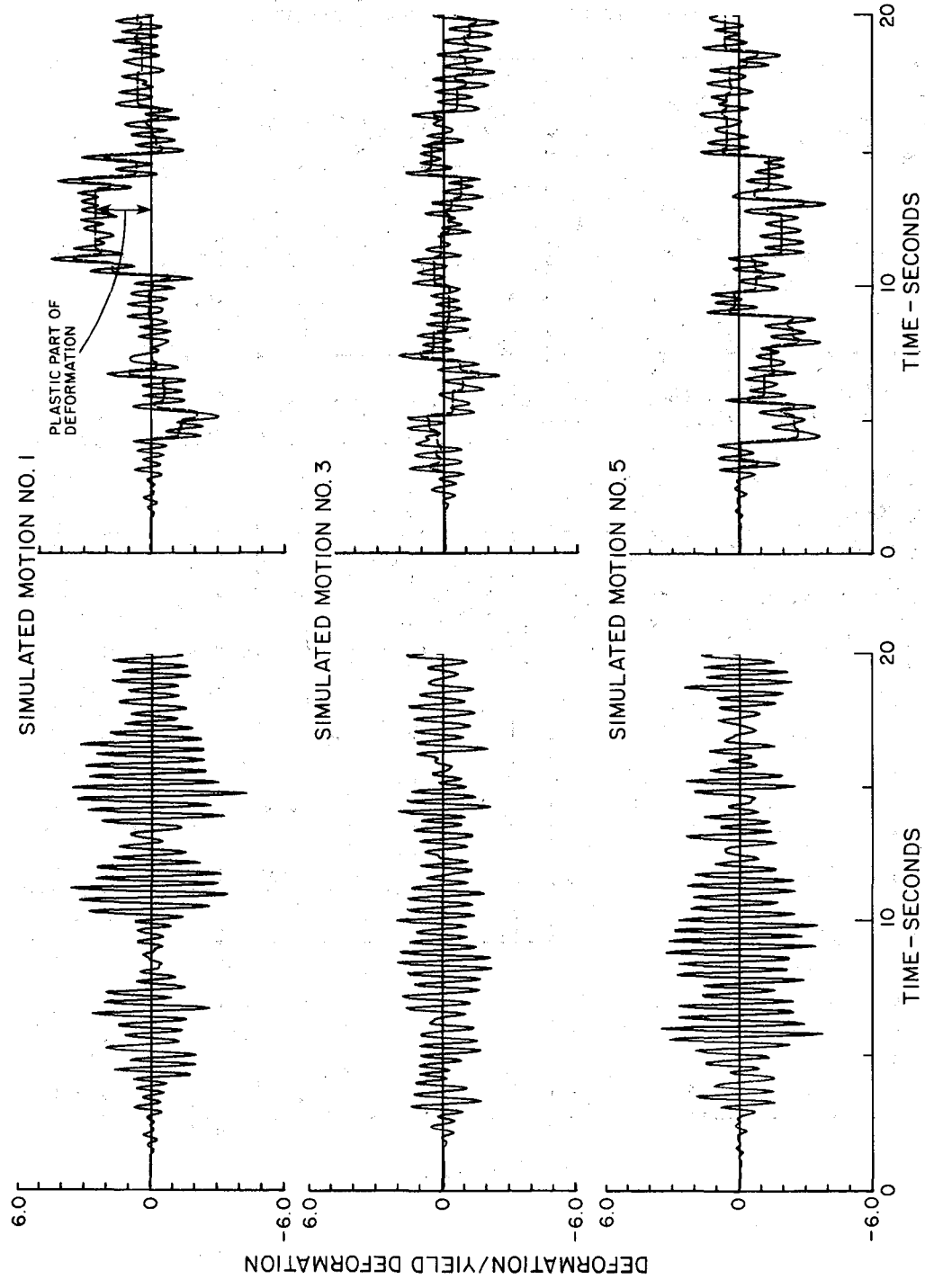

FIG. 9 RESPONSE OF ELASTIC AND ELASTIC-PERFECTLY PLASTIC HYSTERETIC SYSTEMS, BOTH WITH ELASTIC VIBRATION PERIOD = 0.4 SEC, TO SIMULATED GROUND MOTIONS, 1, 3 AND 5.

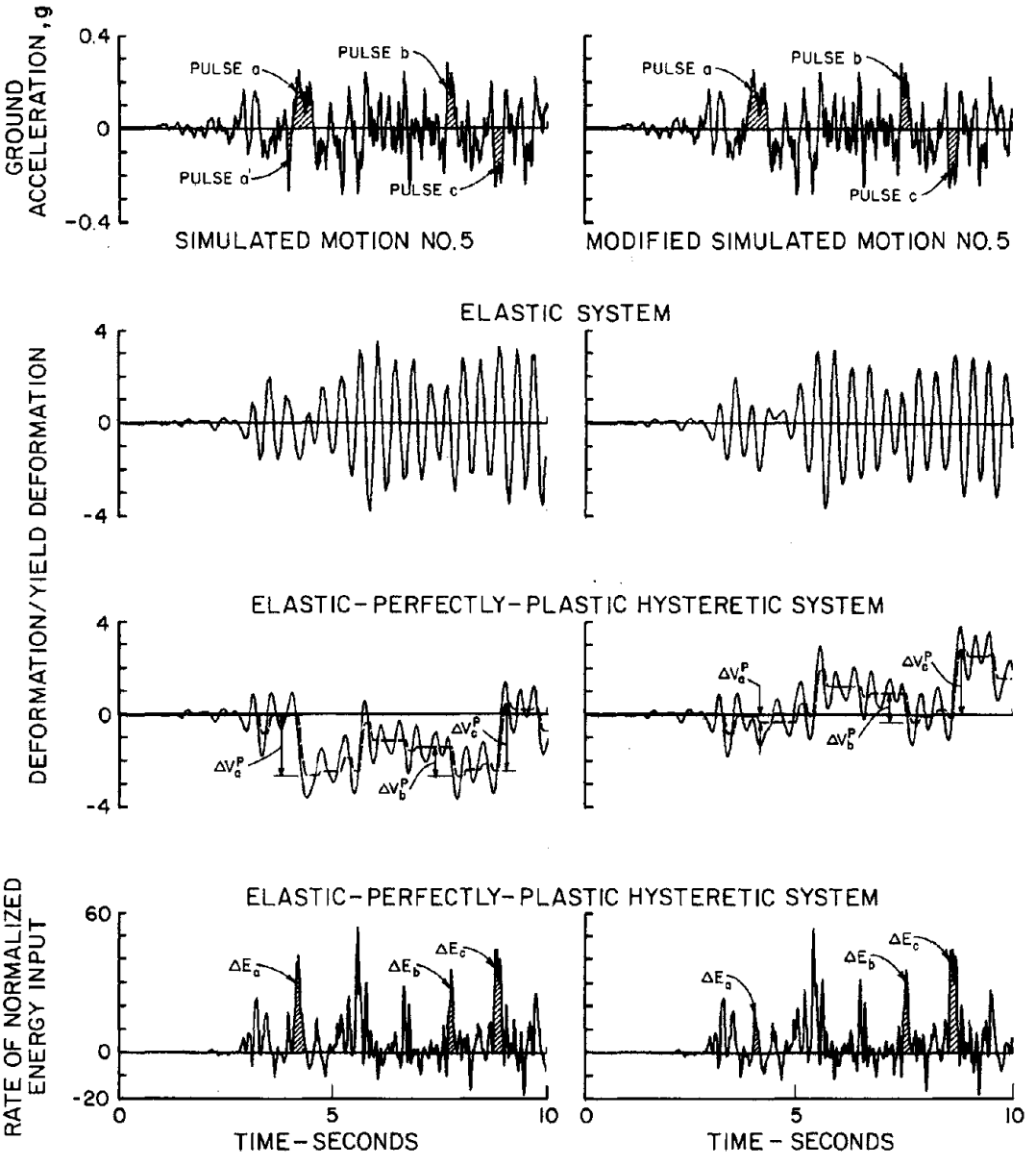

FIG. 10 RESPONSE OF ELASTIC AND ELASTIC-PERFECTLY PLASTIC HYSTERETIC SYSTEMS, BOTH WITH ELASTIC VIBRATION PERIOD = 0.4 SEC, TO ORIGINAL AND MODIFIED VERSIONS OF SIMULATED GROUND MOTION NO. 5

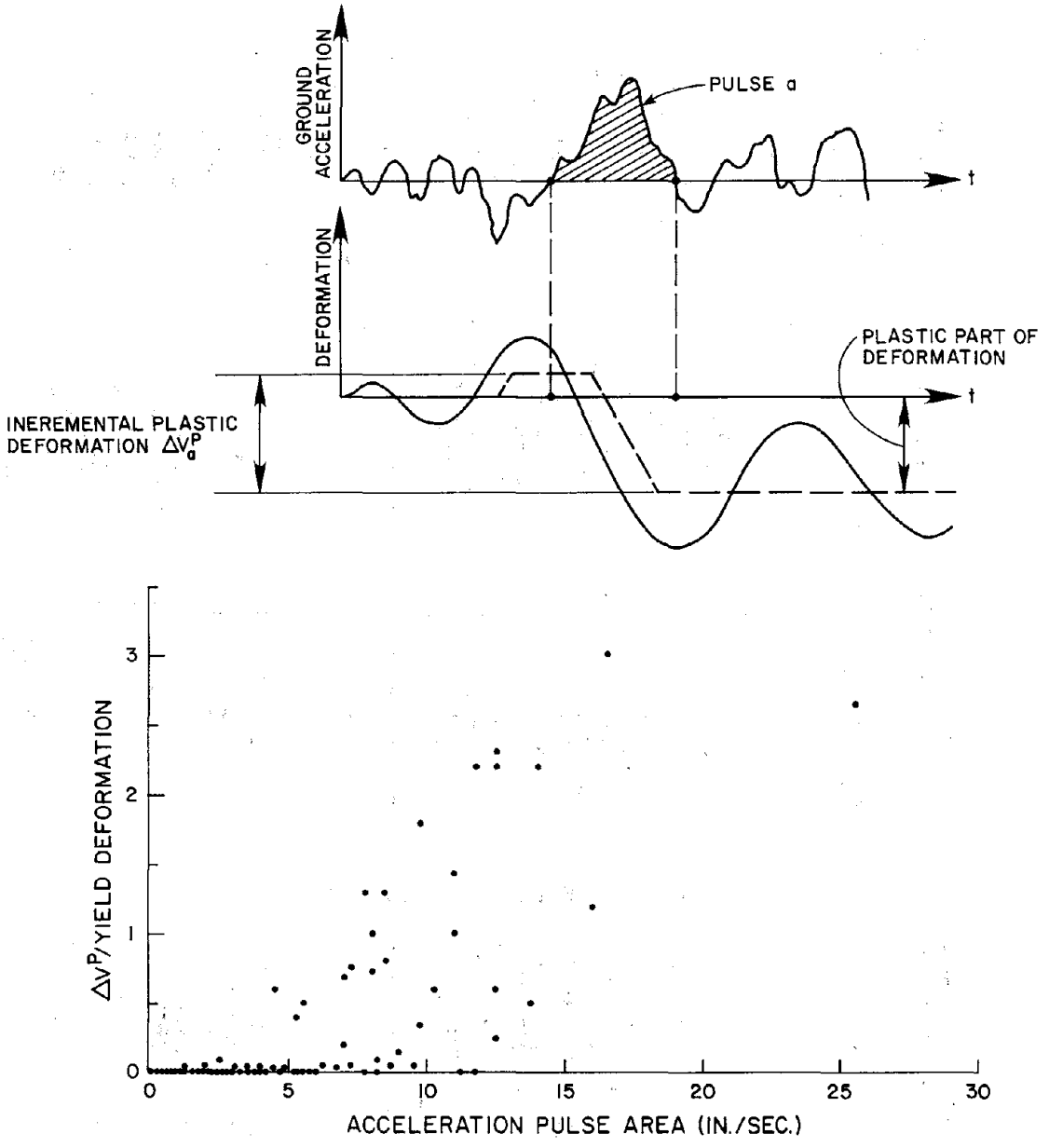

FIG. 11 RELATION BETWEEN ACCELERATION PULSE AREAS AND ASSOCIATED PLASTIC DEFORMATION.

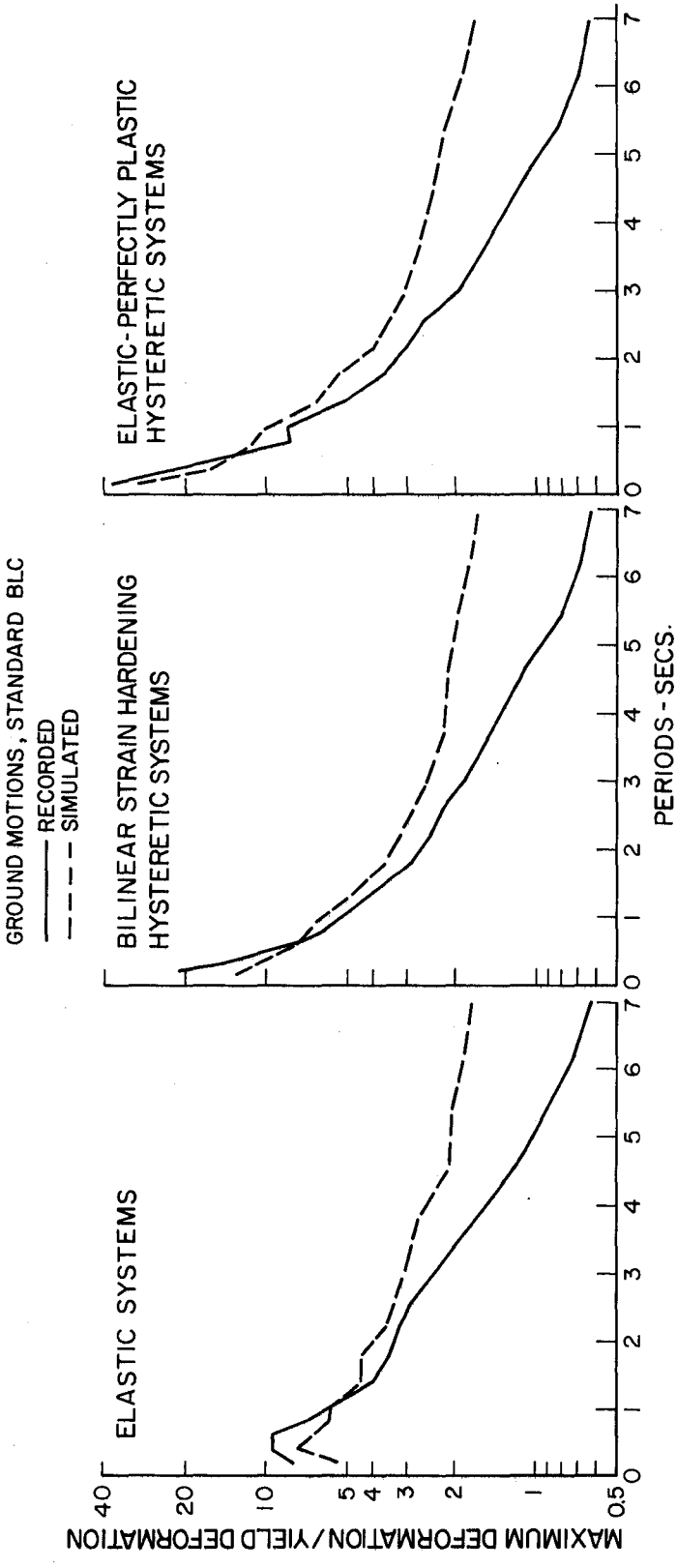

FIG. 12 AVERAGE DEFORMATION RESPONSE SPECTRA.

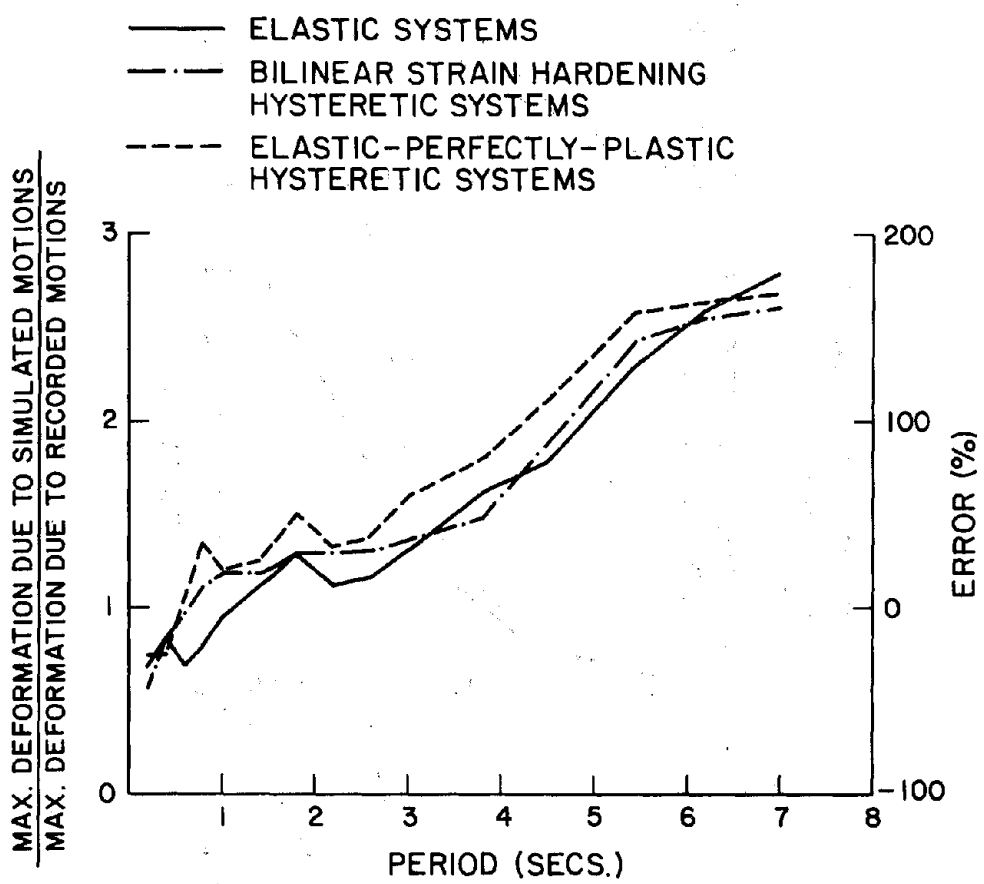

FIG. 13 RATIO OF AVERAGE DEFORMATION RESPONSE SPECTRA FOR SIMULATED AND RECORDED GROUND MOTIONS.

APPENDIX A: ENERGY INPUT BY GROUND MOTION

The equation of motion for a single-degree of freedom system is given by

$$m\ddot{v}(t) + 2\xi m\omega\dot{v}(t) + f(v,\dot{v}) = - m\ddot{v}_g(t) \tag{A.1}$$

where m is the mass of the system, ξ is the damping ratio, ω is the undamped natural frequency, v(t) is the displacement of the mass relative to the base, $f(v,\dot{v})$ is the restoring force, and $\ddot{v}_g(t)$ is the ground acceleration.

The energy input to the system by the ground motion (effective force = $- m\ddot{v}_g(t)$) when the mass moves from position 1 to position 2 is:

$$\Delta W = \int_1^2 [- m\ddot{v}_g(t)]\, \dot{v}(t)\, dt \tag{A.2}$$

Dividing by the elastic strain energy at yield point of the structural system, a dimensionless form of Eq. (A.2) is obtained;

$$\Delta E = \frac{\Delta W}{\frac{1}{2} F_y V_y} = \frac{- \int_1^2 2\ddot{v}_g(t)\dot{\mu}(t)\, dt}{C_y g} \tag{A.3}$$

where $\mu(t) = v(t)/V_y$, and V_y = the yield deformation; $C_y = F_y/mg$ where F_y = yield force for the system and mg is the weight of the system.

The rate of energy input to the structural system during the time increment Δt is:

$$\frac{\Delta E}{\Delta t} = \frac{- 2 \int_t^{t+\Delta t} \ddot{v}_g(t)\dot{\mu}(t)\, dt}{C_y g \Delta t} \tag{A.4}$$

PART TWO

Effects of Gravity Loads and Vertical Ground Motion on Earthquake Response of Buildings

INTRODUCTION

The response of yielding structures to earthquake ground motions has been the subject of numerous studies during the preceding two decades. Most of these studies have been concerned with structural response due to horizontal ground motion, one component at a time, under the assumption that lateral deformations are not large enough for the effects of gravity loads to be significant. A building designed for lateral forces specified in building codes is expected to yield during strong ground shaking, and thus admits the possibility of some plastic drift; if this drift becomes large enough, gravity will become the dominant force and the structure will collapse. Studies aimed at understanding the collapse of structures during strong ground motion have been reported (1), (2). Most buildings are, however, designed to satisfy drift limits, which are small enough so that collapse under gravity loads is not a problem; failure under cyclic lateral forces and deformations is, of course, possible. For such buildings, the effects of initial gravity forces in the structure, including the reduction in yield strength of columns, on the ductility demands imposed by strong ground motion have been studied (3).

Most of the numerous studies on response of yielding structures to earthquake ground motion, including those mentioned above, assume one-dimensional yielding behavior. However, interaction between lateral motion in two orthogonal directions under the action of two components of ground motions in those two directions has been studied earlier (4). Yielding under the combined action of gravity loads and lateral forces associated with horizontal ground motion will lead to

interaction between lateral and vertical motions. This study examines the influence of such interaction on the structural deformations that may be caused by strong ground shaking. Vertical forces in the structure, which are constant and only due to gravity loads when only the horizontal ground motion is considered, and the overturning effects are neglected, vary with time when the vertical component of ground motion is also included. Effects of these fluctuating vertical loads on the yielding behavior of the system and on lateral and vertical deformations are also studied.

SYSTEMS, GROUND MOTIONS AND METHOD OF ANALYSIS

Systems

The idealized system considered has its total weight W concentrated at the top deck and deforms as shown in Fig. 1, with two degrees of freedom: lateral deformation v_1 and vertical deformation v_2. The overturning forces associated with lateral response are not considered in the analysis. Furthermore, the secondary effects of gravity loads, the so called P-delta effects, are neglected.

The relation between total restoring forces and deformations--f_1 and v_1 in the lateral direction and f_2 and v_2 in the vertical direction--are shown in Fig. 1b. The yield values for the lateral and vertical forces f_{1y} and f_{2y} are considered to be equal in the two--positive and negative--directions of deformation. Unloading and reloading from regions of inelastic deformation are assumed to take place along lines parallel to the initial, elastic portion of the diagram. Under the combined action of lateral and vertical forces, the system is elastic within the yield surface, assumed to be circular in terms

of normalized forces, and plastic for forces outside the yield surface (Fig. 1c).

The elastic stiffness $k_{en} = (4\pi^2/T_n^2)(W/g)$, n = 1,2, where W = total weight of the structure, T_1 and T_2 = natural periods of linearly elastic vibration in lateral and vertical directions, respectively and g = acceleration of gravity. The yield strength in the lateral direction f_{ly} = 2KCW where K = a numerical coefficient in the Uniform Building Code (UBC) depending on the structural system, selected herein as 0.67, the value recommended for ductile moment resisting frames; $C = 0.05/T^{1/3}$ is the base shear coefficient in an earlier edition of the UBC (5). The lateral yield strength for the system has been taken as twice the UBC design value, to account for the difference between yield and design stresses as well as for the strengthening influence of non-structural components. Similarly the yield strength of the structure in the vertical direction is taken as twice the gravity load, to account for typical load factor values, e.g. 1.7 for steel buildings, and additional strength due to nonstructural components.

Energy dissipation in the structure due to effects other than inelastic action is represented by viscous damping, effective in both horizontal and vertical motions, with the damping ratio selected as 0.05 for both.

Ground Motions

The ground motions considered are (1) the first 15 seconds of the East and vertical components of the Esso Refinery record obtained during the Managua, Nicaragua earthquake of December 23, 1972, and (2) the first 30 seconds of the SOOE and vertical components of the

El Centro record obtained during the Imperial Valley earthquake of May 18, 1940. The time history of ground acceleration, maximum acceleration, root mean square value of acceleration, and bracketed duration--defined as the time span during which acceleration peaks exceed 0.1g--for each component of the two records are presented in Fig. 2.

Method of Analysis

The response of each system is determined by solving the equations of motion (Appendix A) by a numerical integration procedure (Appendix B). The time scale is discretized into equal time intervals, small enough (0.01 sec or less) to define the accelerogram accurately and no more than a small fraction (1/20th) of the natural period for linearly elastic vibration of the system. Within each small time interval, the horizontal and vertical accelerations of the mass of the system were assumed to vary linearly, and the restoring forces f_1 and f_2 were taken to be constant equal to their values at the beginning of the time interval. For the time intervals during which transition from elastic to inelastic state or vice versa occurred, an iterative process was employed to reduce force unbalance created by the numerical approximation to 1 percent of the effective earthquake load.

RESPONSE TO HORIZONTAL GROUND MOTION

In order to study the effects of gravity loads, the response of an idealized system to horizontal ground motion is analyzed for three different conditions: Effects of gravity loads are rigorously considered including their influence on the inelastic behavior through interaction with lateral forces; only a part of their effect, that of

reducing the lateral yield strength, is considered; and gravity loads are ignored. The structure chosen is the idealized system described in the preceeding section with specified stiffness, strength and damping properties and T_1 and T_2, the natural periods of vibration in lateral and vertical motions, equal to 0.5 and 0.1 sec, respectively. The excitation chosen is the East component of the Managua earthquake record (Fig. 2).

If the effects of gravity loads are rigorously considered, the two equations of motion, governing the lateral and vertical motions, are uncoupled only as long as the system is elastic but become coupled after the initiation of yielding (Appendix A). Coupling arises from the fact that the incremental plastic deformation vector is normal to the yield surface (Fig. 1c) resulting in lateral and vertical deformations. Numerical integration of the coupled equations, using the procedure outlined in the preceeding sections and described in Appendix B, led to the results presented in Fig. 3. Lateral deformations (Fig. 3a) are characterized by a few large increments in the plastic part of the deformation, each causing a shift in the equilibrium position about which the system subsequently oscillates until the next large increment in plastic part of the deformation occurs. Thus, the structure oscillates about several different equilibrium positions during the earthquake motion. The vertical deformation before the beginning of the ground motion (Fig. 3b) is simply the static deformation due to the gravity load (Fig. 3d). It remains unchanged as long as the system remains elastic but begins to accumulate in the downward direction (Figs. 3b and 3d) after the initiation of yielding. This happens when the lateral force reaches 0.87 f_{1y}, the lateral yield

strength reduced due to the effects of vertical load (Figs.3c and 3e). The plastic deformation is always in the downward direction because of the presence of the constant downward load (Figs. 3d and 3e).

Accumulation of plastic deformation in the vertical direction, similar to the predictions of the analyses described above, was observed in experimental tests on steel columns subjected to constant axial force and slowly varying, cyclic horizontal force (6). Fig. 4a shows the experimental set up schematically, and the measured relation between bending moment and axial deformation in the column. For convenient comparison, a portion of the analytical results of Fig. 3 is presented in a different manner: the relation between f_1, the lateral force in the system, and v_2, the vertical deformation (Fig. 4b). The force and deformation quantities in the analytical and experimental results (Figs. 4a and 4b) are not exactly the same, but qualitatively, both results indicate the same phenomenon: plastic deformation accumulates in the vertical direction when the system, under constant vertical load, is subjected to cyclic lateral load, large enough to cause yielding. The only difference in the experimental and analytical results is in the yield force levels; in the experimental test the yield moment increased with increasing strain due to the strain hardening property of steel, but the lateral yield force in the analysis remained constant because perfectly plastic behavior without strain hardening was assumed.

The time variation of the energy dissipated in plastic action $\bar{E}_p$--$\bar{E}_{p1}$ and $\bar{E}_{p2}$ are associated with plastic deformations in horizontal and vertical directions, respectively--; energy dissipated in viscous damping $\bar{E}_D$, the sum of elastic strain energy $\bar{E}_s$ and kinetic energy $\bar{E}_k$,

all normalized with respect to the elastic strain energy associated with horizontal deformation at the yield point--see Appendix C for definitions--, is presented in figure 3f. Energy dissipated in plastic action is much larger than the contribution due to viscous damping. Furthermore, a significant part of the energy dissipated in plastic action is associated with plastic deformations in the vertical direction.

Ignoring coupling between lateral and vertical motions created by yielding of the system, response of the system described earlier to the same excitation is determined by numerical integration of the single equation governing lateral motion (Appendix A); results are presented in Fig. 5. This is equivalent to analysis of lateral response of the system with lateral strength = 0.87 f_{ly} (Fig. 5c and 5e), reduced to account for the vertical load; no other effect of the vertical load is considered. Because coupling between lateral and vertical motions in inelastic response is ignored, there is no plastic deformation in the vertical direction, and the vertical deformation remains constant at its initial static value associated with gravity loads (Figs. 5b and 5d); there is no energy dissipated in plastic deformation in the vertical direction (Fig. 5f); however, lateral deformation response is essentially unaffected (Figs. 3a and 5a). It appears therefore that the simpler analysis, where the gravity load effect is limited to reduction of the lateral yield strength, may be adequate for predicting the lateral response of the system to horizontal ground motion. However, coupling between lateral and vertical motions created by yielding of the system, must be considered in order to predict the vertical deformations.

Completely ignoring gravity loads--which reduces the problem to

the standard case of an inelastic SDOF analysis, the response of the system described earlier to the same excitation is determined by numerical integration of the single equation governing lateral motion (Appendix A); the results are presented in Fig. 6. These results are compared with those in Fig. 3 to evaluate effects of gravity loads on dynamic response. The gravity load reduces the lateral yield strength from f_{ly} to 0.87 f_{ly} (Figs. 3c and 6b), leading to slight increase in lateral deformation and elastic strain energy of the system. In conjunction with lateral forces, the gravity load causes plastic deformation in the vertical direction and significant increase in the plastic energy dissipated (Figs. 3b, 3f, and 6c); however, the lateral deformation response is essentially unaffected. It appears therefore that the standard analysis, where gravity loads are ignored, may be adequate for approximate predictions of the lateral response of the system to horizontal ground motion. However, vertical deformations can be predicted only by considering effects of gravity loads, and, as seen earlier, these must be treated rigorously and coupling between lateral and vertical motions should be included.

RESPONSE TO VERTICAL GROUND MOTION

In order to study how vertical ground motion affects response of structures, the previous analysis of response to horizontal ground motion in which effects of gravity loads were rigorously considered, is repeated with the vertical component of the Managua earthquake record also included as the excitation. Analysis of coupled lateral-vertical motions by numerical integration of the two equations of motion (Appendix A) leads to the results presented in Fig. 7.

Vertical ground motion affects the response of the system as follows: vertical axial force no longer remains constant at the gravity load, fluctuations can be observed around that value (Fig. 7d and e); because of the variation in the vertical force, yielding occurs not always when the lateral force reaches 0.87 f_{ly}--the initial (with gravity loads) value of the lateral yield strength--but at fluctuating values of the lateral force (Fig. 7c), governed by the yield surface (Fig. 7e); elastic oscillations--there is no additional yielding because the strength in vertical direction is rather large--are superimposed over the gradually growing vertical deformation that resulted from horizontal ground motion alone (Figs. 3b and 7b); and because of the velocities associated with elastic oscillations in the vertical direction, additional energy is dissipated through viscous damping (Figs. 3f and 7f). However, vertical ground motion has negligible effect on lateral deformations (Figs. 3a and 7a). Furthermore, because the plastic parts of lateral and vertical deformations are essentially unaffected (Figs. 3a and 7a, 3b and 7b), there is little change in the energy dissipated through yielding (Figs. 3f and 7f).

Whereas, as seen above, vertical ground motion has little influence on lateral deformations of the system, horizontal ground motion affects vertical deformations in an important way. This is evident by comparing vertical deformations due to simultaneous action of horizontal and vertical ground motions with those due to horizontal ground motion alone and vertical ground motion alone. The latter was determined from a separate analysis of a single equation governing the vertical motion, with no horizontal deformation (Fig. 7b). Whereas, the elastic oscillations of vertical deformation are entirely due to

the vertical ground motion, the gradual accumulation of plastic deformations in the downward direction and the resulting shift in the position around which oscillations occur, are due to the lateral forces due to horizontal ground motion, large enough to cause yielding (Figs. 3b and 7b). Thus, there would be little meaning in analysis of vertical deformations due to vertical ground motion alone. On the other hand, the residual vertical deformation at the end of the earthquake is primarily due to the effects of yielding due to horizontal ground motion.

RESPONSE OF SEVERAL SYSTEMS

In the preceding section, dynamic response of the idealized system described earlier with specified properties to a selected ground motion was presented and the response behavior was examined in some detail. In this section, results are presented for response of the same idealized system but with several different period values--T_1 and T_2= 0.25 and 0.13, 0.5 and 0.18, 0.75 and 0.22, 1.0 and 0.25, 1.5 and 0.3, 2.0 and 0.33, 2.5 and 0.37, all in seconds--with the Managua and El Centro ground motion records as excitation. The values selected for natural periods of vertical vibration, relative to those for lateral vibration, were based on Ref. (7). For each system and excitation, response to horizontal ground motion is analyzed for the following two conditions: gravity loads are ignored, and effects of gravity loads are rigorously considered as described in the preceding section; also analyzed is the response to simultaneous action of horizontal and vertical ground motion, with the effects of gravity loads rigorously considered; and the response to vertical ground motion alone including

gravity loads. For each case, a complete set of results, including variation of responses with time, were obtained by numerical integration of the equations of motion. However, only selected response results--maximum lateral deformation, maximum vertical deformation, permanent vertical deformations, and total energy dissipated in plastic deformation--are presented in Figs. 8 and 9.

Gravity loads and vertical ground motion affect the maximum lateral deformation of the system, but with no consistent trend: For a particular ground motion, the lateral deformation may increase or decrease depending on the vibration period of the system; and the deformation of a particular system may increase for some ground motions, but decrease for others (Fig. 8a, 9a). Effects of vertical ground motion on lateral deformation and energy dissipated in plastic action of the system are generally small. Those due to gravity loads are relatively significant, with as much as 30% change in deformation for a system with $T_1 = 1$ and $T_2 = 0.25$ sec. and El Centro ground motion as the excitation (Figs. 8a and 9a), and considerable increase in the energy dissipated in inelastic action (Fig. 8b and 9b).

Values of maximum and permanent deformation in the vertical direction for each system and the two ground motions are presented in Figs. 8 and 9. The permanent deformation remaining after the earthquake consists of two parts: elastic deformation due to gravity loads and plastic deformation associated with yielding of the system. The similarity between maximum and permanent deformations, evident by comparing Figs. 8c and 8d, 9c and 9d, is because of the fact that plastic part of the deformation is always accumulating in the downward direction and the difference between maximum and permanent values is

only due to elastic oscillations caused by vertical ground motion (Figs. 3b and 7b).

Vertical deformations--maximum as well as permanent values--are influenced by horizontal ground motion in an important way (Figs. 8c, 8d, 9c and 9d). Because the plastic part of vertical deformations arises from yielding of the system under large lateral forces, the vertical deformations are closely related to the number of yielding excursions and the extent of yielding during each excursion. Thus, the vertical deformations are dependent on the vibration period T_1 in the same way--generally decreasing with increasing period--as ductility demands for code designed systems. Furthermore, the increase in energy dissipated due to inelastic deformation in the vertical direction is an essentially fixed fraction of the energy dissipated in lateral deformations, independent of the vibration period. Another consequence of the fact that the plastic part of vertical deformations is due to yielding under large lateral loads, is apparent from Figs. 8 and 9: vertical deformations and the associated additional energy dissipated are similar for the two ground motion records because their horizontal components are of similar intensity (Fig. 2), and there is essentially no influence of the large differences in the intensity of the two vertical ground motions (Fig. 2). Although the horizontal components of Managua and El Centro ground motions are of similar intensity, the duration of strong shaking is longer for the latter (Fig. 2), which results in a large number of yielding excursions resulting in larger permanent vertical deformations (Figs. 8d and 9d). Accumulation of these deformations with time is apparent in Fig. 9d.

CONCLUSIONS

1. The dynamic response of yielding systems to horizontal ground motion includes lateral deformation of course--this is the response quantity that has been the subject of numerous studies--and vertical deformation, which is perhaps not an obvious effect. The vertical deformation remains constant at the static value due to gravity loads as long as the system is elastic but gradually accumulates in the downward direction with each excursion into the yield range. The plastic part of the vertical deformation is a consequence of the fact that the incremental plastic deformation vector is normal to the yield surface and has components in lateral and vertical directions.

2. The principal effect of the vertical component of ground motion is to superpose elastic vertical oscillations about the gradually growing vertical deformation that resulted from horizontal ground motion alone.

3. Permanent vertical deformations remaining after the earthquake, arise from yielding of the system under large lateral forces, which are primarily due to horizontal ground motion. These deformations are therefore controlled by horizontal ground motion and it is closely related to the number of excursions into the yield range and the extent of yielding during each excursion. Thus, permanent vertical deformations generally decrease with increasing period, similar to lateral deformation ductility demands for code designed buildings; furthermore they increase with duration of strong shaking.

4. The coupling between lateral and vertical deformations created by yielding of the system must be considered in order to predict the

plastic part of vertical deformations due to horizontal ground motion. However, simpler analyses without such deformation coupling, but with reduction of lateral yield strength due to gravity load, would generally be satisfactory for predicting the lateral response of the system. If the gravity loads are completely ignored, i.e. the full yield strength is used in the analysis, the simpler analysis will not lead to as good results but they may still give adequate estimates.

5. For the earthquakes considered, lateral deformations are not influenced significantly by vertical ground motion; hence they may usually be determined from analysis of response to horizontal ground motion only, unless the vertical ground motion is exceptionally intense.

6. The results presented should not be significantly influenced by the secondary effects of gravity loads, the so called P-delta effects or geometric stiffness effects, which were not included in this study. For short period buildings, the effects of interaction between lateral and vertical motions are significant but the secondary effects of gravity loads will be insignificant because the lateral deformations are small. For long period buildings, the relatively small effects of interaction between lateral and vertical motions would increase somewhat because more yielding would be expected due to secondary effects of gravity loads.

REFERENCES

1. Jennings, P. C. and Husid, R., "Collapse of Yielding Structures during Earthquakes," Journal of the Engineering Mechanics Division, ASCE, Vol. 94, EM5, October 1968, pp. 1045-1065.

2. Sun, C.-K., Berg, G. V., and Hanson, R. D., "Gravity Effect on Single-Degree Inelastic System," Journal of the Engineering Mechanics Division, ASCE, Vol. 99, EM1, February 1973, pp. 183-200.

3. Anderson, J. C. and Bertero, V. V., "Effects of Gravity Loads and Vertical Ground Acceleration on the Seismic Response of Multistory Frames," Report No. EERC 73-23, University of California, Berkeley, September 1973.

4. Nigam, N. C., "Inelastic Interaction in the Dynamic Response of Structures," Ph.D. Thesis, California Institute of Technology, Pasadena, June 1967.

5. Uniform Building Code. International Conference of Building Officials, 1970.

6. Popov, E. P., Bertero, V. V., And Chandramouli, S., "Hysteretic Behavior of Steel Columns," Report No. EERC 75-11, University of California, Berkeley, September, 1975.

7. Kost, G., "Response of Structures to Vertical Accelerations," SEAONC Seismology Committee, November 1969.

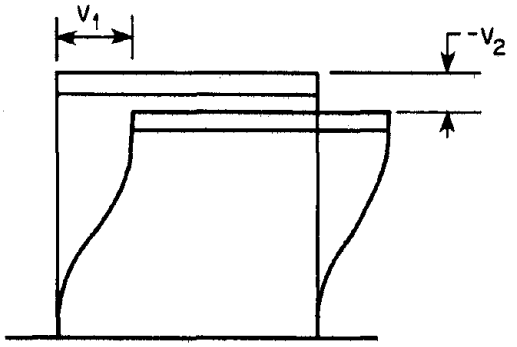

(a) DEFORMATION OF IDEALIZED SYSTEM

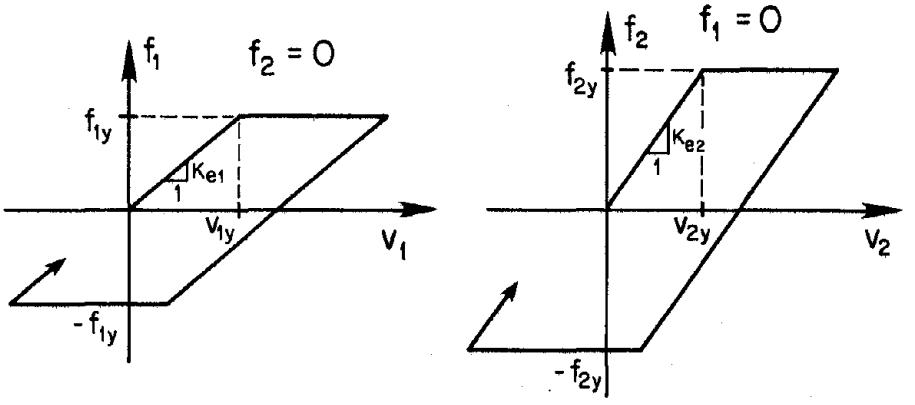

(b) FORCE-DEFORMATION BEHAVIOR

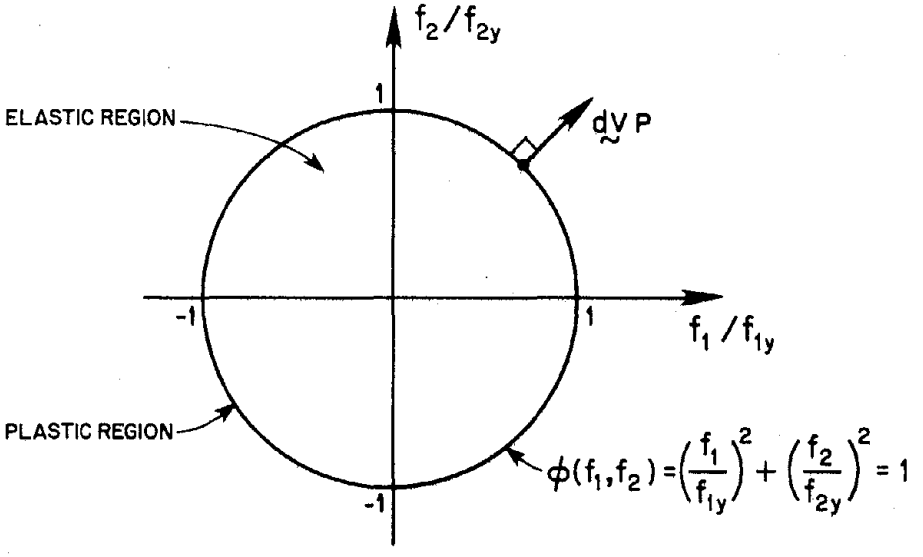

(c) YIELD SURFACE

FIG. 1 PROPERTIES OF IDEALIZED SYSTEM.

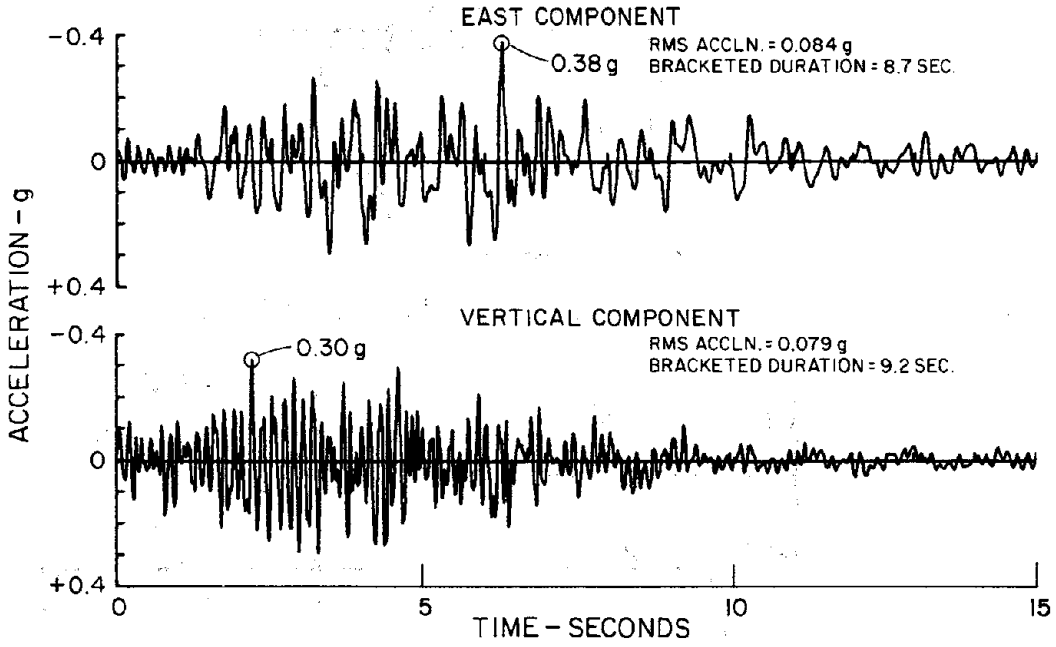

(a) MANAGUA NICARAGUA EARTHQUAKE, DEC. 23, 1972
ESSO REFINERY

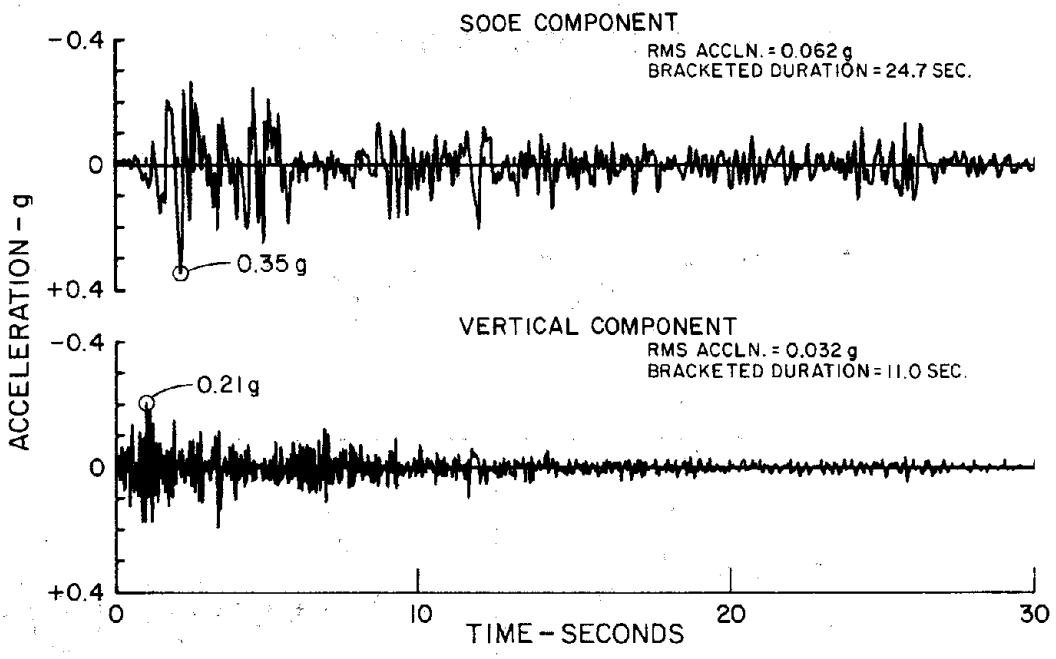

(b) IMPERIAL VALLEY EARTHQUAKE, MAY 18, 1940
EL CENTRO, IMPERIAL VALLEY IRRIGATION DISTRICT

FIG. 2 GROUND ACCELERATION RECORDS.

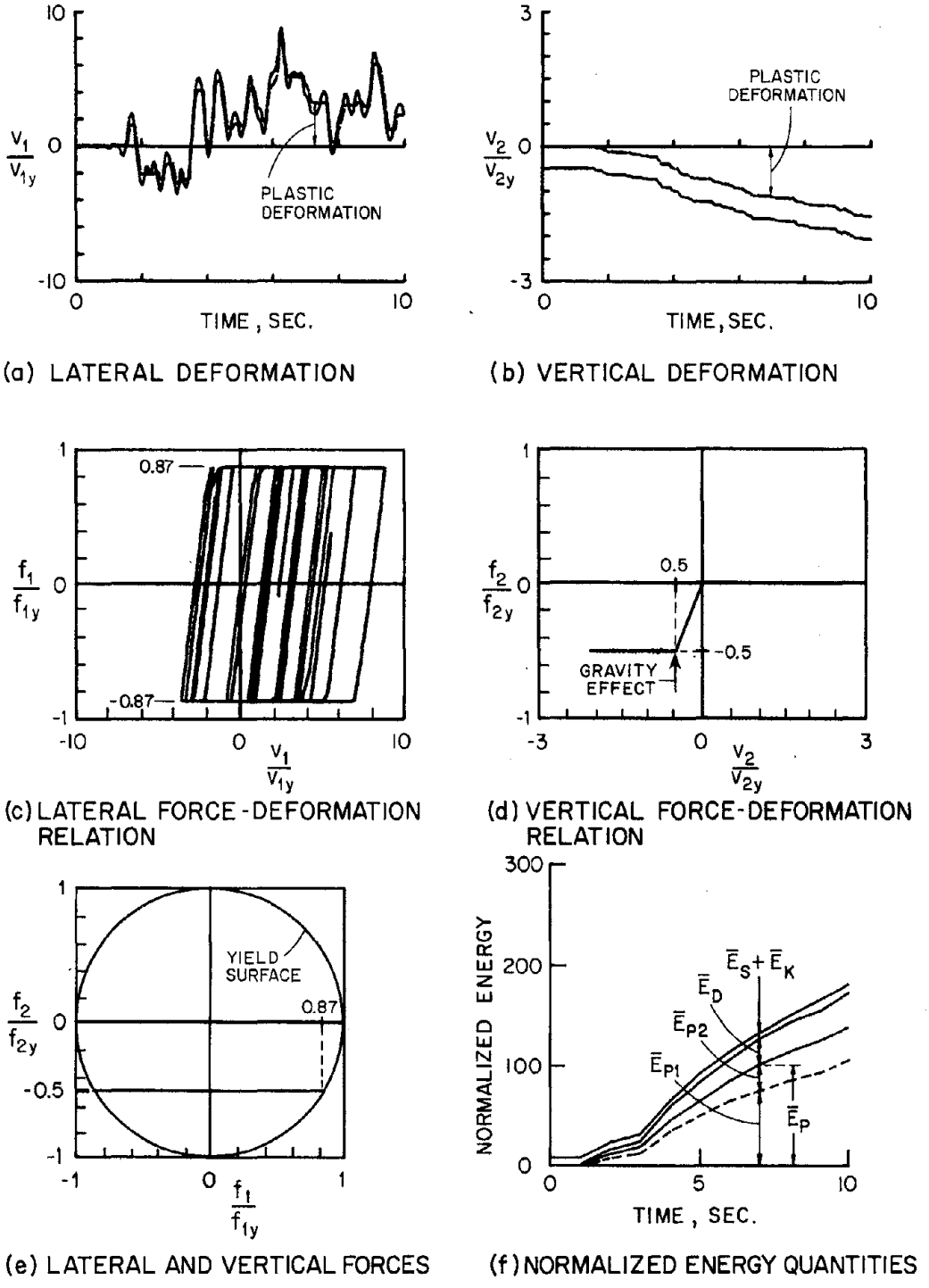

FIG. 3 COUPLED LATERAL-VERTICAL RESPONSE TO HORIZONTAL GROUND MOTION INCLUDING GRAVITY LOADS.

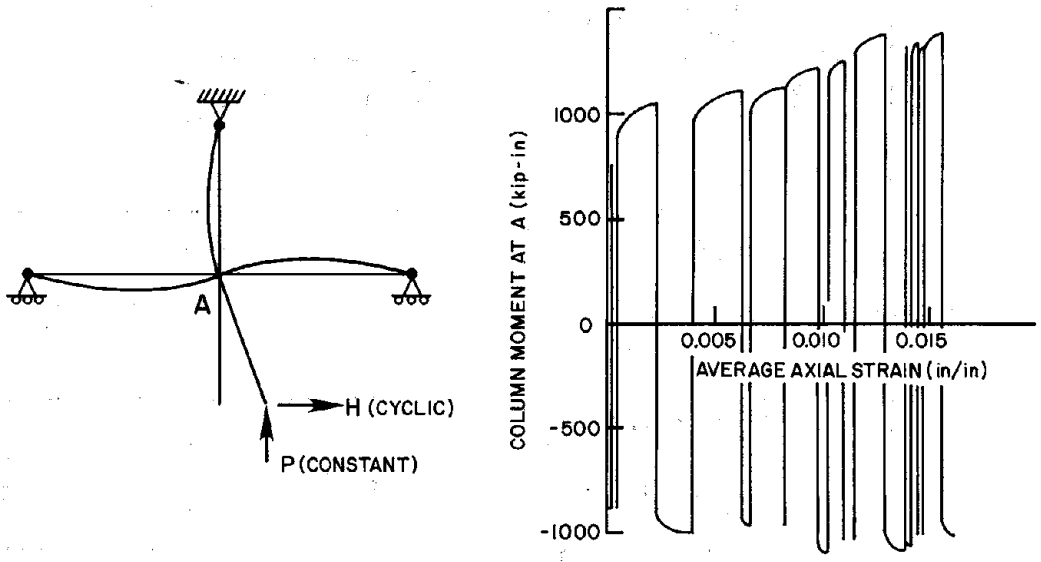

(a) EXPERIMENTALLY OBSERVED ACCUMULATION OF PLASTIC DEFORMATION IN THE VERTICAL DIRECTION (REF. 6)

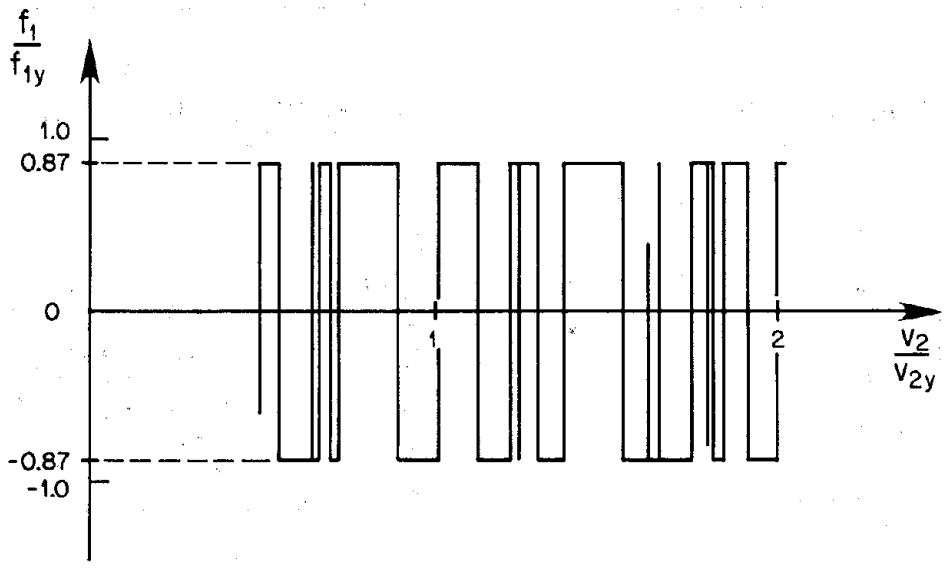

(b) ANALYTICALLY PREDICTED RELATION BETWEEN LATERAL FORCE AND VERTICAL DEFORMATION

FIG. 4 ACCUMULATION OF PLASTIC DEFORMATION IN VERTICAL DIRECTION: COMPARISON BETWEEN EXPERIMENTAL OBSERVATIONS AND ANALYTICAL PREDICTIONS.

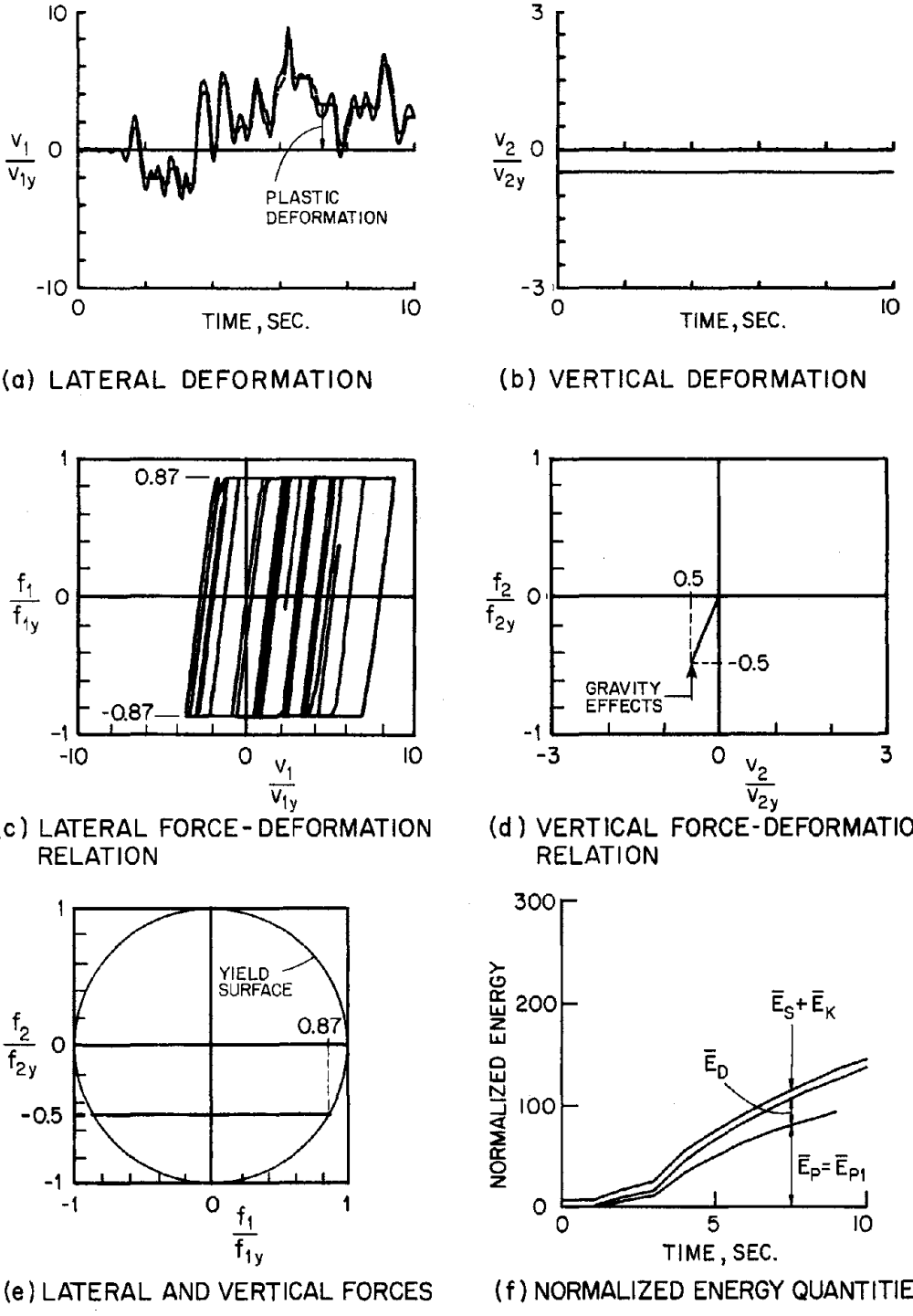

FIG. 5 RESPONSE TO HORIZONTAL GROUND MOTION INCLUDING GRAVITY LOADS BUT NEGLECTING COUPLING BETWEEN LATERAL AND VERTICAL DEFORMATIONS.

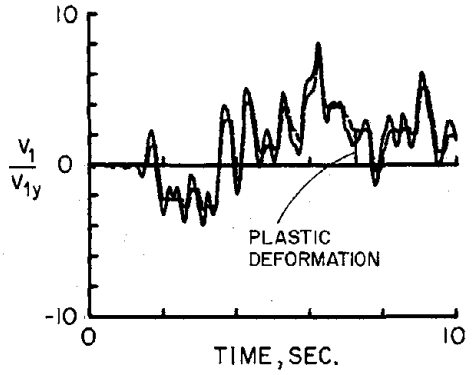

(a) LATERAL DEFORMATION

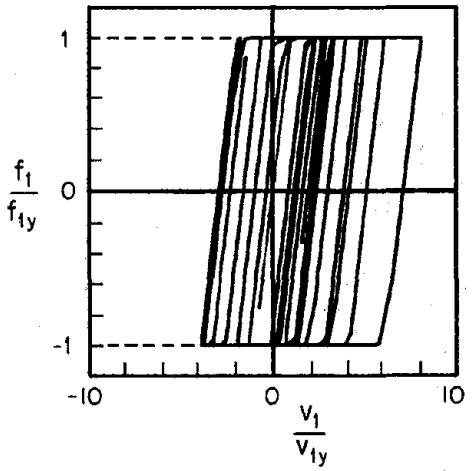

(b) LATERAL FORCE - DEFORMATION RELATION

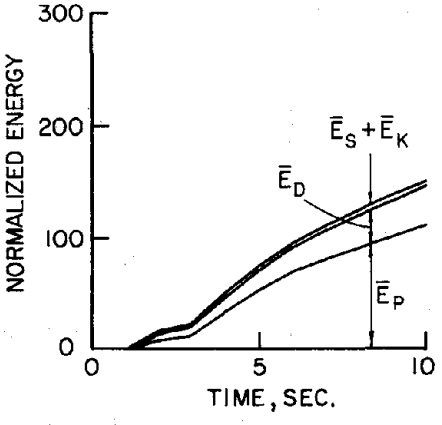

(c) NORMALIZED ENERGY QUANTITIES

FIG. 6 RESPONSE TO HORIZONTAL GROUND MOTION, NEGLECTING GRAVITY LOADS AND COUPLING BETWEEN LATERAL AND VERTICAL DEFORMATIONS: STANDARD ANALYSIS OF A SDOF SYSTEM.

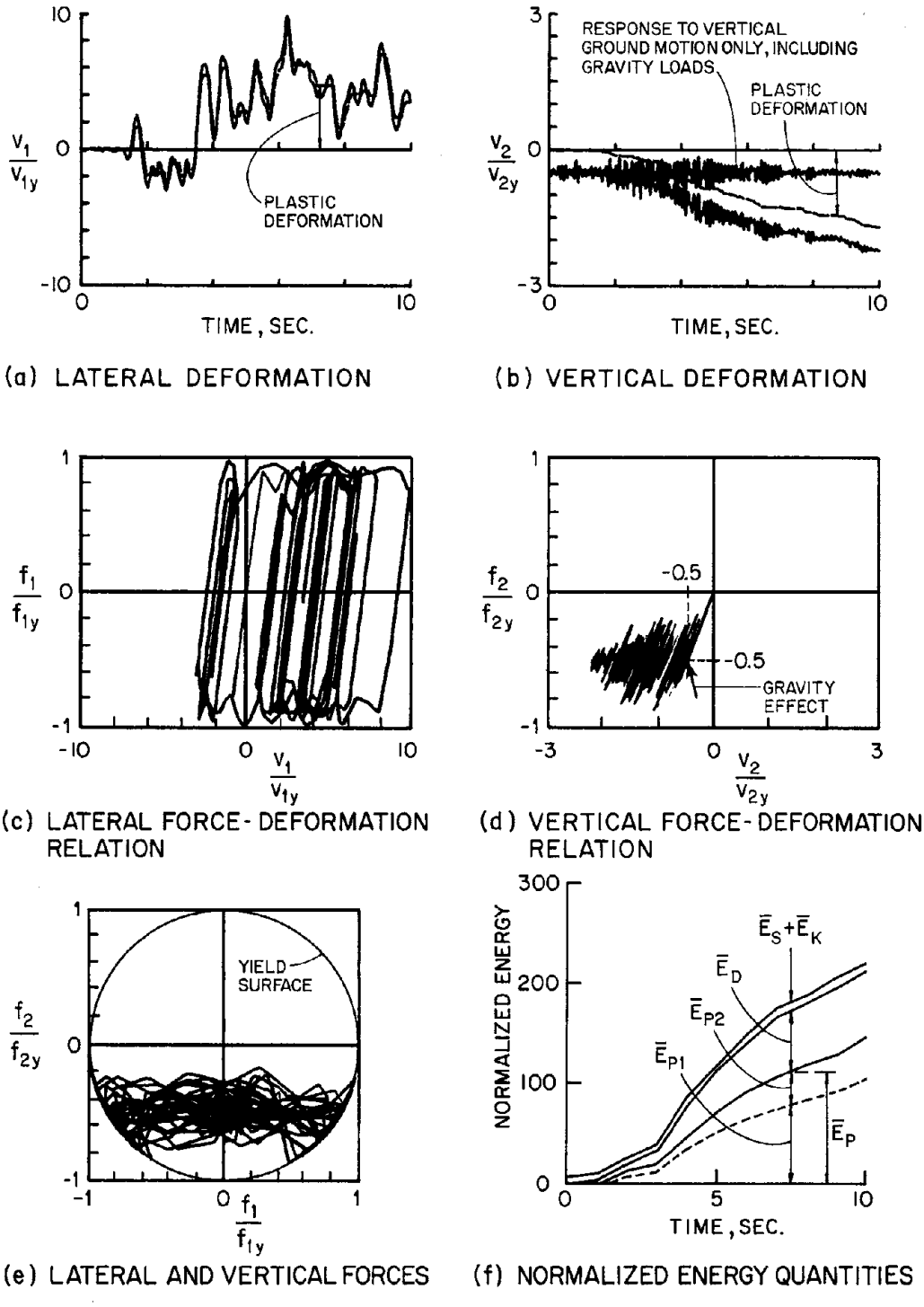

FIG. 7 COUPLED LATERAL-VERTICAL RESPONSE TO SIMULTANEOUS ACTION OF HORIZONTAL AND VERTICAL GROUND MOTIONS, INCLUDING GRAVITY LOADS.

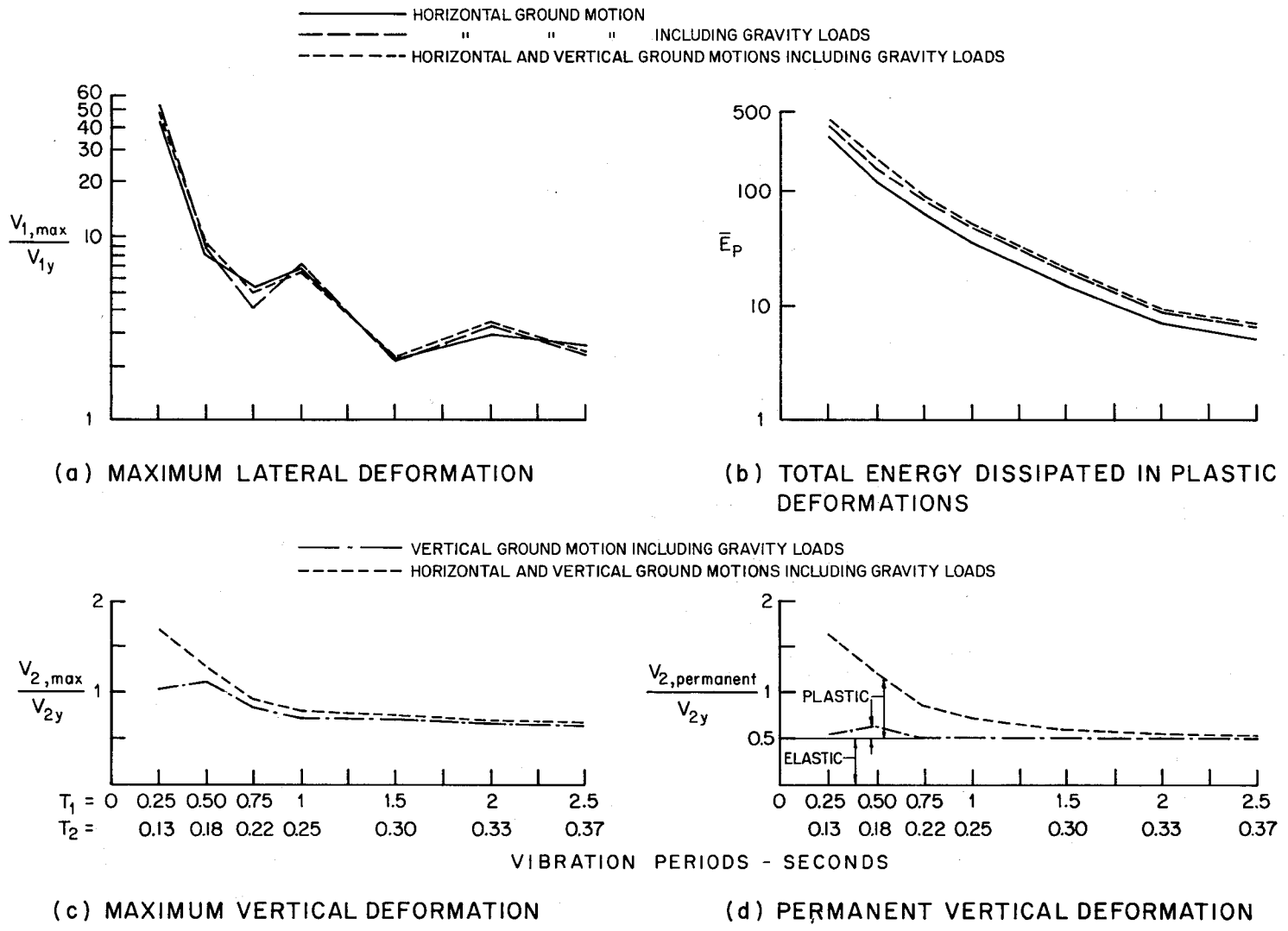

FIG. 8 RESPONSE OF SEVERAL SYSTEMS TO MANAGUA GROUND MOTION.

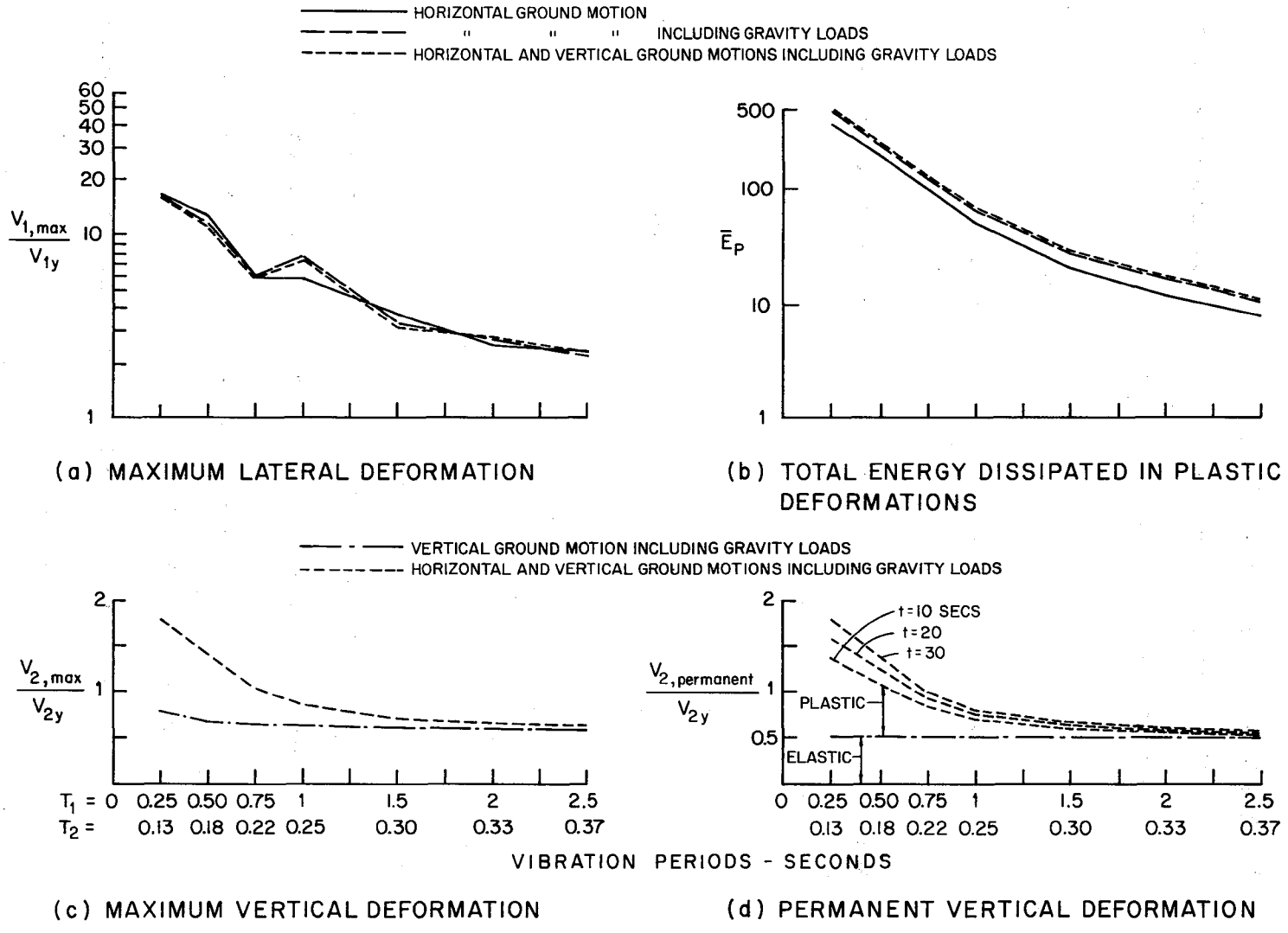

FIG. 9 RESPONSE OF SEVERAL SYSTEMS TO EL CENTRO GROUND MOTION.

APPENDIX A - EQUATIONS OF MOTION

EQUATIONS OF MOTION IN STANDARD FORM

The equations of motion for the system described earlier and illustrated in Figure 1 are as follows:

$$m\,\ddot{V}_1(t) + c_1\dot{V}_1(t) + f_1(t) = -\,m\,\ddot{V}_{g_1}(t) \tag{A.1}$$

$$m\,\ddot{V}_2(t) + c_2\dot{V}_2(t) + f_2(t) = -\,m\,\ddot{V}_{g_2} - W \tag{A.2}$$

and the force-deformation equations are, for elastic and plastic response, respectively:

$$\begin{Bmatrix} d\,f_1 \\ d\,f_2 \end{Bmatrix} = \underline{K}^E \begin{Bmatrix} d\,V_1 \\ d\,V_2 \end{Bmatrix} \quad \text{if} \quad \phi(f_1, f_2) < 1 \text{ or } \phi(f_1, f_2) = 1 \text{ and } d\,W^P < 0 \tag{A.3}$$

$$\begin{Bmatrix} d\,f_1 \\ d\,f_2 \end{Bmatrix} = \underline{K}^{EP} \begin{Bmatrix} d\,V_1 \\ d\,V_2 \end{Bmatrix} \quad \text{if} \quad \phi(f_1, f_2) = 1 \text{ and } d\,W^P \geq 0 \tag{A.4}$$

where

$V_1(t)$ and $V_2(t)$ are the horizontal and vertical deformations, respectively, of the mass with respect to the base;

$V_{g_1}(t)$ and $V_{g_2}(t)$ are the horizontal and vertical ground displacements, respectively;

$f_1(t)$ and $f_2(t)$ are the horizontal and vertical restoring forces, respectively;

m is the mass of the system;

c_1 and c_2 are the horizontal and vertical viscous damping coefficients, respectively;

W is the gravity force equal to m g where g is the acceleration of gravity;

$\phi(f_1, f_2)$ defines the yield surface;

$\underline{K}^E$ and $\underline{K}^{EP}$ are the elastic and elasto-plastic stiffness matrices, respectively; and

d W^P is incremental plastic work.

The force-deformation relation is elastic-perfectly plastic. An elliptical yield surface defines the boundaries of the elastic region.

$$\phi(f_1, f_2) = \left(\frac{f_1}{f_{1y}}\right)^2 + \left(\frac{f_2}{f_{2y}}\right)^2 = 1 \qquad (A.5)$$

where f_{1y} and f_{2y} are the yield horizontal and vertical forces, respectively (Figure 1b).

FORCE-DEFORMATION EQUATIONS

A general form of the force-deformation equation is (1):

$$\underset{\sim}{df} = \underline{K}^t \underset{\sim}{dV} \qquad (A.6)$$

where $\underline{K}^t$ is the tangent stiffness matrix and $\underset{\sim}{df}$ and $\underset{\sim}{dV}$ are the incremental force and deformation vectors, respectively.

For elastic response, $\phi(\underset{\sim}{f}) < 1$ and the tangent stiffness is given by the initial elastic stiffness matrix, $\underline{K}^E$:

$$\underline{K}^E = \begin{bmatrix} K_1 & 0 \\ 0 & K_2 \end{bmatrix} \qquad (A.7)$$

where K_1 and K_2 are the horizontal and vertical elastic stiffnesses, respectively. For plastic behavior, $\phi(\underset{\sim}{f}) = 1$ and the tangent stiffness is given by the elasto-plastic stiffness matrix, $\underline{K}^{EP}$. The following assumptions are made in deriving $\underline{K}^{EP}$:

1. A yield surface exists.

2. The incremental deformation vector can be decomposed into an elastic and plastic part:

$$\underset{\sim}{dV} = \underset{\sim}{dV}^E + \underset{\sim}{dV}^P \tag{A.8}$$

with the elastic part of the vector following Hooke's law:

$$\underset{\sim}{df} = \underline{K}^E \underset{\sim}{dV}^E \tag{A.9}$$

3. The incremental force and plastic deformation vectors are orthogonal:

$$\underset{\sim}{df}^t \underset{\sim}{dV}^P = 0 \tag{A.10}$$

4. The material of which the system is composed is perfectly plastic and the incremental force vector is therefore tangential to the yield surface for plastic response:

$$\underset{\sim}{df}^t \frac{\partial \phi}{\partial \underset{\sim}{f}} = 0 \tag{A.11}$$

where $\frac{\partial \phi}{\partial \underset{\sim}{f}}$ is a vector whose elements are $\frac{\partial \phi}{\partial f_i}$ where i equals 1 or 2.

From Eqs. (A.10) and (A.11) the incremental plastic deformation vector is given by the flow rule:

$$\underset{\sim}{dV}^P = \lambda \frac{\partial \phi}{\partial \underset{\sim}{f}} \tag{A.12}$$

where λ is a positive scalar. Equations (A.8), (A.9), (A.11). and (A.12) are used to obtain λ:

$$\lambda = \left[\left(\frac{\partial \phi}{\partial \underset{\sim}{f}}\right)^t \underline{K}^E \frac{\partial \phi}{\partial \underset{\sim}{f}}\right]^{-1} \left(\frac{\partial \phi}{\partial \underset{\sim}{f}}\right)^t \underline{K}^E \underset{\sim}{dV} \tag{A.13}$$

and from Eqs. (A.4), (A.5), (A.8), and (A.9):

$$\underset{\sim}{df} = \left\{ \underline{K}^E - \underline{K}^E \frac{\partial \phi}{\partial \underset{\sim}{f}} \left[\left(\frac{\partial \phi}{\partial \underset{\sim}{f}}\right)^t \underline{K}^E \frac{\partial \phi}{\partial \underset{\sim}{f}}\right]^{-1} \left(\frac{\partial \phi}{\partial \underset{\sim}{f}}\right)^t \underline{K}^E \right\} \underset{\sim}{dV}$$

or

$$\underset{\sim}{df} = \underline{K}^{EP} \underset{\sim}{dV}$$

where

$$\underline{K}^{EP} = \underline{K}^E - \underline{K}^E \frac{\partial \phi}{\partial \underset{\sim}{f}} \left[\left(\frac{\partial \phi}{\partial \underset{\sim}{f}}\right)^t \underline{K}^E \frac{\partial \phi}{\partial \underset{\sim}{f}}\right]^{-1} \left(\frac{\partial \phi}{\partial \underset{\sim}{f}}\right)^t \underline{K}^E \tag{A.14}$$

For the yield surface described by Eq. (A.5), the elasto-plastic stiffness matrix is given by:

$$\underline{K}^{EP} = \frac{1}{\left(\frac{2f_1}{f_{1y}^2}\right)^2 K_1 + \left(\frac{2f_2}{f_{2y}^2}\right)^2 K_2} \begin{bmatrix} K_1 K_2 \left(\frac{2f_2}{f_{2y}^2}\right)^2 & -4K_1K_2 \frac{f_1}{f_{1y}^2} \frac{f_2}{f_{2y}^2} \\ -4K_1K_2 \frac{f_1}{f_{1y}^2} \frac{f_2}{f_{2y}^2} & K_1 K_2 \left(\frac{2f_1}{f_{1y}^2}\right)^2 \end{bmatrix} \tag{A.15}$$

LOADING AND UNLOADING CRITERIA

The plastic work increment is used to determine whether the system is in a state of loading or unloading:

$$dW^P = \underset{\sim}{f}^t \, d\underset{\sim}{V}^P \tag{A.16}$$

When $dW^P \geq 0$ the system is in a state of loading and the force vector is on the yield surface. When $dW^P < 0$ the system is in a state of unloading and the force vector is on the elastic region.

Equations (A.1) through (A.4) govern the seismic response of the two-degree-of-freedom system. The two equations of motion are uncoupled for elastic response (see Eq. (A.7)) and can be integrated independently, while for plastic response the equations are coupled (see Eq. (A.15)) and must be integrated simultaneously.

EQUATIONS OF MOTION IN DIMENSIONLESS FORM

The equations of motion can be written in dimensionless form by using the following transformations (2):

$$\omega_1^2 = k_1/m \qquad \omega_2^2 = k_2/m$$

$$c_1 = 2m\omega_1\xi_1 \qquad c_2 = 2m\omega_2\xi_2$$

$$\mu_1 = V_1/V_{1y} \qquad \mu_2 = V_2/V_{2y}$$

$$P_1 = f_1/f_{1y} \qquad P_2 = f_2/f_{2y} \tag{A.17}$$

$$a_{1y} = f_{1y}/m \qquad a_{2y} = f_{2y}/m$$

$$\beta = W/f_{2y} = mg/f_{2y} \qquad \tau = t\omega_1$$

$$\delta = \omega_1/\omega_2$$

Derivatives with respect to τ are denoted by $(\,)'$. When equations (A.17) are substituted into Eqs. (A.1) to (A.4), the resulting equations of motion are:

$$\mu_1''(\tau) + 2\xi_1\mu_1'(\tau) + P_1(\tau) = - \frac{\ddot{v}_{g_1}(\tau/\omega_1)}{a_{1y}} \tag{A.18}$$

$$\delta^2\mu_2''(\tau) + 2\xi_2\delta\mu_2'(\tau) + P_2(\tau) = - \frac{\ddot{v}_{g_2}(\tau/\omega_1)}{a_{2y}} - \beta \tag{A.19}$$

and the force-deformation equations are:

$$\begin{Bmatrix} dP_1 \\ dP_2 \end{Bmatrix} = \underline{S}^E \begin{Bmatrix} d\mu_1 \\ d\mu_2 \end{Bmatrix} \quad \text{if} \quad \phi(P_1, P_2) < 1 \text{ or } \phi(P_1, P_2) = 1 \text{ and } dM^P < 0 \tag{A.20}$$

$$\begin{Bmatrix} dP_1 \\ dP_2 \end{Bmatrix} = \underline{S}^{EP} \begin{Bmatrix} d\mu_1 \\ d\mu_2 \end{Bmatrix} \quad \text{if} \quad \phi(P_1, P_2) = 1 \text{ and } dM^P \geq 0 \tag{A.21}$$

where

$$\phi(P_1, P_2) = P_1^2 + P_2^2 = 1 \tag{A.22}$$

The elastic and elasto-plastic stiffness matrices are:

$$\underline{S}^E = \begin{bmatrix} 1 & 0 \\ 0 & 1 \end{bmatrix} \tag{A.23}$$

$$\underline{S}^{EP} = \frac{1}{\omega_1^2\left(\frac{P_1}{a_{1y}}\right)^2 + \omega_2^2\left(\frac{P_2}{a_{2y}}\right)^2} \begin{bmatrix} \omega_2^2\left(\frac{P_2}{a_{2y}}\right)^2 & \frac{-\omega_1^2 P_1 P_2}{a_{1y}^2} \\ \frac{-\omega_2^2 P_1 P_2}{a_{2y}^2} & \omega_1^2\left(\frac{P_1}{a_{1y}}\right)^2 \end{bmatrix} \tag{A.24}$$

The dimensionless plastic work increment is defined as:

$$dM^P = P_1 d\mu_1^P + P_2 d\mu_2^P \qquad \text{(A.25)}$$

APPENDIX B - NUMERICAL INTEGRATION OF EQUATIONS OF MOTION

GENERAL APPROACH

The incremental equations of motion for a two-degree-of-freedom system can be written in general form as:

$$\underset{\sim}{m}\,\Delta\ddot{\underset{\sim}{V}} + \underset{\sim}{c}\,\Delta\dot{\underset{\sim}{V}} + \Delta\underset{\sim}{f} = \Delta\underset{\sim}{P}(t) \tag{B.1}$$

and the force deformation equations as:

$$\Delta\underset{\sim}{f} = \underset{\sim}{K}^{t}\,\Delta\underset{\sim}{V} \tag{B.2}$$

where $\underset{\sim}{m}$, $\underset{\sim}{c}$, and $\underset{\sim}{K}^{t}$ are the mass, damping, and tangent stiffness matrices, respectively, $\underset{\sim}{V}$ is the displacement vector, $\underset{\sim}{f}$ is the force vector, and $\underset{\sim}{P}(t)$ is the exciting force.

The displacements, velocities, accelerations, and forces at time $t + \Delta t$ given those at time t are sought. The equations are solved numerically using a step-by-step procedure. The numerical method can be summarized as follows (3):

(1) Linearization Procedure - The tangent stiffness matrix $\underset{\sim}{K}^{t}$ at time t is formed.

(2) Solution Procedure - Response increments $\Delta\underset{\sim}{V}$, $\Delta\dot{\underset{\sim}{V}}$, and $\Delta\ddot{\underset{\sim}{V}}$ are calculated using the linear acceleration method.

(3) State Determination Problem - Force increments are calculated given deformation increments, $\Delta\underset{\sim}{f} = \underset{\sim}{K}^{t}\,\Delta\underset{\sim}{V}$.

(4) Iterative Procedure to Reduce Unbalanced Forces - Any unbalanced forces in the system are calculated and the solution iterated using a Newton-Raphson scheme until

equilibrium tolerances are satisfied, leading to new response increments $\Delta\underset{\sim}{V}$, $\Delta\dot{\underset{\sim}{V}}$, $\Delta\ddot{\underset{\sim}{V}}$, $\Delta\underset{\sim}{f}$.

(5) Final Solution - The new state of the system at time $t + \Delta t$ is calculated

$$\underset{\sim}{V}(t + \Delta t),\ \dot{\underset{\sim}{V}}(t + \Delta t),\ \ddot{\underset{\sim}{V}}(t + \Delta t),\ \underset{\sim}{f}(t + \Delta t)$$

LINEARIZATION AND SOLUTION PROCEDURE

The tangent stiffness matrix is calculated using the linearization procedure and according to the plasticity laws as described in Appendix A. For elastic behavior, the tangent stiffness is given by Eq. (A.7), and for plastic behavior by Eq. (A.15). The response increments $\Delta\underset{\sim}{V}$, $\Delta\dot{\underset{\sim}{V}}$, $\Delta\ddot{\underset{\sim}{V}}$ are calculated by the linear acceleration method (4). If the acceleration is assumed to vary linearly during the time interval Δt, the kinematic equations for $\Delta\underset{\sim}{V}$ and $\Delta\dot{\underset{\sim}{V}}$ can be written as follows:

$$\Delta\dot{\underset{\sim}{V}} = \ddot{\underset{\sim}{V}}(t)\Delta t + \Delta\ddot{\underset{\sim}{V}}\,\frac{\Delta t}{2} \tag{B.3}$$

$$\Delta\underset{\sim}{V} = \dot{\underset{\sim}{V}}(t)\Delta t + \ddot{\underset{\sim}{V}}(t)\,\frac{\Delta t^2}{2} + \Delta\ddot{\underset{\sim}{V}}\,\frac{\Delta t^2}{6} \tag{B.4}$$

The equations of motion (B.1) and the kinematic equations (B.3) and (B.4) represent a system of 3 vectorial equations with 3 unknown vectors that can be solved for $\Delta\underset{\sim}{V}$, $\Delta\dot{\underset{\sim}{V}}$, and $\Delta\ddot{\underset{\sim}{V}}$ as follows:

$$\Delta\underset{\sim}{V} = (\underline{\bar{K}})^{-1}\,\Delta\underset{\sim}{\bar{P}} \tag{B.5}$$

where $\underline{\bar{K}}$ is the effective stiffness matrix defined by

$$\underline{\bar{K}} = \underline{K}^t + \frac{6}{\Delta t^2}\,\underline{m} + \frac{3}{\Delta t}\,\underline{c} \tag{B.6}$$

and

$$\Delta\bar{\underset{\sim}{P}} = \Delta\underset{\sim}{P} + \underline{m}\left(\frac{6}{\Delta t}\,\dot{\underset{\sim}{V}}(t) + 3\ddot{\underset{\sim}{V}}(t)\right) + \underline{c}\left(3\dot{\underset{\sim}{V}}(t) + \frac{\Delta t}{2}\,\ddot{\underset{\sim}{V}}(t)\right) \tag{B.7}$$

$$\Delta\dot{\underset{\sim}{V}} = \frac{3}{\Delta t}\,\Delta\underset{\sim}{V} - 3\dot{\underset{\sim}{V}}(t) - \frac{\Delta t}{2}\,\ddot{\underset{\sim}{V}}(t) \tag{B.8}$$

$$\Delta\underset{\sim}{V} = -3\ddot{\underset{\sim}{V}}(t) - \dot{\underset{\sim}{V}}(t)\,\frac{6}{\Delta t} + \Delta\underset{\sim}{V}\,\frac{6}{\Delta t^2} \tag{B.9}$$

STATE DETERMINATION PROBLEM

The force increments $\Delta\underset{\sim}{f}$ are calculated given the displacement increments $\Delta\underset{\sim}{V}$. The force-deformation relations are (Eq. (B.2)):

$$\Delta\underset{\sim}{f} = \underline{K}^{t}\,\Delta\underset{\sim}{V} \tag{B.10}$$

For elastic response, $\underline{K}^{t}$ is defined by Eq. (A.7) where K_1 and K_2 are constant during Δt and $\Delta\underset{\sim}{f}$ may be calculated directly from Eq. (B.10). For plastic response, the tangent stiffness matrix $\underline{K}^{t}$ (Eq. (A.15)) is a function of the force vector $\underset{\sim}{f}$, and Eq. (B.10) is expressed by:

$$\Delta\underset{\sim}{f} = \underline{K}^{EP}(\underset{\sim}{f})\,\Delta\underset{\sim}{V} \tag{B.11}$$

To solve for $\Delta\underset{\sim}{f}$ in Eq. (B.11), a numerical integration within time steps must be carried out. The solution process will be described for two transition states: from plastic to plastic state and from elastic to plastic state.

a) Plastic To Plastic State

The state determination problem involved when the system transists from plastic to plastic state is illustrated in Figure (B.1a). The force vector at time t, $\underset{\sim}{f}(t)$, is known and is on the yield surface.

$\Delta\underset{\sim}{f}$ must be determined such that Eq. (B.11) is satisfied and $\underset{\sim}{f}(t + \Delta t) = \underset{\sim}{f}(t) + \Delta\underset{\sim}{f}$ is on the yield surface. A first approximation for the force vector, $\underset{\sim}{f}^1(t + \Delta t)$, is obtained from Eq. (B.11) using the tangent stiffness at time t (Figure B.1b):

$$\underset{\sim}{f}^1(t + \Delta t) = \underset{\sim}{f}(t) + \underline{K}^{EP}(\underset{\sim}{f}(t))\ \Delta\underset{\sim}{V}$$

To obtain a second approximation, the tangent stiffness at $\underset{\sim}{f}^1$ is used in conjunction with a second order Runge-Kutta scheme:

$$\underset{\sim}{f}^2(t + \Delta t) = \underset{\sim}{f}(t) + \frac{1}{2}\left[\underline{K}^{EP}(\underset{\sim}{f}(t)) + \underline{K}^{EP}(\underset{\sim}{f}^1(t + \Delta t))\right]\Delta\underset{\sim}{V}$$

Because the solution is carried out numerically, $\underset{\sim}{f}^2(t + \Delta t)$ will not be exactly on the yield surface and a correction as shown in Figure (B.1b) must be introduced to obtain the final value for the force vector $\underset{\sim}{f}(t + \Delta t)$. Finally,

$$\Delta\underset{\sim}{f} = \underset{\sim}{f}(t + \Delta t) - \underset{\sim}{f}(t)$$

b) Elastic To Plastic State

The state determination problem involved when the system transists from elastic to plastic state is illustrated in Figure (B.2a). The force vector at time t is $\underset{\sim}{f}(t)$ and is on the elastic region. The elastic solution results in forces represented by point A on Figure (B.2a). Assuming this point as the first approximation to the solution, $\Delta\underset{\sim}{f}(t + \Delta t)$ is determined such that Eq. (B.11) is satisfied and the force vector is on the yield surface.

The procedure to determine $\underset{\sim}{f}(t + \Delta t)$ is carried out in two steps. First, the force vector, $\underset{\sim}{f}^2(t + \Delta t)$ is calculated such that it is on the yield surface:

$$\underset{\sim}{f}^2(t + \Delta t) = \underset{\sim}{f}(t) + \alpha\, \Delta\underset{\sim}{f}^1$$

where α is a factor than when used to multiply the second term in the above equation yields a value for $\underset{\sim}{f}^2(t + \Delta t)$ that is on the yield surface and that defines the transition between elastic and plastic states. The plastic force vector is then calculated as previously described for the transition from plastic to plastic state. The incremental displacement for plastic response of the system is given by $(1 - \alpha)\Delta\underset{\sim}{V}$. A second order Runge-Kutta scheme is used to calculate $\underset{\sim}{f}^4(t + \Delta t)$:

$$\underset{\sim}{f}^4(t + \Delta t) = \underset{\sim}{f}^2(t + \Delta t) + \frac{1}{2}\left[\underline{K}^{EP}(\underset{\sim}{f}^2(t + \Delta t)) + \underline{K}^{EP}(\underset{\sim}{f}^3(t + \Delta t))\right](1 - \alpha)\Delta\underset{\sim}{V}$$

where

$$\underset{\sim}{f}^3(t + \Delta t) = \underset{\sim}{f}^2(t + \Delta t) + \underline{K}^{EP}(\underset{\sim}{f}^2(t + \Delta t))(1 - \alpha)\Delta\underset{\sim}{V}$$

Because the solution $\underset{\sim}{f}^4(t + \Delta t)$ is still not on the yield surface, a correction is applied as shown in Fig. (B.2b) to obtain the final value for the force vector $\underset{\sim}{f}(t + \Delta t)$ and

$$\Delta\underset{\sim}{f} = \underset{\sim}{f}(t + \Delta t) - \underset{\sim}{f}(t)$$

REDUCTION OF UNBALANCED FORCES

In solving the equations of motion (Eqs. (B.5) to (B.9)), the tangent stiffness matrix is assumed to be constant during each time step. However, when the system moves from elastic to plastic or plastic to plastic states, the stiffness varies within the time step, dynamic equilibrium is violated, and unbalanced forces are introduced into the system. A Newton-Raphson Iteration is used to reduce the unbalanced forces thus introduced.

The restoring forces that satisfy the dynamic equilibrium equations (B.1) are the first approximations shown in Figures (B.1) and (B.2). The final values for the restoring forces, $\underset{\sim}{f}(t + \Delta t)$, are provided by the solution of the state determination problem. The unbalanced forces introduced into the system are, therefore:

$$\underset{\sim}{f}^{U} = \underset{\sim}{f}(t + \Delta t) - \underset{\sim}{f}^{1}(t + \Delta t)$$

The vector $\overline{\underset{\sim}{\Delta P}}$ in Eq. (B.7) is replaced by the unbalanced force value and additional displacement increments are calculated using an iterative procedure. The process is repeated until equilibrium tolerances are satisfied.

ELASTIC AND PLASTIC DISPLACEMENTS

When the final displacement values have been calculated for each time step, the elastic and plastic parts of the displacement vector (Eqs. (A.8) and (A.9)) are calculated as follows:

$$\underset{\sim}{\Delta v}^{E} = (\underline{K}^{E})^{-1} \underset{\sim}{\Delta f}$$

$$\underset{\sim}{\Delta v}^{P} = \underset{\sim}{\Delta v} - \underset{\sim}{\Delta v}^{E}$$

ENERGY INTEGRALS

The energy equations derived in Appendix C are calculated using the trapezoidal rule. The dimensionless energy increments at each time interval are:

$$\overline{\Delta E}_{I1} = - \frac{\ddot{v}_{g_1}(\tau+\Delta\tau)\ \dot{\mu}_1(\tau+\Delta\tau) + \ddot{v}_{g_1}(\tau)\ \dot{\mu}_1(\tau)}{a_{1y}}\ \Delta\tau$$

$$\Delta\bar{E}_{I2} = - \frac{\ddot{v}_{g_2}(\tau+\Delta\tau)\ \dot{\mu}_2(\tau+\Delta\tau) + \ddot{v}_{g_2}(\tau)\ \dot{\mu}_2(\tau)}{a_{2y}}\ \Delta\tau$$

$$- \beta\left[\dot{\mu}_2(\tau + \Delta\tau) + \dot{\mu}_2(\tau)\right]\Delta\tau$$

where $\Delta\bar{E}_{I1}$ and $\Delta\bar{E}_{I2}$ are input energy terms;

$$\Delta\bar{E}_{K1} = \dot{\mu}_1^2(\tau + \Delta\tau) - \dot{\mu}_1^2(\tau)$$

$$\Delta\bar{E}_{K2} = \delta^2\left[\dot{\mu}_2^2(\tau + \Delta\tau) - \dot{\mu}_2^2(\tau)\right]$$

where $\Delta\bar{E}_{K1}$ and $\Delta\bar{E}_{K2}$ are kinetic energy terms;

$$\Delta\bar{E}_{D1} = 2\Delta\tau\xi_1\left[\dot{\mu}_1^2(\tau + \Delta\tau) + \dot{\mu}_1^2(\tau)\right]$$

$$\Delta\bar{E}_{D2} = 2\Delta\tau\xi_2\delta\left[\dot{\mu}_2^2(\tau + \Delta\tau) + \dot{\mu}_2^2(\tau)\right]$$

where $\Delta\bar{E}_{D1}$ and $\Delta\bar{E}_{D2}$ are daming energy terms;

$$\Delta\bar{E}_{S1} = \mu_1^{E^2}(\tau + \Delta\tau) - \mu_1^{E^2}(\tau)$$

$$\Delta\bar{E}_{S2} = \mu_2^{E^2}(\tau + \Delta\tau) - \mu_2^{E^2}(\tau)$$

where $\Delta\bar{E}_{S1}$ and $\Delta\bar{E}_{S2}$ are strain energy terms; and

$$\Delta\bar{E}_{P1} = \left[P_1(\tau + \Delta\tau) + P_1(\tau)\right]\left[v_1^P(\tau + \Delta\tau) - v_1^P(\tau)\right]$$

$$\Delta\bar{E}_{P2} = \left[P_2(\tau + \Delta\tau) + P_2(\tau)\right]\left[v_2^P(\tau + \Delta\tau) - v_2^P(\tau)\right]$$

where $\Delta\bar{E}_{P1}$ and $\Delta\bar{E}_{P2}$ are terms for energy dissipated plastically.

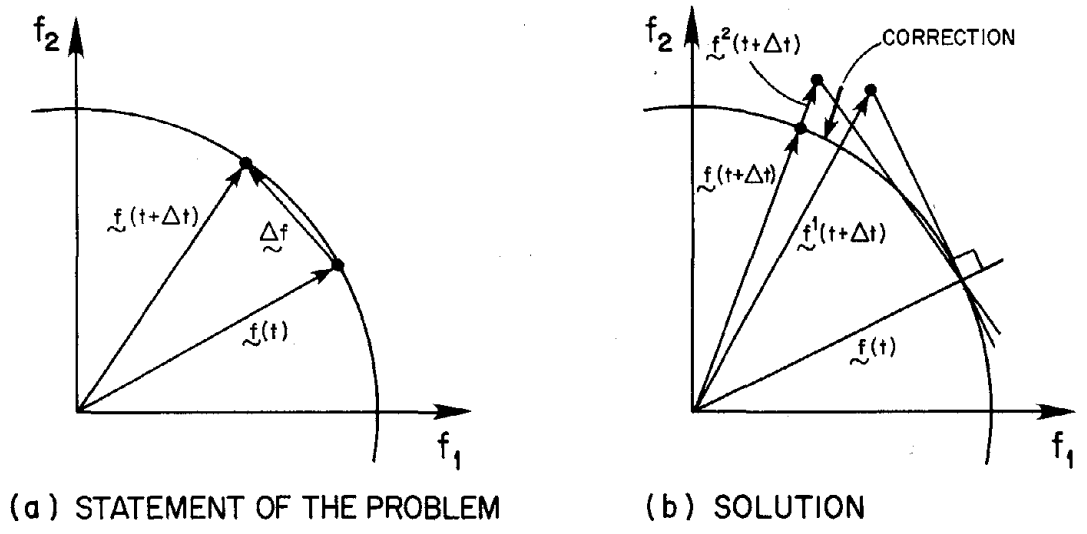

FIG. B.1 SOLUTION OF STATE DETERMINATION PROBLEM: FROM PLASTIC TO PLASTIC STATE.

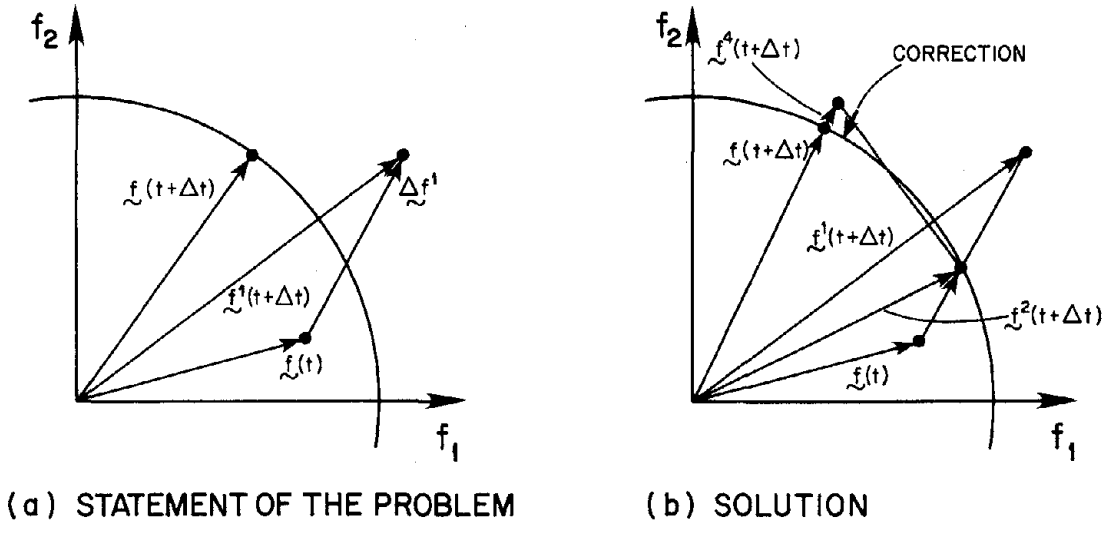

FIG. B.2 SOLUTION OF STATE DETERMINATION PROBLEM: FROM ELASTIC TO PLASTIC STATE.

APPENDIX C - ENERGY EQUATIONS

The equations used to determine the energy input and dissipated in response of the system to the input ground motions are derived below.

The equations of motion (Eqs. (A.1) and (A.2)) can be combined as follows:

$$m\ddot{V}_i + c_i\dot{V}_i + f_i = Q_i(t) \tag{C.1}$$

where i = 1 and 2, and

$$\begin{aligned} Q_1(t) &= - m\ddot{V}_{g_1}(t) \\ Q_2(t) &= - m\ddot{V}_{g_2}(t) - W \end{aligned} \tag{C.2}$$

To obtain the energy equation, Eq. (C.1) must be multiplied by dV_i. Then, integrating between 0 and $V_i(t)$ and decomposing dV_i into elastic and plastic parts, we obtain:

$$\int_0^{V_i(t)} m\ddot{V}_i dV_i + \int_0^{V_i(t)} c_i\dot{V}_i dV_i + \int_0^{V_i(t)} f_i dV_i^E + \int_0^{V_i(t)} f_i dV_i^P = \int_0^{V_i(t)} Q_i dV_i$$

The righthand term represents the energy input to the system by the exciting force during time t, and the lefthand term the energy in the system at time t and energy dissipated by the system during time t. The energy equation can be written as:

$$E_{Ki}(t) + E_{Di}(t) + E_{Si}(t) + E_{Pi}(t) = E_{Ii}(t) \tag{C.3}$$

where

$$E_{Ki}(t) = \int_0^{V_i(t)} m\ddot{V}_i dV_i$$

describes the kinetic energy in the system at time t;

$$E_{Di}(t) = \int_0^{V_i(t)} c_i\dot{V}_i dV_i$$

describes the energy dissipated by damping during time t;

$$E_{Si}(t) = \int_0^{V_i(t)} f_i dV_i^E \tag{C.4}$$

describes the strain energy in the system at time t;

$$E_{Pi}(t) = \int_0^{V_i(t)} f_i dV_i^P$$

describes the energy dissipated plastically during time t; and

$$E_{Ii}(t) = \int_0^{V_i(t)} Q_i dV_i$$

describes the energy input to the system during time t.

The energy equation can be written in dimensionless form by dividing by the elastic energy capacity in the i^{th} direction. For instance:

$$\overline{E}_{Ii}(t) = \frac{E_{Ii}(t)}{\frac{1}{2} f_{iy} V_{iy}}$$

The other terms are similarly derived. Equation (C.3) therefore becomes:

$$\overline{E}_{Ki}(t) + \overline{E}_{Di}(t) + \overline{E}_{Si}(t) + \overline{E}_{Pi}(t) = \overline{E}_{Ii}(t) \qquad (C.5)$$

By using the definitions of Eq. (A.17), the following expression for Eqs. (C.4) are obtained:

$$\overline{E}_{I1}(t) = \frac{-2\omega_1}{a_{1y}} \int_0^t \ddot{v}_{g_1}(t)\dot{\mu}_1(t)\,dt$$

$$\overline{E}_{I2}(t) = \frac{-2\omega_1}{a_{2y}} \int_0^t \ddot{v}_{g_2}(t)\dot{\mu}_2(t)\,dt - 2\beta\omega_1 \int_0^t \dot{\mu}_2(t)\,dt$$

$$\overline{E}_{K1}(t) = \dot{\mu}_1^2(t)$$

$$\overline{E}_{K2}(t) = \delta^2\dot{\mu}_2^2(t)$$

$$\overline{E}_{D1}(t) = 4\xi_1\omega_1 \int_0^t \dot{\mu}_1^2(t)\,dt$$

$$\overline{E}_{D2}(t) = 4\xi_2\delta\omega_1 \int_0^t \dot{\mu}_2^2(t)\,dt$$

$$\overline{E}_{S1}(t) = \left[\mu_1^E(t)\right]^2$$

$$\overline{E}_{S2}(t) = \left[\mu_2^E(t)\right]^2$$

$$\bar{E}_{P1}(t) = 2 \int_0^t P_1(t) d\mu_1^P$$

$$\bar{E}_{P2}(t) = 2 \int_0^t P_2(t) d\mu_2^P$$

At t = 0, all energy values are equal to zero with the exception of the strain energy in the vertical direction which is equal to the work done by the axial force before the ground motion is applied to the system.

$$\bar{E}_{S2}(0) = \bar{E}_{I2}(0) = \beta^2$$

Total energy values include the contribution of both the horizontal and vertical directions of motion to the energy input to and dissipated by the system and are normalized by the elastic energy capacity in the horizontal direction. The total energy input is defined as:

$$E_I(t) = E_{I1}(t) + E_{I2}(t)$$

In dimensionless form, this expression is:

$$\bar{E}_I(t) = \frac{E_I(t)}{\frac{1}{2} f_{1y} V_{1y}}$$

Similarly, the other energy terms, $\bar{E}_K$, $\bar{E}_D$, $\bar{E}_S$ and $\bar{E}_P$ are the dimensionless total kinetic energy, total energy dissipated by damping, total strain energy, and total energy dissipated plastically, respectively.

The above energy formulation holds for a system on a fixed base subjected to applied forces $Q_i(t)$, not for the actual case where the system is excited by base motion. The kinetic energy terms in the equations therefore represent the energy associated with motions relative to the base of the system and not the kinetic energy due to total motion. Because the primary concern in seismic analysis is with deformation of the system, an energy formulation in terms of relative motion is more useful.

REFERENCES

1. Porter, F. L. and Powell, G. H., "Static and Dynamic Analysis of Inelastic Frame Structures," Report No. EERC 71-3, University of California, Berkeley, June 1971.

2. Nigam, N. C., "Inelastic Interaction in the Dynamic Response of Structures," Ph.D. Thesis, California Institute of Technology, Pasadena, June 1967.

3. Mondkar, D. P. and Powell, G. H., "Static and Dynamic Analysis of Nonlinear Structures," Report No. EERC 75-10, University of California, Berkeley, 1975.

4. Clough, R. W. and Penzien, J., Dynamic of Structures, McGraw-Hill, 1975.

EARTHQUAKE ENGINEERING RESEARCH CENTER REPORTS

NOTE: Numbers in parenthesis are Accession Numbers assigned by the National Technical Information Service; these are followed by a price code. Copies of the reports may be ordered from the National Technical Information Service, 5285 Port Royal Road, Springfield, Virginia, 22161. Accession Numbers should be quoted on orders for reports (PB --- ---) and remittance must accompany each order. Reports without this information were not available at time of printing. Upon request, EERC will mail inquirers this information when it becomes available.

EERC 67-1 "Feasibility Study Large-Scale Earthquake Simulator Facility," by J. Penzien, J.G. Bouwkamp, R.W. Clough and D. Rea - 1967 (PB 187 905)A07

EERC 68-1 Unassigned

EERC 68-2 "Inelastic Behavior of Beam-to-Column Subassemblages Under Repeated Loading," by V.V. Bertero - 1968 (PB 184 888)A05

EERC 68-3 "A Graphical Method for Solving the Wave Reflection-Refraction Problem," by H.D. McNiven and Y. Mengi - 1968 (PB 187 943)A03

EERC 68-4 "Dynamic Properties of McKinley School Buildings," by D. Rea, J.G. Bouwkamp and R.W. Clough - 1968 (PB 187 902)A07

EERC 68-5 "Characteristics of Rock Motions During Earthquakes," by H.B. Seed, I.M. Idriss and F.W. Kiefer - 1968 (PB 188 338)A03

EERC 69-1 "Earthquake Engineering Research at Berkeley," - 1969 (PB 187 906)A11

EERC 69-2 "Nonlinear Seismic Response of Earth Structures," by M. Dibaj and J. Penzien - 1969 (PB 187 904)A08

EERC 69-3 "Probabilistic Study of the Behavior of Structures During Earthquakes," by R. Ruiz and J. Penzien - 1969 (PB 187 886)A06

EERC 69-4 "Numerical Solution of Boundary Value Problems in Structural Mechanics by Reduction to an Initial Value Formulation," by N. Distefano and J. Schujman - 1969 (PB 187 942)A02

EERC 69-5 "Dynamic Programming and the Solution of the Biharmonic Equation," by N. Distefano - 1969 (PB 187 941)A03

EERC 69-6 "Stochastic Analysis of Offshore Tower Structures," by A.K. Malhotra and J. Penzien - 1969 (PB 187 903)A09

EERC 69-7 "Rock Motion Accelerograms for High Magnitude Earthquakes," by H.B. Seed and I.M. Idriss - 1969 (PB 187 940)A02

EERC 69-8 "Structural Dynamics Testing Facilities at the University of California, Berkeley," by R.M. Stephen, J.G. Bouwkamp, R.W. Clough and J. Penzien - 1969 (PB 189 111)A04

EERC 69-9 "Seismic Response of Soil Deposits Underlain by Sloping Rock Boundaries," by H. Dezfulian and H.B. Seed 1969 (PB 189 114)A03

EERC 69-10 "Dynamic Stress Analysis of Axisymmetric Structures Under Arbitrary Loading," by S. Ghosh and E.L. Wilson 1969 (PB 189 026)A10

EERC 69-11 "Seismic Behavior of Multistory Frames Designed by Different Philosophies," by J.C. Anderson and V. V. Bertero - 1969 (PB 190 662)A10

EERC 69-12 "Stiffness Degradation of Reinforcing Concrete Members Subjected to Cyclic Flexural Moments," by V.V. Bertero, B. Bresler and H. Ming Liao - 1969 (PB 202 942)A07

EERC 69-13 "Response of Non-Uniform Soil Deposits to Travelling Seismic Waves," by H. Dezfulian and H.B. Seed - 1969 (PB 191 023)A03

EERC 69-14 "Damping Capacity of a Model Steel Structure," by D. Rea, R.W. Clough and J.G. Bouwkamp - 1969 (PB 190 663)A06

EERC 69-15 "Influence of Local Soil Conditions on Building Damage Potential during Earthquakes," by H.B. Seed and I.M. Idriss - 1969 (PB 191 036)A03

EERC 69-16 "The Behavior of Sands Under Seismic Loading Conditions," by M.L. Silver and H.B. Seed - 1969 (AD 714 982)A07

EERC 70-1 "Earthquake Response of Gravity Dams," by A.K. Chopra - 1970 (AD 709 640)A03

EERC 70-2 "Relationships between Soil Conditions and Building Damage in the Caracas Earthquake of July 29, 1967," by H.B. Seed, I.M. Idriss and H. Dezfulian - 1970 (PB 195 762)A05

EERC 70-3 "Cyclic Loading of Full Size Steel Connections," by E.P. Popov and R.M. Stephen - 1970 (PB 213 545)A04

EERC 70-4 "Seismic Analysis of the Charaima Building, Caraballeda, Venezuela," by Subcommittee of the SEAONC Research Committee: V.V. Bertero, P.F. Fratessa, S.A. Mahin, J.H. Sexton, A.C. Scordelis, E.L. Wilson, L.A. Wyllie, H.B. Seed and J. Penzien, Chairman - 1970 (PB 201 455)A06

EERC 70-5 "A Computer Program for Earthquake Analysis of Dams," by A.K. Chopra and P. Chakrabarti - 1970 (AD 723 994)A05

EERC 70-6 "The Propagation of Love Waves Across Non-Horizontally Layered Structures," by J. Lysmer and L.A. Drake 1970 (PB 197 896)A03

EERC 70-7 "Influence of Base Rock Characteristics on Ground Response," by J. Lysmer, H.B. Seed and P.B. Schnabel 1970 (PB 197 897)A03

EERC 70-8 "Applicability of Laboratory Test Procedures for Measuring Soil Liquefaction Characteristics under Cyclic Loading," by H.B. Seed and W.H. Peacock - 1970 (PB 198 016)A03

EERC 70-9 "A Simplified Procedure for Evaluating Soil Liquefaction Potential," by H.B. Seed and I.M. Idriss - 1970 (PB 198 009)A03

EERC 70-10 "Soil Moduli and Damping Factors for Dynamic Response Analysis," by H.B. Seed and I.M. Idriss - 1970 (PB 197 869)A03

EERC 71-1 "Koyna Earthquake of December 11, 1967 and the Performance of Koyna Dam," by A.K. Chopra and P. Chakrabarti 1971 (AD 731 496)A06

EERC 71-2 "Preliminary In-Situ Measurements of Anelastic Absorption in Soils Using a Prototype Earthquake Simulator," by R.D. Borcherdt and P.W. Rodgers - 1971 (PB 201 454)A03

EERC 71-3 "Static and Dynamic Analysis of Inelastic Frame Structures," by F.L. Porter and G.H. Powell - 1971 (PB 210 135)A06

EERC 71-4 "Research Needs in Limit Design of Reinforced Concrete Structures," by V.V. Bertero - 1971 (PB 202 943)A04

EERC 71-5 "Dynamic Behavior of a High-Rise Diagonally Braced Steel Building," by D. Rea, A.A. Shah and J.G. Bouwkamp 1971 (PB 203 584)A06

EERC 71-6 "Dynamic Stress Analysis of Porous Elastic Solids Saturated with Compressible Fluids," by J. Ghaboussi and E. L. Wilson - 1971 (PB 211 396)A06

EERC 71-7 "Inelastic Behavior of Steel Beam-to-Column Subassemblages," by H. Krawinkler, V.V. Bertero and E.P. Popov 1971 (PB 211 335)A14

EERC 71-8 "Modification of Seismograph Records for Effects of Local Soil Conditions," by P. Schnabel, H.B. Seed and J. Lysmer - 1971 (PB 214 450)A03

EERC 72-1 "Static and Earthquake Analysis of Three Dimensional Frame and Shear Wall Buildings," by E.L. Wilson and H.H. Dovey - 1972 (PB 212 904)A05

EERC 72-2 "Accelerations in Rock for Earthquakes in the Western United States," by P.B. Schnabel and H.B. Seed - 1972 (PB 213 100)A03

EERC 72-3 "Elastic-Plastic Earthquake Response of Soil-Building Systems," by T. Minami - 1972 (PB 214 868)A08

EERC 72-4 "Stochastic Inelastic Response of Offshore Towers to Strong Motion Earthquakes," by M.K. Kaul - 1972 (PB 215 713)A05

EERC 72-5 "Cyclic Behavior of Three Reinforced Concrete Flexural Members with High Shear," by E.P. Popov, V.V. Bertero and H. Krawinkler - 1972 (PB 214 555)A05

EERC 72-6 "Earthquake Response of Gravity Dams Including Reservoir Interaction Effects," by P. Chakrabarti and A.K. Chopra - 1972 (AD 762 330)A08

EERC 72-7 "Dynamic Properties of Pine Flat Dam," by D. Rea, C.Y. Liaw and A.K. Chopra - 1972 (AD 763 928)A05

EERC 72-8 "Three Dimensional Analysis of Building Systems," by E.L. Wilson and H.H. Dovey - 1972 (PB 222 438)A06

EERC 72-9 "Rate of Loading Effects on Uncracked and Repaired Reinforced Concrete Members," by S. Mahin, V.V. Bertero, D. Rea and M. Atalay - 1972 (PB 224 520)A08

EERC 72-10 "Computer Program for Static and Dynamic Analysis of Linear Structural Systems," by E.L. Wilson, K.-J. Bathe, J.E. Peterson and H.H.Dovey - 1972 (PB 220 437)A04

EERC 72-11 "Literature Survey - Seismic Effects on Highway Bridges," by T. Iwasaki, J. Penzien and R.W. Clough - 1972 (PB 215 613)A19

EERC 72-12 "SHAKE-A Computer Program for Earthquake Response Analysis of Horizontally Layered Sites." by P.B. Schnabel and J. Lysmer - 1972 (PB 220 207)A06

EERC 73-1 "Optimal Seismic Design of Multistory Frames," by V.V. Bertero and H. Kamil - 1973

EERC 73-2 "Analysis of the Slides in the San Fernando Dams During the Earthquake of February 9, 1971," by H.B. Seed, K.L. Lee, I.M. Idriss and F. Makdisi - 1973 (PB 223 402)A14

EERC 73-3 "Computer Aided Ultimate Load Design of Unbraced Multistory Steel Frames," by M.B. El-Hafez and G.H. Powell 1973 (PB 248 315)A09

EERC 73-4 "Experimental Investigation into the Seismic Behavior of Critical Regions of Reinforced Concrete Components as Influenced by Moment and Shear," by M. Celebi and J. Penzien - 1973 (PB 215 884)A09

EERC 73-5 "Hysteretic Behavior of Epoxy-Repaired Reinforced Concrete Beams," by M. Celebi and J. Penzien - 1973 (PB 239 568)A03

EERC 73-6 "General Purpose Computer Program for Inelastic Dynamic Response of Plane Structures," by A. Kanaan and G.H. Powell - 1973 (PB 221 260)A08

EERC 73-7 "A Computer Program for Earthquake Analysis of Gravity Dams Including Reservoir Interaction," by P. Chakrabarti and A.K. Chopra - 1973 (AD 766 271)A04

EERC 73-8 "Behavior of Reinforced Concrete Deep Beam-Column Subassemblages Under Cyclic Loads," by O. Küstü and J.G. Bouwkamp - 1973 (PB 246 117)A12

EERC 73-9 "Earthquake Analysis of Structure-Foundation Systems," by A.K. Vaish and A.K. Chopra - 1973 (AD 766 272)A07

EERC 73-10 "Deconvolution of Seismic Response for Linear Systems," by R.B. Reimer - 1973 (PB 227 179)A08

EERC 73-11 "SAP IV: A Structural Analysis Program for Static and Dynamic Response of Linear Systems," by K.-J. Bathe, E.L. Wilson and F.E. Peterson - 1973 (PB 221 967)A09

EERC 73-12 "Analytical Investigations of the Seismic Response of Long, Multiple Span Highway Bridges," by W.S. Tseng and J. Penzien - 1973 (PB 227 816)A10

EERC 73-13 "Earthquake Analysis of Multi-Story Buildings Including Foundation Interaction," by A.K. Chopra and J.A. Gutierrez - 1973 (PB 222 970)A03

EERC 73-14 "ADAP: A Computer Program for Static and Dynamic Analysis of Arch Dams," by R.W. Clough, J.M. Raphael and S. Mojtahedi - 1973 (PB 223 763)A09

EERC 73-15 "Cyclic Plastic Analysis of Structural Steel Joints," by R.B. Pinkney and R.W. Clough - 1973 (PB 226 843)A08

EERC 73-16 "QUAD-4: A Computer Program for Evaluating the Seismic Response of Soil Structures by Variable Damping Finite Element Procedures," by I.M. Idriss, J. Lysmer, R. Hwang and H.B. Seed - 1973 (PB 229 424)A05

EERC 73-17 "Dynamic Behavior of a Multi-Story Pyramid Shaped Building," by R.M. Stephen, J.P. Hollings and J.G. Bouwkamp - 1973 (PB 240 718)A06

EERC 73-18 "Effect of Different Types of Reinforcing on Seismic Behavior of Short Concrete Columns," by V.V. Bertero, J. Hollings, O. Küstü, R.M. Stephen and J.G. Bouwkamp - 1973

EERC 73-19 "Olive View Medical Center Materials Studies, Phase I," by B. Bresler and V.V. Bertero - 1973 (PB 235 986)A06

EERC 73-20 "Linear and Nonlinear Seismic Analysis Computer Programs for Long Multiple-Span Highway Bridges," by W.S. Tseng and J. Penzien - 1973

EERC 73-21 "Constitutive Models for Cyclic Plastic Deformation of Engineering Materials," by J.M. Kelly and P.P. Gillis 1973 (PB 226 024)A03

EERC 73-22 "DRAIN - 2D User's Guide," by G.H. Powell - 1973 (PB 227 016)A05

EERC 73-23 "Earthquake Engineering at Berkeley - 1973," (PB 226 033)A11

EERC 73-24 Unassigned

EERC 73-25 "Earthquake Response of Axisymmetric Tower Structures Surrounded by Water," by C.Y. Liaw and A.K. Chopra 1973 (AD 773 052)A09

EERC 73-26 "Investigation of the Failures of the Olive View Stairtowers During the San Fernando Earthquake and Their Implications on Seismic Design," by V.V. Bertero and R.G. Collins - 1973 (PB 235 106)A13

EERC 73-27 "Further Studies on Seismic Behavior of Steel Beam-Column Subassemblages," by V.V. Bertero, H. Krawinkler and E.P. Popov - 1973 (PB 234 172)A06

EERC 74-1 "Seismic Risk Analysis," by C.S. Oliveira - 1974 (PB 235 920)A06

EERC 74-2 "Settlement and Liquefaction of Sands Under Multi-Directional Shaking," by R. Pyke, C.K. Chan and H.B. Seed 1974

EERC 74-3 "Optimum Design of Earthquake Resistant Shear Buildings," by D. Ray, K.S. Pister and A.K. Chopra - 1974 (PB 231 172)A06

EERC 74-4 "LUSH - A Computer Program for Complex Response Analysis of Soil-Structure Systems," by J. Lysmer, T. Udaka, H.B. Seed and R. Hwang - 1974 (PB 236 796)A05

EERC 74-5 "Sensitivity Analysis for Hysteretic Dynamic Systems: Applications to Earthquake Engineering," by D. Ray 1974 (PB 233 213)A06

EERC 74-6 "Soil Structure Interaction Analyses for Evaluating Seismic Response," by H.B. Seed, J. Lysmer and R. Hwang 1974 (PB 236 519)A04

EERC 74-7 Unassigned

EERC 74-8 "Shaking Table Tests of a Steel Frame - A Progress Report," by R.W. Clough and D. Tang - 1974 (PB 240 869)A03

EERC 74-9 "Hysteretic Behavior of Reinforced Concrete Flexural Members with Special Web Reinforcement," by V.V. Bertero, E.P. Popov and T.Y. Wang - 1974 (PB 236 797)A07

EERC 74-10 "Applications of Reliability-Based, Global Cost Optimization to Design of Earthquake Resistant Structures," by E. Vitiello and K.S. Pister - 1974 (PB 237 231)A06

EERC 74-11 "Liquefaction of Gravelly Soils Under Cyclic Loading Conditions," by R.T. Wong, H.B. Seed and C.K. Chan 1974 (PB 242 042)A03

EERC 74-12 "Site-Dependent Spectra for Earthquake-Resistant Design," by H.B. Seed, C. Ugas and J. Lysmer - 1974 (PB 240 953)A03

EERC 74-13 "Earthquake Simulator Study of a Reinforced Concrete Frame," by P. Hidalgo and R.W. Clough - 1974 (PB 241 944)A13

EERC 74-14 "Nonlinear Earthquake Response of Concrete Gravity Dams," by N. Pal - 1974 (AD/A 006 583)A06

EERC 74-15 "Modeling and Identification in Nonlinear Structural Dynamics - I. One Degree of Freedom Models," by N. Distefano and A. Rath - 1974 (PB 241 548)A06

EERC 75-1 "Determination of Seismic Design Criteria for the Dumbarton Bridge Replacement Structure, Vol. I: Description, Theory and Analytical Modeling of Bridge and Parameters," by F. Baron and S.-H. Pang - 1975 (PB 259 407)A15

EERC 75-2 "Determination of Seismic Design Criteria for the Dumbarton Bridge Replacement Structure, Vol. II: Numerical Studies and Establishment of Seismic Design Criteria," by F. Baron and S.-H. Pang - 1975 (PB 259 408)A11 (For set of EERC 75-1 and 75-2 (PB 259 406))

EERC 75-3 "Seismic Risk Analysis for a Site and a Metropolitan Area," by C.S. Oliveira - 1975 (PB 248 134)A09

EERC 75-4 "Analytical Investigations of Seismic Response of Short, Single or Multiple-Span Highway Bridges," by M.-C. Chen and J. Penzien - 1975 (PB 241 454)A09

EERC 75-5 "An Evaluation of Some Methods for Predicting Seismic Behavior of Reinforced Concrete Buildings," by S.A. Mahin and V.V. Bertero - 1975 (PB 246 306)A16

EERC 75-6 "Earthquake Simulator Study of a Steel Frame Structure, Vol. I: Experimental Results," by R.W. Clough and D.T. Tang - 1975 (PB 243 981)A13

EERC 75-7 "Dynamic Properties of San Bernardino Intake Tower," by D. Rea, C.-Y. Liaw and A.K. Chopra - 1975 (AD/A008 406) A05

EERC 75-8 "Seismic Studies of the Articulation for the Dumbarton Bridge Replacement Structure, Vol. I: Description, Theory and Analytical Modeling of Bridge Components," by F. Baron and R.E. Hamati - 1975 (PB 251 539)A07

EERC 75-9 "Seismic Studies of the Articulation for the Dumbarton Bridge Replacement Structure, Vol. 2: Numerical Studies of Steel and Concrete Girder Alternates," by F. Baron and R.E. Hamati - 1975 (PB 251 540)A10

EERC 75-10 "Static and Dynamic Analysis of Nonlinear Structures," by D.P. Mondkar and G.H. Powell - 1975 (PB 242 434)A08

EERC 75-11 "Hysteretic Behavior of Steel Columns," by E.P. Popov, V.V. Bertero and S. Chandramouli - 1975 (PB 252 365)A11

EERC 75-12 "Earthquake Engineering Research Center Library Printed Catalog," - 1975 (PB 243 711)A26

EERC 75-13 "Three Dimensional Analysis of Building Systems (Extended Version)," by E.L. Wilson, J.P. Hollings and H.H. Dovey - 1975 (PB 243 989)A07

EERC 75-14 "Determination of Soil Liquefaction Characteristics by Large-Scale Laboratory Tests," by P. De Alba, C.K. Chan and H.B. Seed - 1975 (NUREG 0027)A08

EERC 75-15 "A Literature Survey - Compressive, Tensile, Bond and Shear Strength of Masonry," by R.L. Mayes and R.W. Clough - 1975 (PB 246 292)A10

EERC 75-16 "Hysteretic Behavior of Ductile Moment Resisting Reinforced Concrete Frame Components," by V.V. Bertero and E.P. Popov - 1975 (PB 246 388)A05

EERC 75-17 "Relationships Between Maximum Acceleration, Maximum Velocity, Distance from Source, Local Site Conditions for Moderately Strong Earthquakes," by H.B. Seed, R. Murarka, J. Lysmer and I.M. Idriss - 1975 (PB 248 172)A03

EERC 75-18 "The Effects of Method of Sample Preparation on the Cyclic Stress-Strain Behavior of Sands," by J. Mulilis, C.K. Chan and H.B. Seed - 1975 (Summarized in EERC 75-28)

EERC 75-19 "The Seismic Behavior of Critical Regions of Reinforced Concrete Components as Influenced by Moment, Shear and Axial Force," by M.B. Atalay and J. Penzien - 1975 (PB 258 842)A11

EERC 75-20 "Dynamic Properties of an Eleven Story Masonry Building," by R.M. Stephen, J.P. Hollings, J.G. Bouwkamp and D. Jurukovski - 1975 (PB 246 945)A04

EERC 75-21 "State-of-the-Art in Seismic Strength of Masonry - An Evaluation and Review," by R.L. Mayes and R.W. Clough 1975 (PB 249 040)A07

EERC 75-22 "Frequency Dependent Stiffness Matrices for Viscoelastic Half-Plane Foundations," by A.K. Chopra, P. Chakrabarti and G. Dasgupta - 1975 (PB 248 121)A07

EERC 75-23 "Hysteretic Behavior of Reinforced Concrete Framed Walls," by T.Y. Wong, V.V. Bertero and E.P. Popov - 1975

EERC 75-24 "Testing Facility for Subassemblages of Frame-Wall Structural Systems," by V.V. Bertero, E.P. Popov and T. Endo - 1975

EERC 75-25 "Influence of Seismic History on the Liquefaction Characteristics of Sands," by H.B. Seed, K. Mori and C.K. Chan - 1975 (Summarized in EERC 75-28)

EERC 75-26 "The Generation and Dissipation of Pore Water Pressures during Soil Liquefaction," by H.B. Seed, P.P. Martin and J. Lysmer - 1975 (PB 252 648)A03

EERC 75-27 "Identification of Research Needs for Improving Aseismic Design of Building Structures," by V.V. Bertero 1975 (PB 248 136)A05

EERC 75-28 "Evaluation of Soil Liquefaction Potential during Earthquakes," by H.B. Seed, I. Arango and C.K. Chan - 1975 (NUREG 0026)A13

EERC 75-29 "Representation of Irregular Stress Time Histories by Equivalent Uniform Stress Series in Liquefaction Analyses," by H.B. Seed, I.M. Idriss, F. Makdisi and N. Banerjee - 1975 (PB 252 635)A03

EERC 75-30 "FLUSH - A Computer Program for Approximate 3-D Analysis of Soil-Structure Interaction Problems," by J. Lysmer, T. Udaka, C.-F. Tsai and H.B. Seed - 1975 (PB 259 332)A07

EERC 75-31 "ALUSH - A Computer Program for Seismic Response Analysis of Axisymmetric Soil-Structure Systems," by E. Berger, J. Lysmer and H.B. Seed - 1975

EERC 75-32 "TRIP and TRAVEL - Computer Programs for Soil-Structure Interaction Analysis with Horizontally Travelling Waves," by T. Udaka, J. Lysmer and H.B. Seed - 1975

EERC 75-33 "Predicting the Performance of Structures in Regions of High Seismicity," by J. Penzien - 1975 (PB 248 130)A03

EERC 75-34 "Efficient Finite Element Analysis of Seismic Structure - Soil - Direction," by J. Lysmer, H.B. Seed, T. Udaka, R.N. Hwang and C.-F. Tsai - 1975 (PB 253 570)A03

EERC 75-35 "The Dynamic Behavior of a First Story Girder of a Three-Story Steel Frame Subjected to Earthquake Loading," by R.W. Clough and L.-Y. Li - 1975 (PB 248 841)A05

EERC 75-36 "Earthquake Simulator Study of a Steel Frame Structure, Volume II - Analytical Results," by D.T. Tang - 1975 (PB 252 926)A10

EERC 75-37 "ANSR-I General Purpose Computer Program for Analysis of Non-Linear Structural Response," by D.P. Mondkar and G.H. Powell - 1975 (PB 252 386)A08

EERC 75-38 "Nonlinear Response Spectra for Probabilistic Seismic Design and Damage Assessment of Reinforced Concrete Structures," by M. Murakami and J. Penzien - 1975 (PB 259 530)A05

EERC 75-39 "Study of a Method of Feasible Directions for Optimal Elastic Design of Frame Structures Subjected to Earthquake Loading," by N.D. Walker and K.S. Pister - 1975 (PB 257 781)A06

EERC 75-40 "An Alternative Representation of the Elastic-Viscoelastic Analogy," by G. Dasgupta and J.L. Sackman - 1975 (PB 252 173)A03

EERC 75-41 "Effect of Multi-Directional Shaking on Liquefaction of Sands," by H.B. Seed, R. Pyke and G.R. Martin - 1975 (PB 258 781)A03

EERC 76-1 "Strength and Ductility Evaluation of Existing Low-Rise Reinforced Concrete Buildings - Screening Method," by T. Okada and B. Bresler - 1976 (PB 257 906)A11

EERC 76-2 "Experimental and Analytical Studies on the Hysteretic Behavior of Reinforced Concrete Rectangular and T-Beams," by S.-Y.M. Ma, E.P. Popov and V.V. Bertero - 1976 (PB 260 843)A12

EERC 76-3 "Dynamic Behavior of a Multistory Triangular-Shaped Building," by J. Petrovski, R.M. Stephen, E. Gartenbaum and J.G. Bouwkamp - 1976

EERC 76-4 "Earthquake Induced Deformations of Earth Dams," by N. Serff and H.B. Seed - 1976

EERC 76-5 "Analysis and Design of Tube-Type Tall Building Structures," by H. de Clercq and G.H. Powell - 1976 (PB 252 220) A10

EERC 76-6 "Time and Frequency Domain Analysis of Three-Dimensional Ground Motions, San Fernando Earthquake," by T. Kubo and J. Penzien (PB 260 556)A11

EERC 76-7 "Expected Performance of Uniform Building Code Design Masonry Structures," by R.L. Mayes, Y. Omote, S.W. Chen and R.W. Clough - 1976

EERC 76-8 "Cyclic Shear Tests on Concrete Masonry Piers," Part I - Test Results," by R.L. Mayes, Y. Omote and R.W. Clough - 1976 (PB 264 424)A06

EERC 76-9 "A Substructure Method for Earthquake Analysis of Structure - Soil Interaction," by J.A. Gutierrez and A.K. Chopra - 1976 (PB 257 783)A08

EERC 76-10 "Stabilization of Potentially Liquefiable Sand Deposits using Gravel Drain Systems," by H.B. Seed and J.R. Booker - 1976 (PB 258 820)A04

EERC 76-11 "Influence of Design and Analysis Assumptions on Computed Inelastic Response of Moderately Tall Frames," by G.H. Powell and D.G. Row - 1976

EERC 76-12 "Sensitivity Analysis for Hysteretic Dynamic Systems: Theory and Applications," by D. Ray, K.S. Pister and E. Polak - 1976 (PB 262 859)A04

EERC 76-13 "Coupled Lateral Torsional Response of Buildings to Ground Shaking," by C.L. Kan and A.K. Chopra - 1976 (PB 257 907)A09

EERC 76-14 "Seismic Analyses of the Banco de America," by V.V. Bertero, S.A. Mahin and J.A. Hollings - 1976

EERC 76-15 "Reinforced Concrete Frame 2: Seismic Testing and Analytical Correlation," by R.W. Clough and J. Gidwani - 1976 (PB 261 323)A08

EERC 76-16 "Cyclic Shear Tests on Masonry Piers, Part II - Analysis of Test Results," by R.L. Mayes, Y. Omote and R.W. Clough - 1976

EERC 76-17 "Structural Steel Bracing Systems: Behavior Under Cyclic Loading," by E.P. Popov, K. Takanashi and C.W. Roeder - 1976 (PB 260 715)A05

EERC 76-18 "Experimental Model Studies on Seismic Response of High Curved Overcrossings," by D. Williams and W.G. Godden - 1976

EERC 76-19 "Effects of Non-Uniform Seismic Disturbances on the Dumbarton Bridge Replacement Structure," by F. Baron and R.E. Hamati - 1976

EERC 76-20 "Investigation of the Inelastic Characteristics of a Single Story Steel Structure Using System Identification and Shaking Table Experiments," by V.C. Matzen and H.D. McNiven - 1976 (PB 258 453)A07

EERC 76-21 "Capacity of Columns with Splice Imperfections," by E.P. Popov, R.M. Stephen and R. Philbrick - 1976 (PB 260 378)A04

EERC 76-22 "Response of the Olive View Hospital Main Building during the San Fernando Earthquake," by S. A. Mahin, R. Collins, A.K. Chopra and V.V. Bertero - 1976

EERC 76-23 "A Study on the Major Factors Influencing the Strength of Masonry Prisms," by N.M. Mostaghel, R.L. Mayes, R. W. Clough and S.W. Chen - 1976

EERC 76-24 "GADFLEA - A Computer Program for the Analysis of Pore Pressure Generation and Dissipation during Cyclic or Earthquake Loading," by J.R. Booker, M.S. Rahman and H.B. Seed - 1976 (PB 263 947)A04

EERC 76-25 "Rehabilitation of an Existing Building: A Case Study," by B. Bresler and J. Axley - 1976

EERC 76-26 "Correlative Investigations on Theoretical and Experimental Dynamic Behavior of a Model Bridge Structure," by K. Kawashima and J. Penzien - 1976 (PB 263 388)A11

EERC 76-27 "Earthquake Response of Coupled Shear Wall Buildings," by T. Srichatrapimuk - 1976 (PB 265 157)A07

EERC 76-28 "Tensile Capacity of Partial Penetration Welds," by E.P. Popov and R.M. Stephen - 1976 (PB 262 899)A03

EERC 76-29 "Analysis and Design of Numerical Integration Methods in Structural Dynamics," by H.M. Hilber - 1976 (PB 264 410)A06

EERC 76-30 "Contribution of a Floor System to the Dynamic Characteristics of Reinforced Concrete Buildings," by L.J. Edgar and V.V. Bertero - 1976

EERC 76-31 "The Effects of Seismic Disturbances on the Golden Gate Bridge," by F. Baron, M. Arikan and R.E. Hamati - 1976

EERC 76-32 "Infilled Frames in Earthquake Resistant Construction," by R.E. Klingner and V.V. Bertero - 1976 (PB 265 892)A13

UCB/EERC-77/01 "PLUSH - A Computer Program for Probabilistic Finite Element Analysis of Seismic Soil-Structure Interaction," by M.P. Romo Organista, J. Lysmer and H.B. Seed - 1977

UCB/EERC-77/02 "Soil-Structure Interaction Effects at the Humboldt Bay Power Plant in the Ferndale Earthquake of June 7, 1975," by J.E. Valera, H.B. Seed, C.F. Tsai and J. Lysmer - 1977 (PB 265 795)A04

UCB/EERC-77/03 "Influence of Sample Disturbance on Sand Response to Cyclic Loading," by K. Mori, H.B. Seed and C.K. Chan - 1977 (PB 267 352)A04

UCB/EERC-77/04 "Seismological Studies of Strong Motion Records," by J. Shoja-Taheri - 1977 (PB 269 655)A10

UCB/EERC-77/05 "Testing Facility for Coupled-Shear Walls," by L. Li-Hyung, V.V. Bertero and E.P. Popov - 1977

UCB/EERC-77/06 "Developing Methodologies for Evaluating the Earthquake Safety of Existing Buildings," by No. 1 - B. Bresler; No. 2 - B. Bresler, T. Okada and D. Zisling; No. 3 - T. Okada and B. Bresler; No. 4 - V.V. Bertero and B. Bresler - 1977 (PB 267 354)A08

UCB/EERC-77/07 "A Literature Survey - Transverse Strength of Masonry Walls," by Y. Omote, R.L. Mayes, S.W. Chen and R.W. Clough - 1977

UCB/EERC-77/08 "DRAIN-TABS: A Computer Program for Inelastic Earthquake Response of Three Dimensional Buildings," by R. Guendelman-Israel and G.H. Powell - 1977 (PB 270 693)A07

UCB/EERC-77/09 "SUBWALL: A Special Purpose Finite Element Computer Program for Practical Elastic Analysis and Design of Structural Walls with Substructure Option," by D.Q. Le, H. Peterson and E.P. Popov - 1977 (PB 270 567)A05

UCB/EERC-77/10 "Experimental Evaluation of Seismic Design Methods for Broad Cylindrical Tanks," by D.P. Clough

UCB/EERC-77/11 "Earthquake Engineering Research at Berkeley - 1976," - 1977

UCB/EERC-77/12 "Automated Design of Earthquake Resistant Multistory Steel Building Frames," by N.D. Walker, Jr. - 1977

UCB/EERC-77/13 "Concrete Confined by Rectangular Hoops Subjected to Axial Loads," by D. Zallnas, V.V. Bertero and E.P. Popov - 1977

UCB/EERC-77/14 "Seismic Strain Induced in the Ground During Earthquakes," by Y. Sugimura - 1977

UCB/EERC-77/15 "Bond Deterioration under Generalized Loading," by V.V. Bertero, E.P. Popov and S. Viwathanatepa - 1977

UCB/EERC-77/16 "Computer Aided Optimum Design of Ductile Reinforced Concrete Moment Resisting Frames," by S.W. Zagajeski and V.V. Bertero - 1977

UCB/EERC-77/17 "Earthquake Simulation Testing of a Stepping Frame with Energy-Absorbing Devices," by J.M. Kelly and D.F. Tsztoo 1977

UCB/EERC-77/18 "Inelastic Behavior of Eccentrically Braced Steel Frames under Cyclic Loadings," by C.W. Roeder and E.P. Popov - 1977

UCB/EERC-77/19 "A Simplified Procedure for Estimating Earthquake-Induced Deformations in Dams and Embankments," by F.I. Makdisi and H.B. Seed - 1977

UCB/EERC-77/20 "The Performance of Earth Dams during Earthquakes," by H.B. Seed, F.I. Makdisi and P. de Alba - 1977

UCB/EERC-77/21 "Dynamic Plastic Analysis Using Stress Resultant Finite Element Formulation," by P. Lukkunapvasit and J.M. Kelly 1977

UCB/EERC-77/22 "Preliminary Experimental Study of Seismic Uplift of a Steel Frame," by R.W. Clough and A.A. Huckelbridge - 1977

UCB/EERC-77/23 "Earthquake Simulator Tests of a Nine-Story Steel Frame with Columns Allowed to Uplift," by A.A. Huckelbridge - 1977

UCB/EERC-77/24 "Nonlinear Soil-Structure Interaction of Skew Highway Bridges," by M.-C. Chen and Joseph Penzien - 1977

UCB/EERC-77/25 "Seismic Analysis of an Offshore Structure Supported on Pile Foundations," by D.D.-N. Liou - 1977

UCB/EERC-77/26 "Dynamic Stiffness Matrices for Homogeneous Viscoelastic Half-Planes," by G. Dasgupta and A.K. Chopra - 1977

UCB/EERC-77/27 "A Practical Soft Story Earthquake Isolation System," by J.M. Kelly and J.M. Eidinger - 1977

UCB/EERC-77/28 "Seismic Safety of Existing Buildings and Incentives for Hazard Mitigation in San Francisco: An Exploratory Study," by A. J. Meltsner - 1977

UCB/EERC-77/29 "Dynamic Analysis of Electrohydraulic Shaking Tables," by D. Rea, S. Abedi-Hayati and Y. Takahashi - 1977

UCB/EERC-78/01 "The Development of Energy-Absorbing Devices for Aseismic Base Isolation Systems," by J.M. Kelly and D.F. Tsztoo 1978

UCB/EERC-78/02 "Effect of Tensile Prestrain on the Cyclic Response of Structural Steel Connections," by J.G. Bouwkamp and A. Mukhopadhyay - 1978

UCB/EERC-78/03 "Experimental Results of an Earthquake Isolation System using Natural Rubber Bearings," by J. M. Eidinger and J.M. Kelly - 1978

UCB/EERC-78-04 "Seismic Behavior of Tall Liquid Storage Tanks," by A. Niwa 1978

UCB/EERC-78/05 "An Approach for Improving Seismic-Resistant Behavior of Reinforced Concrete Interior Joints," by B. Galunic, V.V. Bertero and E.P. Popov - 1978

UCB/EERC-78/06 "Inertia Forces on Submerged Tanks and Cassons Due to Earthquakes," by R.C. Byrd, F. Nilrat, B.C. Gerwick, Jr., J. Penzien and R.L. Weigel - 1978

UCB/EERC-78/07 "Studies of Structural Response to Earthquake Ground Motion," by O.A. Lopez and A.K. Chopra - 1978